Techno-economic assessment of process chains for the manufacturing of external maxillofacial prostheses for the South African ethnic demography using digital and Additive Manufacturing technologies

by

Izél van Heerden

Thesis submitted in fulfilment of the requirements for the degree

Doctor of Health Sciences in Biomedical Technology,

Department of Health Sciences,

Faculty of Health and Environmental Sciences,

Central University of Technology, Free State,

Bloemfontein

Supervisor: Professor Annabel Fossey

Co-supervisor: Doctor Kobus van der Walt

NOVEMBER 2024

Declaration

I, Izél van Heerden, declare that this thesis entitled, ‘Techno-economic assessment of process chains for the manufacturing of external maxillofacial prostheses for the South African ethnic demography using digital and Additive Manufacturing technologies’, is a presentation of my own original research work conducted at the Central University of Technology, Free State. Wherever contributions of others were involved, every effort has been made to indicate this clearly, with due reference to the literature and acknowledgment of collaborative research and discussions. No part of this dissertation has been submitted for any other degree or processional qualification.

The work was conducted under the guidance of Professor Annabel Fossey and Doctor Kobus van der Walt.

……………………………….
Izél van Heerden

November 2024

I certify that the above statement is correct

…………………………………
Professor Annabel Fossey

Acknowledgements

Isaiah 41:10: " So do not fear, for I am with you; do not be dismayed, for I am the Lord your God. I will strengthen you; I will help you. I will uphold you with my righteous hand." When we believe that God is with us, we can have confidence that no matter what we might face, no matter what challenges, difficulties, opposition, enemies, or battles that we face, when we know that God is with us in those things, it can give us the confidence, it provides us with the assurance that comes hell or high water that my God is with me. My God goes before me. He is parting the sea so that I can walk on dry ground. He is making a way where there appears to be no way. He is working behind the scenes. And if we have faith and keep moving forward, if we have trust in Him and keep putting one foot in front of the next, we will discover that at the end of the road, when we would look back, we will see God moved powerfully and mightily on our behalf. – Colby Maier.

Thank you, Heavenly Father, for moving powerfully and mightily on my behalf. Your faithfulness, love, and mercy have no end.

I would like to express my heartfelt gratitude to my supervisor, Prof Annabel Fossey, for making this study successful. Your unwavering support, immense knowledge, experience, encouragement, patience, and understanding have been invaluable to me. Words cannot express how much I admire and appreciate you. I will be forever grateful for having such an exceptional supervisor during my doctoral journey. I would also like to thank my co-supervisor, Dr Kobus van der Walt, for his support and guidance on the practical aspects of the project. You never stop believing in me; your encouragement on many occasions is appreciated.

Thank you to André Heydenrych at the CRPM for your assistance.

How can I begin to thank you, Ettienne, my love? I have always felt more optimistic after speaking to you. Without you, I would never have been able to complete my studies. Your love and hugs, motivational talks in the middle of the night, calming my racing heart; I will cherish it forever. Thank you for all the hours of support with computer-issues and software-issues (my rekenaar-boffin). Love you always and forever.

Pappa Philip and Mamma Elené, your support was enormous. Throughout my academic career, you were always there for me without a second thought. All your prayers and late night-early morning hugs to comfort me through the anxiety kept me going even when I was close to giving up. Your endless love, hundreds of cups of coffee, and healthy cooked meals helped me to keep going. How can I ever say thank you enough? You never stop believing in me. I am what and who I am today because of you. My heart is overflowing with love for you.

My brother Attie, thank you for everything and all your help with experiments. Thank you for all your love. Ja ek is uiteindelik klaar! To my sister-in-law, Danielle, thank you for all your support and all the delicious, cooked meals for family dinners on Sundays. I love you and Sion so much.

My Aunt Noeleen, thank you for all your prayers and beautiful early morning messages. I love you.

Christelle, my best friend. A heartfelt thank you for your endless prayers and regular check-ins. You are such a gift from God. May our friendship last for another 32 years. Lief vir jou vriendin.

Abba Vader neem my hand veilig in U hand en lei my op die pad wat U vir my beplan.

Ek sien uit na my toekoms met U aan my sy.

Table of Contents

List of Tables

List of Figures

Abbreviations and Trademarks

Abbreviations

2D	Two-dimensional
3D	Three-dimensional
AM	Additive manufacturing
BPR	Best Preview Render
CAD	Computer-aided design
CAM	Computer-aided manufacturing
CRPM	Centre for Rapid Prototyping and Manufacturing
CT	Computed tomography
CUT	Central University of Technology, Free State
DICOM	Digital Imaging and Communications in Medicine
DSR	Design science research
ED	Ear deformity (model)
MANOVA	Multivariate Analysis of Variance
MD	Mean distance
MIP	Medical image processing
MRI	Magnetic resonance imaging
ND	Nose deformity (model)
RMS	Root Mean Square
ROI	Region of interest
RP	Rapid prototyping
RTV	Research test volume
SD	Standard deviation
SR	Standardised Rating
STL	Stereolithography file format, Standard Triangle Language, or Standard Tessellation Language
USRI	Unweighted Standardised Rating Index
UV	Ultraviolet

Trademarks

3D Coat	Developed by Pilgway® LLC. Yuliya Zdanozska street, 03022, Kyiv, Ukraine.

3D Doctor™	Developed by Able Software Corp. 5 Appletree Lane Lexington, MA 02420, Massacusetts, USA.
3D Slicer™	Developed by The Slicer Community. Brigham and Women's Hospital (BWH), a teaching affiliate of Harvard Medical School.
Artec Studio	Developed by Artec 3D®. 4 Rue Lou Hemmer, L-1748 Senningerberg, Luxembourg.
CloudCompare	Developed by Telecom ParisTech and the R&D division of EDF and Daniel Girardeau Montaut.
Geomagic® Freeform®	Developed by 3D Systems®, Inc. 333 Three D Systems Circle Rock Hill, 29730, South Carolina, United States. Currently owned by Oqton.
Geomagic® Control X™	Developed by 3D Systems®, Inc. 333 Three D Systems Circle Rock Hill, 29730, South Carolina, United States. Currently owned by Oqton.
InVesalius	Developed by CTI (Renato Archer Information Technology Center), a research institute of the Brazilian Science and Technology Center. Dom Pedro I Highway (SP-65), Km 143,6 - Chácaras Campos dos Amarais, Campinas - SP, 13069-901, Brazil.
Magics®	Developed by Materialise®. Technologielaan 15, 3001 Leuven, Belgium.
Meshmixer	Developed by Autodesk®, Inc. The Landmark @ One Market, Ste. 400 San Francisco, California, 94105 United States.
Mimics®	Developed by Materialise®. Technologielaan 15, 3001 Leuven, Belgium.
Mudbox™	Developed by Autodesk®, Inc. The Landmark @ One Market, Ste. 400 San Francisco, California, 94105 United States.
ZBrush™	Developed by Pixologic®, Inc. 6410 Santa Monica Blvd Bldg 10, Los Angeles, California, 90038, United States. Currently owned by Maxon.

Abstract

Introduction: Maxillofacial trauma can significantly impact a person's life, affecting vital functions such as vision, smell, hearing, speech, breathing, eating, and facial appearance. Treating such trauma is challenging since the face plays a key role in expressing emotions and identity. In South Africa, the impact of facial trauma is extensive, not only for individuals but also for their families. Many patients, especially those reliant on government healthcare, lack the funding to access advanced technologies for the manufacturing of external maxillofacial prostheses. Therefore, given the high costs, research is needed to identify cheaper production options that still produce quality prostheses. To improve access for patients with limited financial resources, identifying cost-effective alternatives is crucial while ensuring the quality of these prostheses matches industry-benchmarks. In this study, process chains incorporating medical image processing (MIP) and computer-aided design (CAD) software using computed tomography (CT) volumetric data were evaluated against the industry-benchmark, which combines Mimics and Geomagic Freeform software applications. Additionally, process chains using surface scan data in conjunction with CAD software were tested and compared to the industry-benchmark.

Main research question: The main research question probed in this study was: "Which process chain(s) can produce external maxillofacial prostheses of acceptable quality at a price relevant to the South African demography?" The answer to this question was explored by employing a design science research approach to find practical solutions to real-world problems, aligning with the pragmatic goal of generating useful, actionable knowledge with tangible outcomes.

Methods: The objective was to determine which process chains could effectively meet the requirements for designing external maxillofacial prostheses. To systematically explore and validate affordable alternatives to the industry-benchmark, the research was divided into four distinct phases.

In **Phase 1**, MIP and CAD software with potential for inclusion in the test process chains were identified through a comprehensive systematic literature review.

In **Phase 2**, MIP software was selected based on its features and ability to segment CT data obtained from two human subjects. Errors in the segmented geometries were evaluated using Meshmixer, while the alignment of the test geometries with the control mesh was analysed and compared using CloudCompare.

In **Phase 3**, the selected CAD software was tested for its features and sculpting capabilities. Sculpting functionality was evaluated using an anti-oloid mesh as the test object. Meshmixer was also used to detect any errors introduced during the sculpting process.

Finally, in **Phase 4**, 3D models of human ears and noses were designed using the potential alternative process chains, which combined the selected MIP and CAD software and compared them to the industry benchmark. Additionally, the process chains that used surface scan data and CAD software to design ears and noses were also compared to the industry-benchmark. The ears and noses produced by the different process chains were analysed using Meshmixer, CloudCompare, and Geomagic Control X. To further assess the performance of each process chain, an Unweighted Standardised Rating Index was calculated to rate the various process chains based on quality. The process chains were also compared based on cost.

Results: Following a thorough examination of over 700 scholarly publications, 73 were found to be suitable for identifying MIP and CAD software that may be suitable for testing in process chains related to the manufacturing of external maxillofacial prostheses. By applying a stepwise process of excluding software that did not fit the criteria, five MIP (out of 21) and nine CAD software applications (out of 37) were chosen for testing besides the industry-benchmarks. After testing the MIP software mainly for their segmenting capabilities, 3D Slicer and InVesalius were selected for testing in process chains. The systematic comparison of CAD software for digital sculpting in the manufacturing of external maxillofacial prostheses revealed that 3D Coat and ZBrush should be tested in process chains. The

study's findings showed that the four test process chains combining MIP software with CAD software, and the two chains using scanned data with CAD software, produced products of comparable quality to those created by the control process chains. Among these, the combination of 3D Slicer with either 3D Coat or ZBrush resulted in the highest quality products. In contrast, the combinations of InVesalius with ZBrush, as well as surface scan data with 3D Coat or ZBrush, yielded lower-quality outcomes. In terms of cost, surface scan data combined with 3D Coat was the most affordable option for the South African demographic. For CT data, however, the combination of 3D Slicer or InVesalius with 3D Coat was the most cost-effective.

Significance: By identifying alternative, cheaper, and more readily available processes to produce maxillofacial prostheses, more patients suffering from facial trauma will be able to access these life-changing technologies. When patients undergo reconstructive interventions, their self-esteem improves, which in turn helps them to reintegrate into society more quickly.

Keywords: medical image processing software; computer-aided design software; external maxillofacial prostheses; process chains

Chapter 1

Introduction to the Study

1.1 Introduction

A person's facial disfigurements have a significant effect on their psychosocial well-being. Because they are viewed as abnormal, society typically rejects these individuals. As a result, people with obvious facial malformations frequently experience anxiety, extreme despair, and low self-esteem (Sykes et al., 1972; Sarwer et al., 2022). Disfigurement, defined by the Collins Dictionary (2022), is "a part of someone's body which is not the normal shape because of injury or illness, or because they were born this way."

Worldwide, the prevalence of trauma is still rising. Facial trauma is a major health problem that is often associated with incidents such as vehicle accidents, assaults, and cancer (Yadav & Shrestha, 2017; Al-Ali et al., 2022). Any damage to the soft and hard tissues of the jaws, face, and other corresponding structures is referred to as maxillofacial trauma (Pillay et al., 2018). All the soft tissues of the face, including the frontal, nasal, zygomatic, ethmoid, maxillary bones, and mandible, are included in the maxillofacial region (Gokharman et al., 2023). Abrasions, burns, lacerations, bruising, avulsions, and missing tissues are examples of soft tissue injuries. Hard tissue injuries include dental trauma, temporomandibular joint dislocations, and fractures of the bony maxillofacial complex (Pillay et al., 2018; Gómez Roselló et al., 2020). The primary salivary glands, blood vessels, cranial nerves, muscles, connective tissue, facial bones, and the sensory organs, namely the eyes, ears, and nose, can all be impacted by these soft and hard tissue injuries in the face (Hogg & Horswell, 2006). Losing the auricle, nasal, and orbital anatomy can significantly impact an individual's life.

There are several different causes of maxillofacial trauma that have been reported in the literature. Among the significant factors that contribute to facial trauma statistics are burns, road traffic accidents, assaults (including firearm injuries), and cancer (Al-Ali et al., 2022; Gokharman et al., 2023). Congenital disorders, accidents at work, falls, sports injuries, animal attacks by both domestic and wild animals, and freak accidents are some more causes of facial disfigurements. Severe burns accounted for approximately 11 million medical admissions worldwide in 2004 alone and are the fourth most common cause of injuries behind road traffic accidents, falls, and interpersonal violence (Peck, 2011). Both in industrialised and developing nations, burn injuries continue to be a serious public health concern (Iqbal et al., 2013). Despite a worldwide decline in burn injuries, Africa still experiences approximately twice the global average when considering disability-adjusted life years (James et al., 2020; Jeschke et al., 2020; Chen et al., 2022). South Africa has exceptionally high rates of burn injury morbidity, which remain a significant concern (Angelou et al., 2022; Davies et al., 2024). Burns represent 3.2% of all occurrences of facial trauma in South Africa each year, of which the majority of victims are children and young people (Teo et al., 2012; Alemayehu et al., 2020). The leading causes of burns in South Africa include fires caused by kerosene (paraffin) cookstoves and unattended candles in crowded informal housing settlements (Maritz et al., 2012). These fires are frequently triggered by alcohol and drug intoxication (Davies et al., 2024). The statistics of face trauma patients in South Africa include not only burns but also high rates of road traffic accidents and attacks, especially in disadvantaged communities.

Road traffic deaths and injuries remain a significant global health challenge. An estimated 1.19 million road traffic deaths occurred in 2021 (Supramaniam et al., 2024). According to the World Health Organization, 3 000 individuals lose their lives daily on the roads, with a minimum of 30 000 others sustaining serious injuries or becoming disabled. Annually, over 1.2 million people die, while an additional 50 million suffer severe injuries (World Health Organization, 2023). More than half of the individuals impacted have experienced multiple traumas and need interdisciplinary treatment from trauma surgeons, otolaryngologists, plastic surgeons, ophthalmologists, anaesthesiologists, and oral and maxillofacial surgeons (Malik et al., 2017). Underdeveloped nations have considerably higher incidences of road traffic accidents, ranging from approximately 55 to 91% (Lee et al., 2017). South Africa had a 2.2% increase in traffic fatalities on the road when comparing statistics from 2019 and 2021, and 26.2% more in 2021 compared to 2020 (Road Traffic Management Corporation, 2022).

Assault acts of interpersonal violence, intimate partner (domestic) violence, gender-based violence, and violence against children are increasingly acknowledged as significant factors contributing to facial trauma and deformities. Many of these assaults involve the use of illegal firearms (Tobin-Tyler, 2023). According to a study conducted by Pillay et al. (2018) at Zithulele Hospital, Eastern Cape in South Africa, interpersonal violence accounted for most maxillofacial trauma cases at 55%, followed by road traffic accidents at 16%, falls at 10%, and injuries caused by animals at 4%. These results demonstrate how critical it is to address violence and enhance safety protocols in order to lower these kinds of incidents (Lanchimba et al., 2023; Cookson et al., 2024). Maxillofacial trauma is a common occurrence in the rural areas of South Africa, with interpersonal violence being the primary cause. Men aged between 18 and 24 years are frequent victims (Pillay et al., 2018).

One of the leading causes of maxillofacial trauma worldwide is cancer. Melanoma of the skin is the 17th most prevalent form of cancer globally, which is the 13th most common in men and the 15th most common in women (World Cancer Research Fund International, 2020). The number of newly diagnosed cases of melanoma is anticipated to increase by 7.3% in 2024 (Siegel et al., 2024). Skin cancer occurrences have intensified due to South Africa's high ambient ultraviolet (UV) radiation environment (Gordon et al., 2016). Although white individuals are most susceptible to skin cancer, it can affect any individual regardless of their skin colour (Gordon et al., 2016). The highest occurrence of squamous cell carcinoma, basal cell carcinoma, and cutaneous melanoma is in white people, followed by coloured people, and has considerably lesser incidence in black and Asian/Indian populations (Norval et al., 2014; Ndlovu et al., 2022; Statistics South Africa, 2023). The most common type of skin cancer in black people is squamous cell carcinoma. Unfortunately, many black South Africans tend to delay seeking medical help, which can result in advanced-stage melanoma metastasis (Gordon et al., 2016; The Skin Cancer Foundation, 2024). This can lead to the growth of large cancerous tumours, which can cause significant facial trauma and deformity.

Maxillofacial trauma can affect an individual in significant ways. It disrupts several vital bodily functions essential for daily activities, such as breathing, eating, speaking, hearing, smelling, vision, and facial appearance (Yadav & Shrestha, 2017; Cristache et al., 2021; Pan et al., 2022). Treatment for maxillofacial trauma is challenging and complex since the face is an integral part of who people are and how they express emotions (De et al., 2023). A patient with maxillofacial trauma may need multiple constructive and plastic surgeries, which can lead to prolonged hospital stays (Al-Ali et al., 2022). The effective management of maxillofacial trauma requires coordinated care from various disciplines (Malik et al., 2017).

1.2 Problem statement

External maxillofacial prosthesis manufacture has been practiced for several decades. The traditional approach is creating wax replicas and employing carving methods (Sakib-Uz-Zaman & Khondoker, 2023). These traditional methods include several challenging processes and depend on a clinician's expertise and a designer's artistic aptitude (Ozdemir-Karatas et al., 2011; Cristache et al., 2021). These steps involve creating a duplication of the affected area by taking an impression of the area, modelling a clay or wax model of the anatomical structure(s) for which a prosthesis will be constructed, producing a mould of the clay or wax model, and finally fabricating the prosthesis in the desired material (Liacouras et al., 2011). A human likeness is hand-painted onto the prosthesis once it has been created. These traditional carving techniques are time-consuming and uncomfortable for patients, requiring them to be present for lengthy periods (Liacouras et al., 2011; Goyal et al., 2014).

Innovative approaches to the manufacturing of external maxillofacial prosthetics have been made possible by new and sophisticated technologies. Technologies such as digital imaging, computer-aided design (CAD), computer-aided manufacturing (CAM), and additive manufacturing (AM) have changed the landscape of external maxillofacial prosthesis reconstruction (Bai et al., 2014; Cruz et al., 2020c). Although AM technologies have been available for many years, they have become powerful and valuable tools in medical product development and prosthesis manufacturing (Petrovic et al., 2012). Furthermore, with newer materials and techniques available, external maxillofacial prostheses can be custom-made to fit a patient's unique anatomy with greater flexibility (Cruz et al., 2020b; Generalova et al., 2024). The implementation of medical image processing (MIP), CAD, and AM technologies has primarily replaced traditional carving techniques, resulting in less invasive and time-consuming procedures that are rapidly gaining popularity among medical practitioners (Petrovic et al., 2012; Cristache et al., 2021).

In South Africa, the effects of facial injuries and deformity are far-reaching, impacting not just the individual but also their extended family. The economic ramifications of this impact include lost pay, prolonged care for the individual while they cope with emotional stress, and the commitment of family resources (Yadav & Shrestha, 2017). These people frequently go to doctors in search of reconstructive procedures to enhance their physical appearance. Nevertheless, many South African patients, particularly those who receive government funding and who need external maxillofacial reconstruction, do not have access to these cutting-edge treatments. As a result, protocols and procedures that can help these patients get the appropriate medical care must be developed. Research is required to find less expensive production techniques that produce prostheses of acceptable quality, as these procedures can be costly. Despite the growing use of digital technologies in face prosthesis production, little is known about the low-cost process chains involved in facial prosthesis manufacturing (Jablonski et al., 2023).

1.3 Aim of this study

The external maxillofacial prosthesis production process requires an interdisciplinary team of professionals to generate digital data and produce a prosthesis. Engineers, designers, and medical professionals are among the experts participating in this process. A production process chain's primary activities are acquiring and processing digital data, designing a digital geometry, and manufacturing an external maxillofacial prosthesis. There are several options for every process chain event, some of which are more expensive than others. To increase the accessibility of these prostheses for patients with low financial resources, alternative and less costly choices for each step in the process chain are essential. However, as external maxillofacial prostheses are meant to be used by patients, the quality of medical items produced using alternative choices has to meet standard options with the International Organization for Standardization (ISO) certification. As such, the following was the primary research question that this project posed:

Which process chain(s) can produce external maxillofacial prostheses of acceptable quality at a price relevant to the South African demography?

To answer this question entailed testing several potential alternative process chains with pertinent digital technologies to provide patient-specific, high-quality, and affordable external maxillofacial prostheses.

To achieve the aim of this study, the following objectives were devised:

1. To conduct a comprehensive systematic review of the literature to identify commonly used MIP and CAD software with the potential to be tested in process chains for the manufacture of external maxillofacial prostheses;

2. To select and evaluate MIP software based on specific criteria related to software features and digital segmentation functionality;

3. To select and evaluate CAD software based on specific criteria related to software features and digital sculpting capabilities; and

4. To evaluate the selected MIP and CAD software as well as different data options within process chains to identify alternatives that compare favourably with industry-benchmark software, thereby enhancing patient access to external maxillofacial prostheses.

1.4 Summary of the methods

The aim of this research project was to design one or more cost-effective process chains for the manufacturing of affordable external maxillofacial prostheses, focusing on the use of low-cost software. This design science research (DSR) project sought practical solutions to real-world problems, aligning with the pragmatic approach of generating useful, actionable knowledge that has tangible outcomes. To systematically explore and validate affordable alternatives to existing industry-benchmarks, the study was structured into four distinct phases:

- **Phase 1: Selection of potential MIP and CAD software**

A comprehensive systematic review of the literature was conducted to identify commonly used MIP and CAD software with the potential for inclusion in the process chains. This phase established the foundation for software testing in the subsequent stages.

- **Phase 2: Evaluation of potential MIP software**

In this phase, computed tomography (CT) data from two human subjects were obtained and used to test the MIP software. The selection of software was based on specific criteria, particularly its features and segmentation functionality.

- **Phase 3: Evaluation of potential CAD software**

This phase focused on testing CAD software, selected according to its features and sculpting capabilities. The goal was to assess which software could adequately meet the requirements for designing external maxillofacial prostheses.

- **Phase 4: Identification of cost-effective process chains**

In the last phase, potential alternative process chains were produced. These process chains were evaluated using both surface scan and volumetric CT data. These models were assessed in comparison to those generated by the industry-benchmark. The investigation revealed alternate process chains that performed favourably in comparison to the industry-benchmark, offering a more accessible solution to produce external maxillofacial prostheses.

1.5 Limitations and delimitations

In this study, only the production process chains used for manufacturing external maxillofacial prostheses were considered, while the manufacturing of internal maxillofacial prostheses was excluded. Furthermore, the retention of prostheses was also excluded from this study. The AM of external maxillofacial prostheses was not evaluated in this study.

1.6 Value of study

A maxillofacial prosthesis can be costly because they are custom-made. Many South African patients depend on government support, and obtaining the expensive technologies required to produce these prostheses is difficult. The development of substitute, more affordable, and easily accessible manufacturing methods for maxillofacial prostheses will increase the number of individuals with facial disfigurements who can benefit from these transformative technologies. Reconstructive procedures boost patients' self-esteem, which facilitates their quicker reintegration back into society.

1.7 Ethical considerations

The Faculty Research and Innovation Committee of the Central University of Technology, Free State, granted the ethical clearance with the reference number FHES2017001 (Appendix A). Ethical clearance was also obtained and granted by the Health Sciences Research Ethics Committee of the University of the Free State in April 2018, with reference number UFS-HSD2018/0051/2404 (Appendix B). All the datasets collected with a CT and handheld structured light scanner were handled confidentially, and no identifying information was captured. All the participants were given a project information sheet to read before any data collection commenced (Appendix C). Written informed consent was obtained from all the participants on the day the datasets (CT volumetric dataset and handheld surface scan datasets) were captured (Appendix D and E).

1.8 Funding

This research project received financial support from the South African Research Chair's Initiative of the Department of Science and Innovation and National Research Foundation of South Africa (DST-NRF Innovation Doctoral Scholarship [Reference: SFH180602339062, Grant №: 118360]); the Council for Scientific and Industrial Research (CSIR), and Collaborative Programme in Additive

Manufacturing (CPAM) [Contract № CSIR-NLC-CPAM-15-MOA-CUT-01]; and the Central University of Technology, Free State Research Grant Scheme.

1.9 Layout of thesis

This thesis is arranged into eight chapters:

Chapter 1: Introduction to the study

This chapter provides background information about the research question, the problem statement, the aim of the study, and the main objectives performed to meet the aim.

Chapter 2: Literature review

This chapter provides an overview of the background for the research. Several topics are covered and discussed in this chapter. These topics include: the conventional carving techniques; the use of digital imaging technologies such as CT and magnetic resonance imaging (MRI) scanning, structured light scanning, and photogrammetry for digital data capturing; MIP and CAD software used to design digital geometries to manufacture maxillofacial prostheses; AM and 3D printing processes used to manufacture maxillofacial prostheses; and the future of maxillofacial prosthesis design and manufacturing.

Chapter 3: Study design and conceptual framework

In this chapter, the theoretical paradigms, research methodology, study design, and data collection methods are discussed.

Chapter 4: Medical image processing and computer-aided design software selection

In this chapter, a systematic review of the literature revealing the most relevant MIP and CAD software used when manufacturing maxillofacial prostheses is presented. This review was used to identify MIP and CAD software for inclusion in the study.

Chapter 5: Medical image processing software evaluation

In this chapter, the results of the evaluation of the MIP software are presented. These evaluations were based on software functionality, accuracy, and quality of the industry-benchmark software.

Chapter 6: Computer-aided design software evaluation

In this chapter, the results of the evaluation of the CAD software are presented. These evaluations were based on software functionality, accuracy, and quality of the industry-benchmark software.

Chapter 7: Alternative process chains for external maxillofacial prosthesis manufacturing

In this chapter, the results of the evaluation of the potential alternative process chains are compared with the industry-benchmark (control) process chain to select alternative process chains of acceptable quality at a price relevant to the South African demography.

Chapter 8: Discussion and conclusion

This chapter discusses the research findings, the study's limitations, and future research avenues.

The content of Chapters 3 and 4 was reported on in two accredited international conferences:

- Van Heerden, Fossey, Van der Walt, 2018. Maxillofacial prostheses production through computer-aided design and manufacturing technologies – review of state of the art. *RAPDASA 2018 Conference Proceedings*, pp.77 – 83. ISBN 978-0-620-80987-0. (Appendix F).

- Van Heerden and Fossey, 2019. Changing world of external maxillofacial prosthesis manufacturing. *RAPDASA 2019 Conference Proceedings*, pp.362 – 370. ISBN 978-0-6398390-0-4. (Appendix G).

Appendixes

A: Ethical approval from the Central University of Technology, Free State.

B: Ethical approval from the University of the Free State.

C: Project information brochure.

D: Participant consent form for collecting CT volumetric data.

E: Participant consent form for collecting surface scan data.

F: RAPDASA 2018 Conference Proceedings Article.

G: RAPDASA 2019 Conference Proceedings Article.

Chapter 2

Literature Review

2.1 Introduction to the literature review

External maxillofacial prostheses are critical advancements in medical technology that address the needs of people with facial disfigurements brought on by disease, trauma, or congenital conditions. Giving these people access to high-quality prosthetic solutions can significantly improve their quality of life by enhancing both their physical and mental appearance (Prakash et al., 2021).

The use of maxillofacial prostheses can significantly enhance a patient's quality of life and self-esteem by addressing deformities caused by trauma or surgical procedures. These prosthetic solutions play a crucial role in improving a patient’s overall well-being (De Caxias et al., 2019). Maxillofacial prostheses are categorised as either restorative or complementary, depending on their intended purpose. Maxillofacial reconstruction involves creating artificial replacements for both internal and external structures, including implants for the maxilla, mandible, oesophagus, cranial bones, palate, as well as the eyes, ears, and nose (De Caxias et al., 2019; Pawar et al., 2023). Typically, these extraoral prostheses are crafted from acrylic resin and silicone, tailored to fit the patient's unique facial structure (Pawar et al., 2023). They are secured and supported by various means, such as osseo-integrated implants, the remaining skin with or without adhesive, body cavities, and teeth (Fernández-Cedrón Bermejo et al., 2024). Over the years, a variety of techniques, materials, and clinical methods have been utilized in the design and manufacturing of maxillofacial prostheses.

Restorative prostheses are designed to replace lost bone or to correct facial deformities. They can be either placed internally within the tissue or externally as oral, ocular, or facial prostheses. According to De Caxias et al. (2019), complementary prostheses support plastic surgery patients prior to, during, and after the procedure, as well as during radiation treatments. The overall design of the prosthesis and the mechanical and physical characteristics of the materials employed play a major role in the outcome of prosthetic rehabilitation (Annamma et al., 2024). Research and development in this field are driven by the goal of finding a maxillofacial prosthetic material that closely resembles the appearance and properties of the afflicted tissues.

In the field of maxillofacial reconstruction, innovative technologies such as digital imaging, computer-aided design (CAD), computer-aided manufacturing (CAM), and additive manufacturing (AM) have opened novel approaches to producing external maxillofacial prostheses (Bai et al., 2014; Cruz et al., 2020a). AM technologies have evolved into powerful and valuable tools for medical product development and prosthesis manufacture (Petrovic et al., 2012). Furthermore, with new materials and processes, external maxillofacial prostheses can be tailored to a patient's specific anatomy with greater flexibility (Cruz et al., 2020c). The use of medical image processing (MIP), CAD, and AM technologies has largely superseded conventional carving processes, resulting in less invasive and time-consuming treatments that are rapidly gaining appeal among medical professionals (Petrovic et al., 2012).

2.2 Past techniques used in maxillofacial prosthesis design and manufacturing

A prosthesis is an artificial device that replaces missing anatomical parts in the human body. The term prosthesis is derived from the Greek word '*prostithenai,*' meaning addition, application, or attachment (Muneer & Pearce, 2016). The earliest discovery of facial prostheses production to reconstruct facial deformities was in 3000 B.C.E. during the Egyptian dynasty, and it was made from various materials found throughout that time (Dostalova et al., 2011). During the sixteenth century, more in-depth research on maxillofacial prostheses was undertaken, and the evidence was documented. The famous

French surgeon Ambroise Paré (1510 - 1590) first described nasal prostheses made from gold, silver, and "paper mâché" (Dostalova et al., 2011). These prostheses were held in place on the face with a string tied around the patient's head.

During the 20th century, a major revolution in maxillofacial prosthesis manufacturing was the use of silicone. Barnhart, in 1960, pioneered the use of silicone materials for the creation of maxillofacial prostheses (Mitra et al., 2014). Barnhart was among the first to explore its applications in the field of prosthetics. His work demonstrated the potential of silicone rubber as a material for fabricating maxillofacial prostheses, which was a significant advancement in the field. The use of silicone offered improved biocompatibility, durability, and flexibility, making it a superior material for facial reconstruction and prosthetic devices. Its success in providing a more natural appearance and enhancing patient comfort led to further research into alternative materials such as polyurethane (Gonzalez, 1978), phenylene (Lewis & Castleberry, 1980), and modified polysiloxane elastomers (Lontz, 1990).

Successful facial rehabilitation hinges on a well-devised treatment plan that integrates both surgical and prosthetic components. However, practitioners often overlook fundamental principles of prosthetic design (Gowd et al., 2017). In the late 19th century, Claude Martin pioneered a technique for creating facial prostheses using living bone and muscle, involving the surgical removal of the maxilla and mandible to facilitate complex facial reconstructions. While this approach remains in practice today, it often led to significant trauma and deformity at the donor site, as well as prolonged recovery times (Dostalova et al., 2011). Despite advancements in surgical interventions to address facial trauma and deformities, aesthetic outcomes can still be unsatisfactory, frequently necessitating multiple procedures (Annamma et al., 2024). Thus, a combination of surgical reconstruction and external prostheses is essential for restoring both aesthetics and functionality for patients with facial deformities.

Prosthetic rehabilitation has emerged as a compelling alternative to major surgery, particularly for patients with severe functional and aesthetic defects (Leonardi et al., 2008). This approach not only aids in the patient's psychological recovery but also fosters social acceptance and reintegration (Leonardi et al., 2008; Goiato et al., 2009). The creation of maxillofacial prostheses typically involves a collaborative effort among maxillofacial surgeons, implantologists, prosthodontists, and clinical technicians. The early 20th century saw the introduction of synthetic polymer prostheses, which significantly improved performance and ultimately replaced natural materials that had been in use for millennia (Li et al., 2023). These prostheses can be pre-fabricated and applied immediately post-surgery, offering protection to the surgical cavity.

2.3 Traditional techniques used in maxillofacial prosthesis design and manufacturing

Traditionally, the manufacturing of maxillofacial prostheses has predominantly involved subtractive processes. These methods involve removing excess material from a preliminary three-dimensional model to create the desired artefact, with the techniques varying based on the specific type of disfiguration being addressed (Al Mardini et al., 2005; Zardawi, 2012). Typically, external maxillofacial prostheses are crafted by hand, involving the carving of the missing anatomical features in wax to create a mould into which pigmented silicone elastomer is poured (Jindal et al., 2018). This conventional method comprises multiple intricate steps and is labour-intensive, relying significantly on the artistic skills of maxillofacial technicians and clinicians (Ozdemir-Karatas et al., 2011; Cristache et al., 2021; Jablonski et al., 2021).

The process begins with taking a precise impression of the area needing a prosthesis. The selection of appropriate impression materials depends on the defect's location, size, and the presence of any undercuts. Materials range from flexible substances such as hydrocolloid alginates and elastic silicone polymers to rigid ones such as plaster of Paris (Zardawi, 2012). While plaster of Paris can capture fine details, its rigidity poses challenges when severe undercuts are present, potentially damaging soft tissues or breaking the impression material during removal. Consequently, flexible, or elastic materials are preferred in cases of significant undercuts.

Pre-surgical impressions preserve the details of the area to be replaced. A positive stone plaster model is cast from the negative impression, serving as a reference for sculpting the anatomy in wax or clay. This model is meticulously carved to replicate the natural morphological details (Zardawi, 2012). Maxillofacial technicians often create these details using photos, pre-operative moulds, or similar anatomical structures from the patient's relatives. The wax or clay model's fit is then verified on the patient before being transferred into the final silicone material through conventional flasking methods. After removing the wax and lubricating the cast, silicone rubber mixed with skin colouring agents is applied, with the prosthesis being finished by hand to match the patient's skin tone (Zardawi, 2012; Zardawi et al., 2015a; Pawar et al., 2023).

Despite its widespread use, traditional maxillofacial prosthesis manufacturing has several limitations. It is an expensive, time-consuming process requiring significant technical skill (Jablonski et al., 2023). Patients often experience discomfort during the impression-taking process due to the weight of the impression material and, in some instances, they have trouble breathing due to the impression material's obstruction in the airway (Feng et al., 2010). Additionally, inaccuracies can occur due to soft-tissue compression, reflex movements, or lack of structural support during impression-taking (Jablonski et al., 2021). Over time, these prostheses deteriorate, with changes in colour and consistency leading to mismatches with the patient's skin. Prolonged contact with human skin and mucosa, along with exposure to environmental factors and daily handling, accelerates this degradation (Zardawi et al., 2015b).

2.4 New technological advances in prosthesis design and manufacturing

The manufacturing of a maxillofacial prosthesis involves a multi-step process that integrates various advanced technologies, including medical imaging, MIP, CAD, and AM. In this process, a prosthesis is produced that is anatomically accurate, aesthetically pleasing, and functionally effective. The process is complex and requires the use of cutting-edge technologies to create custom, high-quality prosthetic devices. Each step, from data acquisition to final fitting, is critical in ensuring that the prosthesis meets the functional and aesthetic needs of the patient. The key steps include data acquisition, image processing and segmentation, prosthesis design, prosthesis manufacturing, and prosthesis fitting and adjustment.

2.4.1 Data acquisition

To acquire anatomical medical images in the initial step of the process involves acquiring high-resolution medical images of the affected area. In recent decades, advancements in medical imaging have been instrumental in accurately capturing intricate details of human anatomy beyond traditional two-dimensional (2D) images (Hussain et al., 2022; Suresh et al., 2022). Digital Imaging and Communications in Medicine (DICOM) files obtained from computed tomography (CT) and magnetic resonance imaging (MRI) are the world's leading standard for medical imaging information (Kamio et al., 2020). The use of DICOM files has revolutionised the visualisation of clinical images in three-dimensions (3D), leading to the widespread use of volumetric models (Hussain et al., 2022).

Besides acquiring CT or MRI images, surface scanning can be employed to capture the external geometry of the patient's face. Handheld scanners, such as the Artec Spider, use structured light or laser technology to create a detailed 3D model of the facial surface (Erolin, 2023; Schipper et al., 2024). These tools are valuable for generating high-quality datasets with fine surface details and even colour, which are essential for the effective assessment and planning of prostheses design and manufacturing (Farook et al., 2020; Erolin, 2023). Surface scanners, typically handheld laser, or structured light scanners, are portable and fast, making them advantageous for capturing digital data. High-end scanners produce highly accurate results in terms of colour and texture capture with high mesh accuracy (AlShaibani et al., 2021; Unkovskiy et al., 2022; Schipper et al., 2024). However, they have limitations in capturing extremely dark, transparent, or shiny surfaces and do not obtain internal features such as CT or MRI scans (Paxton et al., 2022; Erolin, 2023).

Another technology that is also used to capture surface anatomical data is photogrammetry. Photogrammetry involves taking numerous 2D images of an object from various angles to produce a 3D reconstruction. This technology is widely accessible and can be used with smartphones and free software (Farook et al., 2022; Erolin, 2023). One of its primary advantages is its ability to capture the colour of the object being scanned and produce high-quality texture maps, making it a preferred choice for creating detailed 3D models (Unkovskiy et al., 2022). However, photogrammetry may struggle to adequately capture translucent and glossy surfaces, as well as holes and undercuts (Paxton et al., 2022).

2.4.2 Image processing and segmentation

Medical image processing software plays a critical role in the visualisation, analysis, and interpretation of medical imaging data. These software applications convert raw imaging data from modalities such as CT, MRI, and ultrasound into meaningful visualisations that assist in diagnosis, treatment planning, and research (AlShaibani et al., 2021). The processing involves various techniques such as image reconstruction, segmentation, registration, and enhancement to produce clear and accurate 3D models of anatomical structures (Zhou et al., 2016). The segmentation process involves delineating the region of interest (ROI), segmenting stacked 2D images, and then converting them into a 3D model format, typically the stereolithography (STL) file format, which is the most used file format for 3D printing (Kamio et al., 2020). This conversion is necessary to bridge the gap between medical imaging and 3D modelling using CAD software (Kamio et al., 2020; Paxton et al., 2022). Although CT and MRI scans capture both internal and external features, they do not record colour information, which can make manual segmentation time-consuming (Hussain et al., 2022).

2.4.3 Prosthesis design

After segmenting the ROI, CAD software was used to design the 3D model of the prosthesis. These tools facilitate the translation of anatomical data into functional designs that can be manufactured using various techniques, including 3D printing, and milling (Zhou et al., 2016; AlShaibani et al., 2021). The software is used for detailed sculpting, texturing, and refinement of the prosthesis model, ensuring that it matches the patient's anatomy accurately and aesthetically (Pilgway, 2021; Pixologic, 2021). The digital model is customised to ensure a proper fit and functionality. This may involve virtual fitting sessions where the prosthesis model is superimposed onto the patient's digital facial model to check for alignment and comfort (Blender Foundation, 2021).

2.4.4 Prosthesis manufacturing

After the design step, AM technologies are used to print the finished 3D model. Depending on the production strategy, this step may involve printing negative moulds that are later used for casting or directly printing the prosthesis itself (Unkovskiy et al., 2018). For negative mould printing, materials such as high-strength resins or thermoplastics are typically employed to ensure precision and durability during the casting process. Once the mould is ready, biocompatible silicone or other suitable polymers are cast into it to create the prosthesis (Das et al., 2023). Alternatively, direct 3D printing of the prosthesis can be done using biocompatible materials that offer flexibility and skin-like texture (Unkovskiy et al., 2018). Following printing, the prosthesis goes through post-processing procedures such as cleaning, curing, and finishing (Generalova et al., 2024). This could entail applying skin-like textures and colours to match the patient's complexion in addition to making manual modifications to improve the fit and appearance (Zardawi, 2012).

2.4.5 Prosthesis fitting and adjustment

The newly produced prosthesis is finally fitted to the patient to check proper aesthetic alignment and comfort. Any necessary adjustments are made to ensure that the prosthesis is functional and satisfactory (Jablonski et al., 2021). Once the trial fitting is successful, the prosthesis is finalised and delivered to the patient. Instructions for care and maintenance are provided to ensure the longevity and effectiveness of the prosthesis (Pawar et al., 2023; Chander et al., 2024).

2.5 Advances in medical software

Advancements in the development of advanced medical software have transformed the process chain for prosthesis manufacturing. Software provides a robust foundation for digital prosthesis design and manufacturing of maxillofacial prostheses. The current industry-benchmark for medical imaging and processing software is Mimics, developed by Materialise (Bertolini et al., 2021; Buonamici et al., 2022). Mimics is widely recognised for its robust capabilities in handling complex segmentation tasks, converting DICOM files into 3D models, and preparing models for 3D printing (Mandolini et al., 2022). Its applications span across orthopaedics, cardiovascular, cranio-maxillofacial surgery, and other medical fields. The software is praised for its precision and the quality of its outputs, which is critical for creating patient-specific prostheses, making it a preferred choice in clinical and research settings (Marro et al., 2016; Nikitichev et al., 2018).

The current industry-benchmark CAD software in the medical field is Geomagic Freeform, developed by 3D Systems, Inc. It is renowned for its powerful digital sculpting and design tools, which allow for the creation of highly detailed and anatomically accurate models. Geomagic Freeform supports a range of file formats and integrates well with other software and hardware used in medical manufacturing, making it a versatile tool for maxillofacial prosthesis design and other applications (Memon et al., 2020). The integration of CAD software into prosthesis manufacturing has transformed the field, enabling the production of highly customised, patient-specific prostheses on demand with high repeatability.

2.5.1 Strengths and limitations of the industry-benchmarks

Mimics is known for its advanced capabilities in processing and analysing medical images, making it a valuable tool in surgical planning and anatomical modelling. On the other hand, Geomagic Freeform excels in complex 3D design and haptic modelling, providing exceptional versatility in the creation of highly detailed and personalised prostheses. The main strengths and weaknesses of these industry-benchmark programs are listed in Table 2.1. The table outlines the unique features of each software program and considers the advantages and limitations within external maxillofacial prostheses manufacturing.

Table 2.1 Key strengths and weaknesses of the industry-benchmark software

Key strength	Description	Reference
Precision and accuracy	Both Mimics and Geomagic Freeform offer high precision. Mimics excels in converting medical imaging data into accurate 3D models, while Geomagic Freeform provides detailed sculpting tools that are essential for creating anatomically accurate prostheses.	Marro et al. (2016)
Comprehensive toolsets	Mimics includes a range of tools for segmentation, analysis, and 3D printing preparation. Similarly, Geomagic Freeform offers advanced sculpting, surface modelling, and voxel-based design tools that enhance the design process.	Nikitichev et al. (2018)
Integration and compatibility	Both software applications integrate well with other systems and devices used in medical imaging and manufacturing,	Memon et al. (2020)

Key weakness	Description	Reference
	facilitating a seamless workflow from image acquisition to final product creation.	
Cost	One of the significant limitations of these industry-benchmarks is their high cost. The expense associated with purchasing and maintaining these software solutions can be prohibitive, especially for institutions and practitioners in low-resource settings.	Marro et al. (2016)
Complexity	The advanced features and comprehensive toolsets come with a steep learning curve. Users often require extensive training to effectively use all the capabilities of Mimics and Geomagic Freeform, which can be a barrier for new users.	Nikitichev et al. (2018)
Resource requirements	Both software applications require high-performance computing resources to operate efficiently, which can be another barrier for institutions and practitioners with limited technological infrastructure.	Marro et al. (2016)

2.5.2 MIP software alternatives to industry-benchmark

Medical image and processing software play a key role in transforming raw image data into detailed 3D models essential for diagnostic and therapeutic purposes. The industry-benchmark Mimics has traditionally dominated the field because of its accurate and robust qualities (Bertolini et al., 2021; Buonamici et al., 2022). The software supports the creation of custom prostheses by allowing for the direct translation of anatomical models into designs that can be 3D printed (Zabala-Travers, 2021). Research has demonstrated that the use of Mimics in the construction of maxillofacial prostheses leads to high accuracy and faster prosthesis production (Buffinton et al., 2023). However, the investigation into more affordable and accessible alternatives has become necessary because of the high cost and complexity of this software (Mandolini et al., 2022; Yap Abdullah et al., 2024). There are several MIP software alternatives that hold promise for providing comparable functionality to Mimics that could be considered for prosthesis manufacturing (Table 2.2). Each software has unique strengths that cater to different aspects of medical image processing, making them suitable for various clinical and research applications.

Table 2.2 Alternative MIP software to the industry-benchmark

Software	Description
3D Slicer	3D Slicer is an open-source software platform for the analysis and visualisation of medical images. It is widely used in research because of its flexibility and extensibility through plugins. *Versatility and cost-effectiveness*: As an open-source platform, 3D Slicer is accessible and cost-effective. It supports various modules for image segmentation, 3D modelling, and surgical planning, all of which are critical in the design of prostheses (Fedorov et al., 2012). *Custom prosthesis manufacturing*: The software's ability to integrate with other open-source tools and 3D printing technologies has made it an asset in the manufacturing of custom prostheses. Researchers have highlighted its use in the design of craniofacial implants, where precise anatomical replication is required (Tantisatirapong et al., 2023).
Materialise 3-Matic	Materialise 3-Matic is another key tool from Materialise, designed to enhance the capabilities of Mimics by allowing further design and optimisation of 3D models. *Advanced mesh processing*: 3-Matic is particularly strong in mesh processing and design optimisation. This makes it a valuable tool in prosthesis manufacturing, where the refinement of mesh structures is crucial for creating durable and lightweight prostheses (Srivastava et al., 2024). *Customisation and fit*: The software allows for detailed surface editing and texturing, enabling the customisation of prostheses to better match the patient's skin texture and appearance. Studies have shown that this capability is essential in creating prostheses that not only fit well but also meet the aesthetic needs of patients (Mian et al., 2022).
InVesalius	InVesalius is a free, open-source MIP software developed by the Renato Archer Information Technology Centre in Brazil. It is designed to assist in the visualisation

	and reconstruction of anatomical structures from DICOM files (Amorim et al., 2015). InVesalius supports multiple imaging modalities, including CT and MRI, and it offers a user-friendly interface that makes it accessible to both novices and experienced users. One of its key strengths is its effective segmentation tools, which allow for precise delineation of anatomical regions. Additionally, InVesalius can export models in various formats, such as *STL*, which is essential for 3D printing and further CAD processing (Amorim et al., 2017).
ITK-SNAP	ITK-SNAP is a user-friendly, open-source software application that focuses on the segmentation of anatomical structures in medical images. It uses a semi-automatic segmentation approach that combines manual editing with automation. This hybrid approach facilitates the accurate segmentation of complex anatomical features with minimal user intervention. ITK-SNAP is particularly useful for research applications and has been widely adopted because of its intuitive interface and robust performance (Yushkevich et al., 2016).
OsiriX	OsiriX is a comprehensive DICOM viewer and MIP software designed specifically for Mac OS. It provides a range of advanced imaging tools, including 2D and 3D reconstructions, surface rendering, and volumetric analysis. OsiriX is available in both a free Lite version and a more advanced MD version, which offers additional features tailored for clinical use. Its cutting-edge visualisation capabilities and support for a wide array of imaging modalities are advantageous (Spiriev et al., 2017).
Amira	Amira is a high-end, commercial software application that combines MIP and visualisation capabilities. It is widely used in biomedical research for tasks such as image segmentation, visualisation, and analysis. Amira supports a broad range of file formats and offers advanced features such as multi-modal image registration and quantitative analysis. While it is a commercial product, Amira is often considered because of its comprehensive toolset and ability to handle large, complex datasets (Buffinton et al., 2023).

2.5.3 CAD software alternatives to industry-benchmark

In the design and manufacturing of external maxillofacial prostheses, CAD software is indispensable.

The industry-benchmark software Geomagic Freeform has set a high bar due to its advanced sculpting capabilities, intuitive haptic feedback system, and robust modelling tools (Tanveer et al., 2023; Sharma et al., 2023; Farsil et al., 2024). However, the high costs and specific hardware requirements of such premium software pose accessibility challenges. There are several CAD software alternatives that offer comparable features and functionalities, that may provide a cost-effective solution for the design and production of maxillofacial prostheses (Memon et al., 2020; Das et al., 2023). Each software offers unique strengths that cater to different aspects of the design process, making them suitable for various clinical and research applications (Table 2.3). The choice of software often depends on the specific application, the level of customisation required, and the resources available.

Table 2.3 Alternative CAD software to the industry-benchmark

Software	**Description**
SolidWorks	SolidWorks is a widely used CAD software in various engineering disciplines, including biomedical engineering. Its robust modelling capabilities and user-friendly interface has made it a popular choice for designing prosthetic components. *Parametric design*: SolidWorks excels in parametric design, allowing for the creation of complex, adjustable models that can be easily modified to fit the unique anatomical structures of patients (Vanaclocha-Saiz et al., 2022). *Simulation and analysis*: The software has various simulation tools, such as stress analysis and fluid dynamics, which are crucial for ensuring that prostheses are both functional and durable under real-world conditions. Research has shown that using SolidWorks for the design and testing of prosthetic limbs can improve their performance and longevity (Mondal et al., 2023; Torres-Sanmiguel, 2022).
Autodesk Fusion 360	Autodesk Fusion 360 is another powerful CAD tool that combines design, engineering, and manufacturing capabilities in a single platform. Its cloud-based nature and accessibility have made it a popular choice for both professionals and educational institutions. *Integrated workflow*: Fusion 360 offers an integrated workflow that spans the entire design process, from conceptual sketches to final manufacturing. This seamless integration is particularly beneficial in prosthesis manufacturing, where design changes must be rapidly implemented and tested (Górski's et al., 2022).

	Collaboration and accessibility: As a cloud-based tool, Fusion 360 supports collaborative design and remote access, which is advantageous in multidisciplinary projects involving clinicians, engineers, and designers. This feature has been highlighted in the design of prosthetic hands, where team collaboration is critical (Manero et al., 2019).
Rhinoceros (Rhino)	Rhinoceros, commonly known as Rhino, is a CAD software that excels in freeform modelling and is particularly favoured in the design of organic shapes and complex surfaces, making it well-suited for maxillofacial prostheses. *Surface modelling*: Rhino's strength lies in its ability to create highly detailed, organic surfaces through its NURBS (Non-Uniform Rational B-Splines) modelling capabilities. This is essential in designing facial prostheses that need to match the intricate contours of the human face (Kim et al., 2011). *Customisation and flexibility*: Rhino is highly customisable through various plugins, such as Grasshopper, which allows for parametric design and automation of complex tasks. This flexibility has been leveraged in the creation of custom prostheses, where precise fitting and aesthetics are critical (Guo et al., 2024).
Autodesk Inventor	Autodesk Inventor is a professional-grade CAD software known for its mechanical design capabilities. It is commonly used in the design and manufacturing of prosthetic components, particularly in complex mechanical systems such as prosthetic joints. *Mechanical design and simulation*: Inventor provides advanced tools for the design and simulation of mechanical systems, which are essential in creating functional prosthetic limbs. Its dynamic simulation capabilities allow for the testing of prosthetic joints under various conditions, ensuring optimal performance (Górski et al., 2024). *Assembly modelling*: The software's ability to manage large assemblies is beneficial in the design of modular prosthetic systems, where different components must be designed to work together seamlessly. Studies have shown that using Inventor in the design of prosthetic hands can enhance their modularity and ease of customisation (Saberpour et al., 2023).
PTC Creo	PTC Creo is a powerful CAD software that offers a suite of tools for parametric and direct modelling, as well as simulation and analysis. It is particularly known for its robust feature set in mechanical design. *Parametric and direct modelling*: Creo combines parametric and direct modelling, allowing designers to quickly create and modify prosthetic designs. This flexibility is

	essential in prototyping, where changes are often needed based on patient feedback (Raju Jithin, 2024). *Advanced simulation*: Creo offers comprehensive simulation tools that can analyse the mechanical properties of prostheses, such as stress distribution and material behaviour under load. This ensures that prostheses are not only functional but also durable (Mahajan, 2018).
3D Coat	3D Coat is a versatile and powerful CAD software that excels in voxel sculpting, UV mapping, and retopology. Its key features include dynamic tessellation, which allows for detailed sculpting without significant performance loss, and auto-retopology, which simplifies the creation of clean, animatable meshes from sculpted models. 3D Coat is widely praised for its intuitive user interface and extensive toolset, making it accessible to both beginners and experienced designers. Its ability to import and export in various file formats, including *STL*, *OBJ*, and *FBX*, enhances its compatibility with different 3D printing and modelling workflows (Pilgway, 2021).
ZBrush	ZBrush, developed by Pixologic, is known for its sculpting and painting capabilities. It employs a unique "pixol" technology that combines 3D modelling and 2D painting attributes, allowing for adding intricate details and textures. ZBrush is particularly favoured in industries such as gaming, film, and medical modelling, because of its high-resolution sculpting tools and efficient workflow. The software supports a wide range of file formats and includes features such as DynaMesh for dynamic tessellation, ZRemesher for automatic retopology, and advanced rendering options. ZBrush's strong community and extensive tutorials make it a robust alternative to Geomagic Freeform (Pixologic, 2021).
Blender	Blender is a free, open-source CAD software that offers a comprehensive suite of tools for modelling, sculpting, animation, and rendering. Its powerful sculpting features, including dynamic topology and multi-resolution modelling, make it a viable option for creating detailed anatomical models. Blender's extensive add-ons and community support further enhance its capabilities, making it a flexible tool for both artistic and technical applications. The software's integration with various 3D printing workflows and support for multiple file formats, including *STL*, *OBJ*, and *PLY*, provide a seamless transition from digital design to physical production (Blender Foundation, 2021).
Meshmixer	Meshmixer, developed by Autodesk, is a free CAD software specifically designed for working with 3D meshes. It is particularly useful for preparing models for 3D

	printing, with features such as automatic repair, hollowing, and support generation. Meshmixer also offers robust sculpting tools and an intuitive interface, making it accessible for quick edits and prototyping. Its ability to handle complex mesh operations efficiently makes it a practical alternative for creating maxillofacial prostheses, especially in resource-constrained environments (Autodesk Inc., 2021).
FreeCAD	FreeCAD is an open-source parametric CAD software that supports a wide range of design and engineering applications. It offers robust modelling tools, including a feature-based approach that allows for easy modifications and iterations. FreeCAD's modular architecture enables users to extend its functionality through plugins and custom scripts, making it highly adaptable to specific needs (FreeCAD Project, 2021).

2.6 Additive manufacturing

Additive manufacturing, commonly known as 3D printing, has revolutionised the field of prosthesis manufacturing. In contrast to subtractive manufacturing where material is removed from a solid block, AM adds material only where it is required. Using CAD software, a 3D digital computer model is created, and material is subsequently added layer by layer to make the tangible object (Tanveer et al., 2023). By building an object layer by layer from a digital model, complex geometries that are frequently impossible or prohibitively expensive to achieve with typical subtractive manufacturing techniques can be created (Gibson et al., 2015; Gibson et al., 2021). According to Gibson et al. (2015), this capability is necessary for designing intricate and anatomically accurate prostheses. Because of its versatility and ability to work with a variety of materials, including metals, ceramics, and polymers, this procedure can be used to create a wide range of prosthetic devices (Vennam et al., 2024).

In prosthesis manufacturing, AM plays a critical role in several stages of the production process. There are various benefits associated with AM. It allows for the rapid prototyping and customisation of prosthetic devices tailored to the specific anatomical and functional needs of patients (Pirozzi et al., 2023). This customisation is particularly important in maxillofacial prostheses, where the fit and appearance must be precisely matched to the patient's unique facial structure (Mazzoli, 2013; Sharma et al., 2023; Kouhi et al., 2024). This technology enables the quick production of prototypes, which can be tested and refined before creating the final prosthesis. This accelerates the design process and reduces the time from concept to final product. The additive nature of AM results in significantly less waste and can be more cost-effective (Pirozzi et al., 2023; Amaya-Rivas et al., 2024). Compared to traditional manufacturing techniques, AM can be more affordable for small-scale production and customised prostheses, especially when considering the reduction in waste and the elimination of expensive tooling and moulds (Tofail et al., 2018; Kouhi et al., 2024).

Several disadvantages are associated with AM. Even though AM can employ a wide range of materials, compared to traditional methods, the selection of materials appropriate for prosthesis manufacturing is currently relatively limited (Rajaguru et al., 2020; Ornaghi et al., 2023). Additionally, it is possible that 3D printed materials' mechanical qualities differ from those of conventionally created materials (Bogue, 2013). To obtain the appropriate smoothness and intricacy, further post-processing may be needed for the surface finish of 3D printed products. Factors such as print resolution and layer thickness can also have an impact on the end product's accuracy (Gibson et al., 2015; Gibson et al., 2021). High-quality 3D printers and the associated software can be expensive, representing a significant initial investment for facilities looking to implement AM (Chen et al., 2021). The relatively new nature of AM in medical applications means that there are ongoing challenges related to regulatory approval and the standardisation of materials and processes (Tofail et al., 2018; Korpela et al., 2021).

2.7 Methodologies for evaluating MIP and CAD Software

Evaluating MIP and CAD software involves a systematic approach to ensure that the selected tools meet the specific requirements for external maxillofacial prosthesis manufacturing. Software is evaluated mainly in terms of its specific software features, capabilities, and performance in process chains. The key criteria to consider when evaluating MIP and CAD software for maxillofacial prosthesis design are presented in Table 2.4.

Table 2.4 Key criteria to consider when evaluating MIP and CAD software

Criterion	Description	Reference
Segmentation accuracy	The ability of MIP software to accurately segment anatomical structures from medical images is critical. Accurate segmentation ensures that the prosthesis fits well and functions correctly.	Jablonski et al. (2023)
Usability and workflow integration	The software should be user-friendly and integrate seamlessly into existing clinical workflows. This includes compatibility with other software and hardware used in the prosthesis manufacturing process.	Binhuraib et al. (2023)
Customisation and sculpting capabilities	For CAD software, the ability to customise and digitally sculpt detailed anatomical features is essential. This involves tools for precise modelling, texturing, and adjustments to ensure the prosthesis meets aesthetic and functional requirements.	Parthasarathy (2014)
Cost-effectiveness	Given the study's focus on finding cheaper alternatives, the cost of software and associated hardware is a significant consideration. The selected software should provide a balance between cost and functionality.	Rengier et al. (2010)
MIP and CAD in process chains		
Benchmarking against industry-benchmarks	The selected software combinations are compared against established industry-benchmarks, such as Mimics for MIP and Geomagic Freeform for CAD. This comparison helps in assessing the performance and quality of the alternative software.	Ma et al. (2024) Yap Abdullah et al. (2024)
Performance metrics	Metrics such as segmentation accuracy, model fidelity, processing time, and user satisfaction are used to evaluate the performance of each process chain. These metrics	Chen et al. (2024)

	provide quantitative and qualitative data to support the evaluation.

2.8 Low-cost prosthesis manufacturing

When investigating low-cost prosthesis manufacturing, it is essential to improve affordability and accessibility, particularly in areas with limited resources. Several case studies have documented the successful use of alternative technologies in prosthesis manufacturing. Notably, the adoption of 3D printing and open-source software has been a game-changer in producing affordable prosthetics (Alturkistani et al., 2020). The e-NABLE project uses 3D printing to create prosthetic hands for children (Manero et al., 2019; Parry-Hill, 2019). Volunteers have manufactured working prosthetics for a tenth of the cost of standard devices using inexpensive 3D printers and free design files. According to Parry-Hill (2019), the effort has shown efficacy in offering customised solutions that are reasonably priced and flexible enough to accommodate children's developmental stages. The Project Daniel, initiated by Not Impossible Labs, has effectively used 3D printing to create prosthetic limbs in South Sudan, a country devastated by conflict. The initiative has enabled locals to produce and maintain prosthetics by establishing local 3D printing laboratories, providing community members with training, and providing low-cost, and decentralised manufacturing (Tria, 2023). The Jaipur Foot Project is renowned for producing prosthetics with high-functionality at a reasonable cost. The organisation makes use of simple yet efficient materials and methods. Their prosthetics are designed to meet the needs of amputees in underdeveloped nations, offering low-cost mobility and improving quality of life (Bhargava, 2019). Although the use of digital technology in the production of facial prostheses is becoming more popular, little is known about the low-cost process chains for the manufacturing of facial prostheses (Jablonski et al., 2023).

Comparative research has provided insight into the efficacy of less expensive prosthetic systems in comparison to more expensive counterparts. These studies frequently point out the advantages and disadvantages of each strategy. The costs and results of 3D-printed prosthetic hands were compared with those of commercially available devices in a study conducted by (Wendo et al., 2022). The findings indicated that while high-cost prosthetics offer superior durability and aesthetics, low-cost 3D-printed alternatives provide comparable functionality at a significantly lower price, making them a viable option for many users (Alturkistani et al., 2020; Abbady et al., 2022). A study by Copeland et al. (2022) compared user satisfaction of 3D-printed prosthetics to conventional prosthetics. The study concluded that while traditional prosthetics were preferred for their robustness, 3D-printed models scored higher in terms of affordability and customisation, making them particularly appealing to users with budget constraints. A comparison study by Engdahl et al. (2024) assessed the functional performance of high-cost myoelectric prosthetics versus low-cost body-powered prosthetics. The results highlighted that while high-cost devices offer advanced features and smoother operation, low-cost prosthetics were effective in basic daily functions and were more accessible to a broader population. These studies have shown that integrating these technologies can significantly enhance the efficiency and scalability of prosthesis production (Barrios-Muriel et al., 2020).

2.9 Implications of alternative low-cost software

The use of alternative MIP and CAD software has significant implications for the manufacturing of external maxillofacial prostheses. An important factor to consider is the quality of a prosthesis made with alternative software. Research has demonstrated that MIP and CAD software that is free and open-source can produce results that compare well with industry-benchmarks in terms of accuracy and capability. Farook et al. (2021) demonstrated that prostheses designed using open-source software such as Blender and Meshmixer exhibited high precision in anatomical detail and fit, comparable to those created with high-cost proprietary software. Patient satisfaction with prosthetics depends critically on their aesthetic qualities, including texture and colour matching. According to Dong et al. (2024), lower-cost software can effectively produce prostheses with a high degree of aesthetic detail, although some manual finishing may be required to achieve optimal results. It is also notable that alternative software works with different kinds of materials used in 3D printing, which is important because printing materials can influence the prosthesis's durability and appearance (Rengier et al., 2010).

Alternative software can drastically cut costs associated with prosthetic manufacturing, making these solutions more affordable in environments where resources are limited. Substantial investment costs, such as software licenses and specialised hardware, are associated with the industry benchmarks such as Mimics and Geomagic Freeform. On the other hand, inexpensive or free alternative software significantly lowers up-front costs (Bibb et al., 2015). Ongoing costs associated with maintenance, updates, and training are lower for alternative software (Ventola, 2014). Open-source software often has a large support community, reducing the need for expensive proprietary support services.

A comprehensive comparison of process chains for the manufacturing of maxillofacial prostheses is notably absent in the current literature. While some studies have examined isolated elements of the process chain, such as Yap Abdullah et al. (2024), who compared open-source MIP software against commercial software for 3D skull reconstruction, most analyses do not extend to full, step-by-step process chain evaluations. Farook et al. (2020) provided valuable insight by comparing two complete process chains, one using commercial and the other using open-source software, and found that the open-source chain could achieve aesthetically and volumetrically comparable results. However, these studies do not offer a thorough, comparative exploration of each stage within the process chain and also do not include sculpting CAD software.

2.10 Technological and financial barriers in South Africa

The accessibility of medical prostheses in South Africa is hindered by numerous challenges, including limited availability, high costs, and inadequate healthcare infrastructure. Ennion and Johannesson (2018) stated that there are large differences in the nation's access to prosthetic services, with underserved and rural areas being disproportionately impacted. Because prosthesis manufacturing facilities are unevenly distributed and frequently concentrated in urban areas, rural residents have few options to obtain essential prosthetic devices. In addition to making accessibility even more problematic, traditional prosthesis manufacture is expensive (Ennion & Johannesson, 2018; Mduzana et al., 2020). Conventional techniques are more expensive overall because they require specialised materials and skilled technicians in addition to being labour-intensive (Jablonski et al., 2023).

The patients' own financial constraints are also important. Since many people who need prostheses originate from lower-income families, the expense of these devices may be prohibitive for them. Because of this financial obstacle, patients frequently postpone or abandon therapy, which has a negative impact on their physical and mental well-being (Kharade, 2020), lowers their quality of life, and increases their reliance on others for everyday tasks (Reis et al., 2018; Sarwer et al., 2022). By implementing cost-effective prosthesis manufacturing solutions can significantly reduce the costs associated with prosthesis design and manufacturing, and enhance accessibility for a broader population, particularly in rural and underserved areas (Ennion & Johannesson, 2018; Mduzana et al., 2020).

2.11 Conclusion

The future of low-cost prosthesis production is promising, especially in underdeveloped countries where access to advanced medical technology is limited. The dearth of comparisons among different software used in maxillofacial prosthesis manufacturing in the literature necessitates exploring more cost-effective options for patients to improve accessibility. By integrating low-cost alternatives into the manufacturing of prostheses could yield significant societal benefits, particularly by improving the quality of life for individuals who require prosthetic interventions. As software features and capabilities evolve and 3D printing technologies proliferate, low-cost alternatives are expected to improve, making them increasingly accessible for widespread clinical use. Therefore, by comparing alternative process chains using cheaper technologies with industry benchmarks could yield important information about more cost-effective solutions, which will enable greater patient access to vital medical devices.

Chapter 3

Research Philosophies and Conceptualisation of the Research Project

3.1 Introduction

People across the world have facial disfigurements because of accidents, cancer, and congenital limitations. In South Africa, high rates of traffic accidents, assaults, and untreated cancer are factors contributing to facial trauma and disfigurements, in addition to the alarming numbers of burn victims from shack fires and primus stoves (Maritz et al., 2012; Iqbal et al., 2013). Many patients, who might require external facial prostheses, come from underprivileged backgrounds and are government-funded; therefore, they are unable to afford the sophisticated technologies needed to make prostheses. Investigating low-cost prosthesis production is essential to improving affordability and accessibility, particularly in areas with limited resources.

The creation of maxillofacial prostheses follows a multi-step procedure using medical imaging, medical image processing (MIP), computer-aided design (CAD), additive manufacturing (AM), and other state-of-the-art technology. By adopting process chains that employ these technologies, a person's anatomy can be used to develop a patient-specific, aesthetically pleasing prosthesis. The current industry benchmark for MIP software is Mimics, developed by Materialise. Mimics is known for its robust capabilities in handling challenging segmentation tasks, converting Digital Imaging and Communications in Medicine (DICOM) files into three-dimensional (3D) models, and preparing models for 3D printing (Marro et al., 2016; Nikitichev et al., 2018). Geomagic Freeform, developed by 3D Systems, Inc., is recognised as the industry benchmark for advanced digital sculpting. However, the high cost and complexity associated with these tools have necessitated the exploration of more accessible and cost-effective alternatives. Consequently, this study was undertaken to explore alternative imaging processes, and the use of MIP and CAD software in process chains for the manufacturing of external maxillofacial prostheses. Thus, the main research question for this study was:

Which process chain(s) can produce external maxillofacial prostheses of acceptable quality at a price relevant to the South African demography?

3.2 Philosophies underpinnings of the study

A research project's conceptual underpinnings serve as both support and direction. The development of research topics, the choice of appropriate methodologies, and the interpretation of findings are all guided by research philosophies (Crotty, 1998). "*A system of beliefs and assumptions about the development of knowledge*" defines research philosophy (Saunders et al., 2009). An ontological assumption describes the nature of reality, is related to the study topic, and has an impact on the research questions and objectives that are investigated (Tengli, 2020). There is a general epistemological assumption made about knowledge, which can involve textual, numerical, or even visual data. The axiological assumption is made about values and beliefs. It is the researcher's responsibility to be impartial on values and beliefs that might affect the course, results, and conclusions of the study.

3.2.1 Design science research

The design science research (DSR) paradigm originated from engineering and the sciences of the artificial. Bayazit (2004) asserted that DSR could broadly be characterised as "… *the study, research, and investigation of the artificial made by human beings, and the way these activities have been directed either in academic studies or manufacturing organisations*." The primary goal of DSR initiatives is to find practical solutions to everyday problems (Aburamadan & Trillo, 2020; Steuck et al., 2024). It is, therefore, a paradigm for resolving issues where the production of novel artefacts advances human understanding (Vom Brocke et al., 2020). Theoretically, science and technology are used to create innovative artefacts that address problems that affect the actual world (Hevner et al., 2004; Weigand et al., 2021). As a result, DSR is an applied science that employs design in all its forms to achieve a particular research project's objective (Niiniluoto, 2014). In a broad sense, artefacts include anything created by humans, including models, processes, constructions, and procedures used to address difficult issues (Weigand et al., 2021).

There are primarily three methods for employing DSR. These methods were characterised by Horváth (2007) as (i) research in design; (ii) design-inclusive research; and (iii) practice-based design research. Research in the context of design refers to disciplinary inquiries and research in design that have many beneficial similarities with basic scientific research. The design-inclusive research approach states that contextualisation and the synthesis of scientific and design information occur during design processes and ultimately result in artefacts (Kotzé et al., 2015; Coetzee, 2019; De Sordi et al., 2020). This approach is to achieve a deeper integration of knowledge. Contextualised practical knowledge serves as a strong foundation for design knowledge in the practice-based design research approach. A design-inclusive research strategy served as the cornerstone of this study's methodological implementation.

3.2.2 Pragmatic inquiry

The aim of this project was to provide a workable solution to a real-world query. This typical pragmatic investigation was, therefore, to generate knowledge that would be applicable and have real-world implications (Kelly & Cordeiro, 2020). According to pragmatists, research initiatives start with a problem and conclude with practical solutions that direct the application of future practices (Saunders et al., 2009). Acting on issues in the "real-world" is another point of emphasis for pragmatists (Creswell et al., 2003; Rorty et al., 2004). Because the outcome of this project is to find a real-world solution to some of the costly technologies used in the manufacturing of external maxillofacial prostheses, the project is typically a pragmatic inquiry.

3.2.3 Abductive reasoning

The two primary methods of deductive and inductive thinking are the subject of most of the conventional research. Deductive reasoning begins with the statement of a general rule and works its way down to a particular conclusion. Conversely, inductive reasoning starts with narrowly focused and specific data and works its way up to a plausible generalised conclusion. In addition to deductive and inductive reasoning, a third type of logic, known as abductive reasoning, the process of imagining what "might be so," is needed for creating hypothetical futures (Kolko quoted by Faste & Faste, 2012: 2).

Abductive reasoning starts with an incomplete collection of observations and works its way down to the most likely explanation. The shortcomings of deductive and inductive procedures are addressed by an abductive approach (Faste & Faste, 2012). Deductive reasoning is specifically criticised for being unclear when it comes to choosing a theory to test through the formulation of hypotheses. In their critique of inductive reasoning, Faste and Faste (2012) argued that a theory is not always constructed by a large body of empirical evidence. As a third alternative, abductive reasoning overcomes these weaknesses by adopting a pragmatist perspective. When it comes to using abductive reasoning to develop ideas and draw logical conclusions, it is comparable to deductive and inductive methods (Faste & Faste, 2012). The real-world issue of identifying more reasonably priced MIP and CAD software for the process chains of external maxillofacial prostheses was best solved via an abductive reasoning approach.

In conclusion, this design-inclusive research project can be compared to peeling back the layers of the research onion developed by Saunders et al. (2009, 2019) (Figure 3.1). To accomplish the study's aim, a multi-method quantitative and qualitative experimental research design was used, along with a pragmatic approach and abductive reasoning.

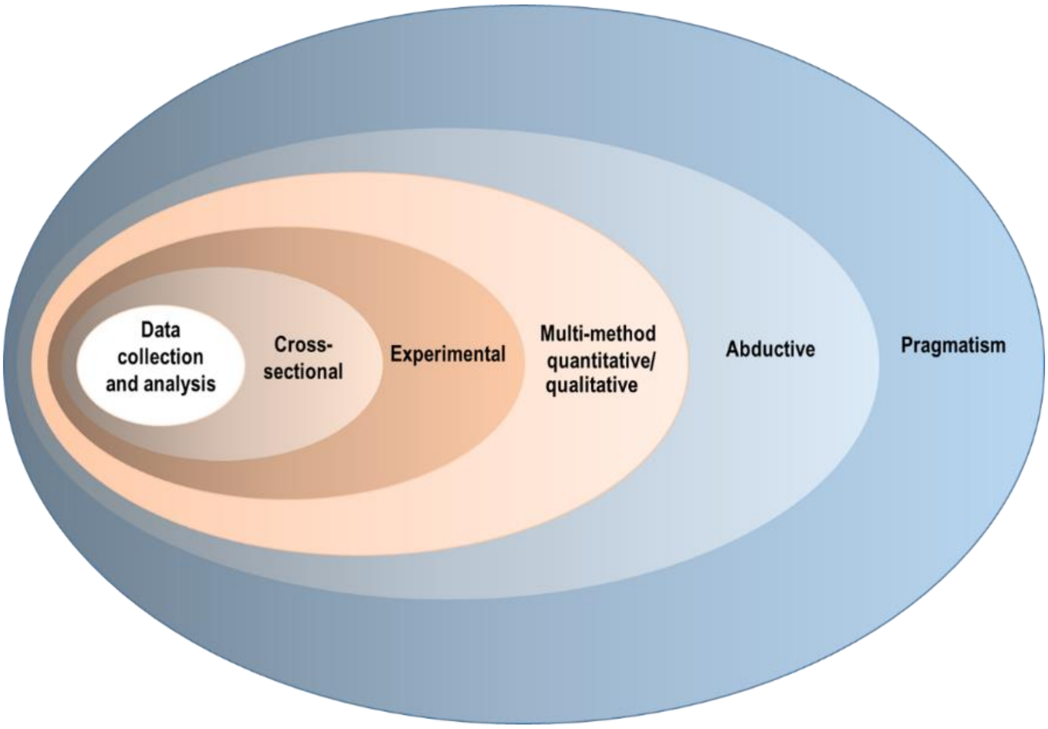

Figure 3.1 Research onion depicting the research philosophies and methodological approaches followed in this study

3.3 Conceptualisation of the project

The conceptualisation of this project necessitated a comprehensive understanding of the process chain involved in the design and manufacturing of external maxillofacial prostheses. The first step in this process is the acquisition of digital images of the anatomy of a patient, which in this study were obtained using computed tomography (CT) and structured light surface scans. The CT scan data, in DICOM format, are imported into MIP software. Within this software, the data are processed, and the region of interest (ROI) is segmented. The segmented data are then exported as a 3D model in a stereolithography (*STL*) file format. This *STL* file is subsequently imported into CAD software, where the prosthesis is designed. When using surface scan data of a patient's anatomy, the data are imported directly into CAD software for the design of the prosthesis, bypassing the MIP stage. Finally, the design is exported for the additive manufacturing (AM) of the prosthesis.

This study focused on the evaluation of the use of surface scan data, and MIP and CAD software, with the aim of identifying more cost-effective alternatives to the expensive industry-benchmarks. Real-world data of a human ear and nose were used in the evaluation following four sequential research actions (Figure 3.2).

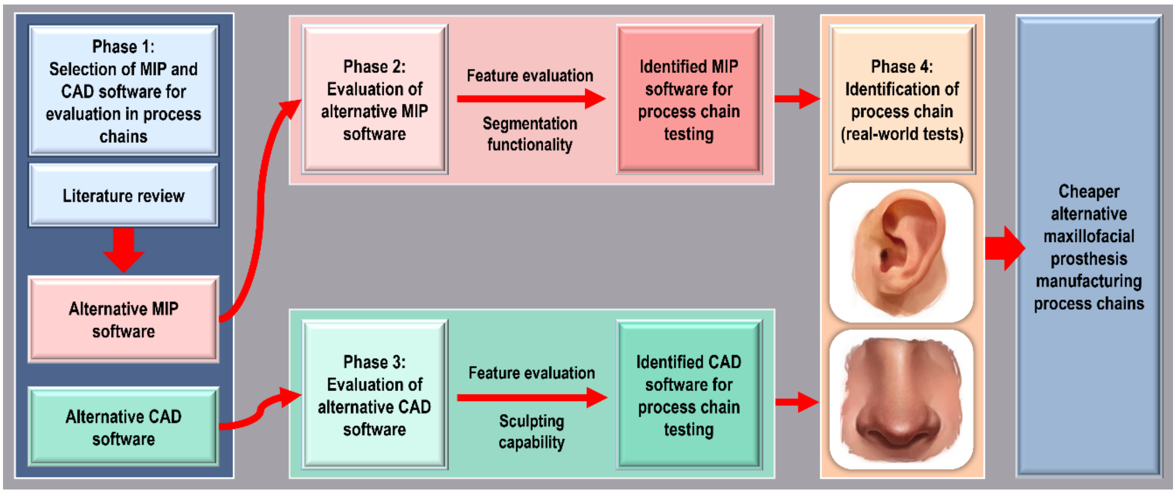

Figure 3.2 Diagram showing the study design of the project

To achieve the aim of identifying more affordable process chain options for the manufacturing of external maxillofacial prostheses, the study was divided into four phases. By structuring the project into these phases ensured a systematic approach into exploring and validating cost-effective alternatives for prosthesis manufacturing. Each phase addressed a specific sub-question and included related objectives. Table 3.1 outlines these phases, the corresponding sub-questions, and their objectives.

Table 3.1 Phases with related sub-questions and objectives, and chapter in which the results are presented

Phase	Sub-question	Objective	Chapter reported in
Phase 1: ***Selection of potential MIP and CAD software for testing in process chains***	What are the commonly used MIP and CAD software options suitable for external maxillofacial prosthesis manufacturing?	OBJ1: To conduct a comprehensive systematic review of the literature to identify commonly used MIP and CAD software with the potential to be tested in process chains.	4
Phase 2: ***Evaluation of potential MIP software***	Which MIP software can be selected and tested based on specific software features and digital segmentation functionality criteria?	OBJ2: To source CT data from two human subjects to use in the software tests. OBJ3: To select MIP software based on specific criteria related to software features. OBJ4: To test and select MIP software based on specific criteria related to digital segmentation functionality.	5
Phase 3: ***Evaluation of potential CAD software***	Which CAD software can be selected and tested based on specific software features and digital sculpting capability criteria?	OBJ5: To select and test CAD software based on specific criteria related to software features. OBJ6: To test and select CAD software based on digital sculpting capability.	6
Phase 4: ***Identification of process chains that are cheaper than the industry-benchmark***	Which alternative process chains produce external maxillofacial prostheses of comparable quality to those produced by the industry benchmark?	OBJ7: To source surface scan data of a human nose and ear. OBJ8: To produce 3D models using process chains assembled using the selected MIP and CAD software. OBJ9: To produce 3D models using process chains assembled using the surface scan data and CAD software. OBJ10: To evaluate the selected process chains to identify alternatives that compare favourably with industry-benchmark software, thereby enhancing access to external maxillofacial prostheses.	7

3.4 Materials and methods

The researcher independently executed all the software-related tasks and procedures detailed in this thesis. To make the chapters easier to read, the procedures for each chapter are included in the relevant chapters where the results have been presented.

3.5 Conclusion

This DSR project was planned and executed to identify more cost-effective process chain alternatives for external maxillofacial prostheses manufacturing. The methodology was divided into four distinct phases to ensure a systematic and comprehensive evaluation of the quality and cost of the products produced by potential alternative maxillofacial prostheses manufacturing process chains. The integration of surface scan data, and MIP and CAD software alternatives into the process chain was compared to the industry benchmarks. The purpose of these comparisons was to find alternative process chains that produced products that match the functionality and quality of the current industry benchmark process chains, while also providing improved accessibility because of their lower costs. By enhancing access to these technologies, especially in resource-constrained settings such as South Africa, this project holds significant potential to improve the accessibility and affordability of external maxillofacial prostheses.

In conclusion, the systematic approach adopted in this study provides a robust framework for identifying affordable, alternative process chains. By enhancing access to these technologies, especially in resource-constrained settings such as South Africa, this project holds significant potential to improve the accessibility and affordability of external maxillofacial prostheses.

Chapter 4

Medical Image Processing and Computer-Aided Design Software Selection

4.1 Introduction

The manufacturing of external maxillofacial prostheses involves two critical process chain events that rely heavily on specialised software. These events involve medical image processing (MIP) and computer-aided design (CAD). MIP software is essential for processing data extracted from 3D volumetric datasets of a patient's anatomical area of interest generated by computed tomography (CT). The primary consideration in selecting MIP software is its ability to perform segmentation, which involves the process of accurately separating the anatomical region of interest (ROI) from the volumetric datasets. CAD software, on the other hand, is used to design a prosthesis using the patient's anatomical data as a guide. The digital sculpting capabilities of CAD software is important when selecting suitable software. Digital sculpting mimics the physical process of sculpting with tools on clay by manipulating a 3D mesh using specialised CAD tools.

The current industry benchmark for MIP software is Mimics, developed by Materialise. The software is FDA-cleared and complies with medical device regulations, making it a preferred choice in clinical and research settings (Marro et al., 2016; Nikitichev et al., 2018). It is widely recognised for its precision and high-quality outputs during medical image processing. Mimics offers specialised and extensive tools for the segmentation of medical scans, 3D reconstruction of anatomical structures, preoperative planning, and patient-specific design. Similarly, Geomagic Freeform, developed by 3D Systems, Inc., is the leading CAD software in the medical industry. It is renowned for its advanced sculpting and powerful design tools that make it possible to create highly detailed and anatomically accurate models (Reilingh et al., 2017; Memon et al., 2020). Therefore, in *Phase 1* of this study, a comprehensive review of the literature was conducted to identify alternative MIP and CAD software that could be evaluated in process chains for external maxillofacial prosthesis manufacturing. The objective was to ascertain whether the selected alternative software could effectively replace the industry benchmarks, Materialise's Mimics and 3D Systems Inc.'s Geomagic Freeform for prostheses manufacturing. As a result, the following sub-question was addressed in this phase:

What are the commonly used MIP and CAD software options suitable for external maxillofacial prosthesis manufacturing?

Figure 4.1 presents a flow diagram of the process followed to select alternative MIP and CAD software from the literature that could undergo further evaluation in process chains for the manufacturing of external maxillofacial prostheses.

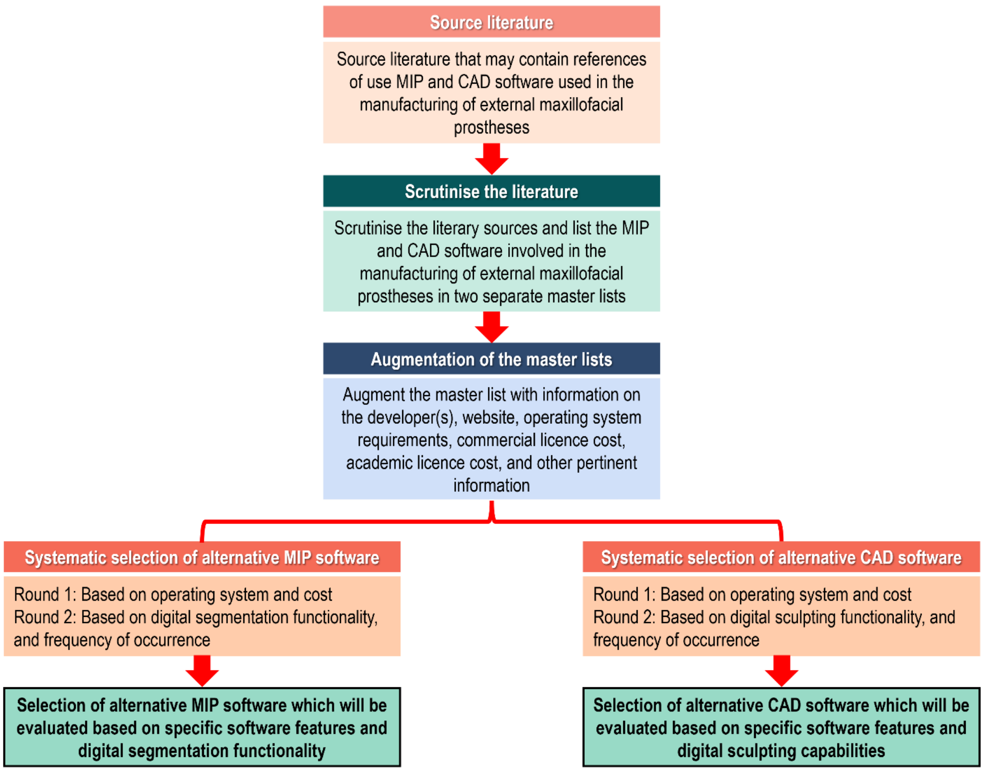

Figure 4.1 Presentation of the research process to identify alternative MIP and CAD software applications in the literature

4.2 Methods

In the initial phase of this study, suitable, alternative MIP and CAD software applications were selected so that their functionality could be evaluated in prosthesis manufacturing process chains. A thorough review of the literature was undertaken to identify and select alternative software applications. Table 4.1 details the four key procedures that were followed to identify and select alternative software for evaluation.

Table 4.1 Steps followed to identify alternative MIP and CAD software that can progress to the testing phases

Step	Aim
1. Source literature	A systematic review of the literature was conducted to identify suitable alternative MIP and CAD software for testing in the manufacturing process chains of external maxillofacial prostheses. The aim was to identify software applications that meet specific requirements, focusing on functionalities such as segmentation accuracy for MIP software and advanced sculpting capabilities for CAD software.
2. Scrutinise sourced literature	The sourced literature was reviewed to identify MIP and CAD software that are frequently used in the process chains for the manufacturing of external maxillofacial prostheses. Several filters were applied to facilitate the identification of relevant MIP and CAD software.
3. List potentially relevant software	Two master lists were created in Excel, one for the MIP software and one for the CAD software. Each of these master lists was supplemented with information that may be of relevance during the selection process, for example, the name of the developers, the operating system, and the costs.
4. Select software for testing in the study	From the MIP and CAD master lists, relevant software was selected based on a defined set of selection criteria. This selection process aimed to identify software applications suitable for further evaluation of their integration into the manufacturing process chains of external maxillofacial prostheses.

4.2.1 Sourcing of literature

To conduct the systematic literature review in Step 1, several literature databases were searched using different search criteria. Among the literature databases searched for this study were ScienceDirect, Emerald Insight, Taylor and Francis Online, PubMed Central, Sage Journals, Whiley Online Library, Research Gate, SpringerLink, Ebscohost, Semantic Scholar, and Google Scholar. A wide net was cast for search term (words and phrases) selection to include terms broadly linked to the design and the manufacture of external maxillofacial prostheses to ensure a thorough scrutiny of the literature. To further enhance the literature search, search phrases were modified to include relevant terms such as 'external facial prosthesis production' and 'external facial prosthesis design and manufacturing.' The search terms selected belonged to five distinct search themes (Table 4.2). Although some search terms belonged to more than one theme, they are listed under one theme in the table. For example, 'craniofacial design' is listed under the theme 'design' but can also be listed under the theme 'medical.'

Table 4.2 Search themes and examples of search terms used to source relevant literature

Search theme	Examples of search terms in a search theme
Imaging/scanning	• medical imaging software • medical image processing software • medical image processing software for medical application • medical image analysis software • medical image editing software • medical image editing software for medical application • CT and MRI imaging for cranio-maxillo-facial implants and prostheses • medical imaging software for digital data processing • CT and MRI scanning for maxillofacial implants and prostheses
Design	• computer-aided design • medical design software • CAD software for medical application • implant design • prostheses design • craniofacial (implant) • craniofacial design

	• medical geometry design • digital sculpting software • digital sculpting software for medical application • CAD used in external maxillofacial reconstruction
Digital	• digital image processing • digital design for facial reconstruction • digital design for facial prosthesis manufacturing • digital geometry design
Facial reconstruction	• maxillofacial facial prosthesis • external facial prosthesis design • external prosthetic design • external facial prosthesis production • external facial prosthesis design and manufacturing
Medical	• medical design • medical product design • medical product development • CAD software for medical application • medical image editing software for medical application • medical image analysis software • medical image processing

4.2.2 Scrutinising the literature

In Step 2, the sourced literature was carefully examined to determine whether the sources contained information relevant to the selection of alternative MIP or CAD software that can be evaluated in prosthesis manufacturing process chains. To find the pertinent literary sources, four screening filters were used in a step-by-step fashion. Table 4.3 describes the four filters that were applied during the scrutiny of the sourced literature.

Table 4.3 Descriptions of the screening filters applied during the scrutiny of the sourced literature

Screening filter	Description of the filter
1.	This filter was applied to exclude duplicate literary sources.
2.	This filter was applied to exclude sources that were non-medical in nature.
3.	This filter was applied to exclude sources that do not refer to 'cranio-maxillo-facial' topics.
4.	This filter was applied to exclude sources that do not refer to external maxillofacial prostheses design and manufacturing.

4.2.3 Listing of relevant software

After the screening filters were applied and the irrelevant literary sources excluded, the remaining literature was thoroughly inspected in Step 3 to identify MIP and CAD software. The identified MIP and CAD software were listed in separate master lists created in Excel spreadsheets. Besides the information that could be gleaned from the literature about the MIP and CAD software, the master lists were supplemented with additional information obtained from the developers' web pages. This information included the version of the software, year of release, the general aim of the software, the operating system, and cost (if available).

4.2.4 Selection of the software for evaluation

In Step 4, MIP and CAD software were selected for further evaluation in process chains for the manufacturing of external maxillofacial prostheses. Four inclusion criteria were applied to the MIP and CAD software master lists to select software (Table 4.4). Initially, a first round of software selection was performed on the software in the master lists using the first two criteria. The software found in the first round was then subjected to the final two criteria, yielding MIP and CAD software that were deemed suitable for advancing to further evaluation. Because the performance of the selected software applications was benchmarked against Materialise Mimics software (MIP software) and Geomagic Freeform, from 3D Systems, Inc. (CAD software) as recommended by the Centre for Rapid Prototyping and Manufacturing (CRPM) at the Central University of Technology, Free State, these software were also included in the selection.

Table 4.4 Descriptions of the inclusion criteria used to select the MIP and CAD software for further evaluation

Criterion	Description of software inclusion criteria
1. Operating system	A software application must use the Microsoft Windows operating system.
2. Cost	A software application must be priced at ≤ R100K.
3. Functionality	A MIP software application must have digital segmentation functions. A CAD software application must have digital sculpting functions.
4. Frequency	A software's frequency of occurrence will also be the final consideration in the selection process.

4.3 Results

4.3.1 Sourced literature

Approximately 700 publications, from 2000 to 2023, were reviewed in the search for relevant MIP and CAD software. After applying the first two filters, the duplicate literary sources, and sources referencing unrelated software information, non-medical applications, and non-applicable medical applications, were removed (Figure 4.2). The remainder of the sources were deemed appropriate (n = 274) for further scrutiny to identify alternative MIP and CAD software that could be advanced for further evaluation. A comprehensive range of medical applications of MIP and CAD software was identified in this literature. These applications covered topics from designing and manufacturing external maxillofacial prostheses to medical and educational uses, pre-operative planning modelling, anthropological studies, dentistry, prosthetics for limb amputees, and facial implants for severe internal structural trauma and deformities. In 71% of these sources, the topic of maxillofacial reconstruction was covered, which included 73 sources that made specific reference to external maxillofacial prostheses.

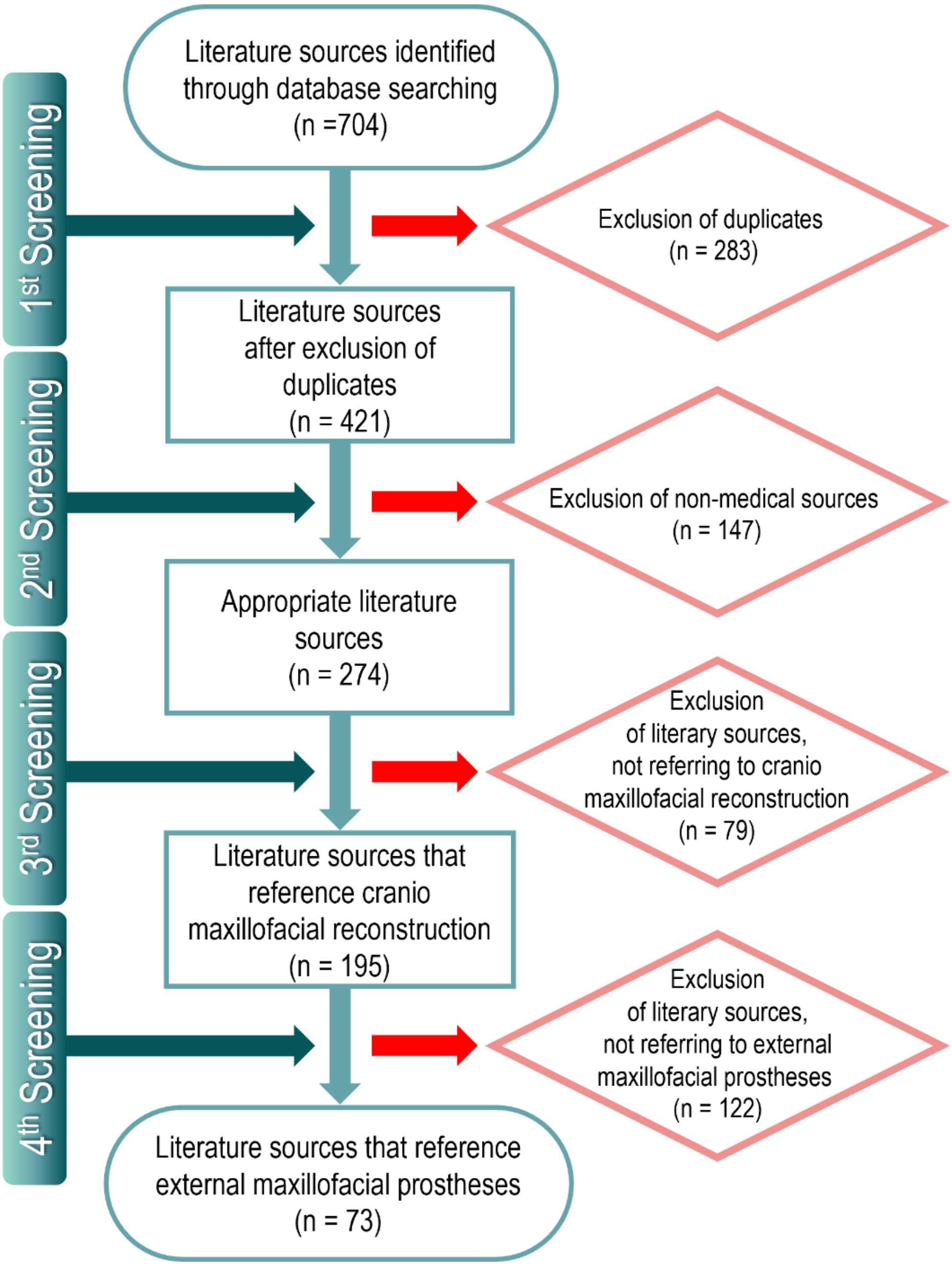

Figure 4.2 Flow diagram depicting the systematic approach followed to eliminate irrelevant literary sources

4.3.2 Selected MIP software

The master list of the MIP software included applications referenced in 73 literary sources. This list contained 21 different MIP software applications, including the control software, Mimics. By applying the first two selection criteria, operating system compatibility and cost, it was determined that 10 of the software applications operated on the Microsoft Windows platform and were priced at or below R100 000. Table 4.5 displays the 21 software applications listed in the master list and the ten applications that were selected after the application of the first two inclusion criteria. Since Mimics Materialise software was considered the industry benchmark and served as the benchmark against which the other MIP software was evaluated, its specifications are indicated as ‘included’ in the table, making up a total of 11 ‘included’ MIP software applications.

Central University of Technology, Free State

Table 4.5 MIP software master list showing the included software based on the operating system and cost

	Software/Developer	Website	Operating system	License	Commercial license cost (SA Rand)	Academic license cost (SA Rand)	Software included/ excluded
1	**3D Doctor™** Able Software Corp	https://www.ablesw.com/	Microsoft Windows	Open Source/ Proprietary	< R85K (per license)	> R43K (per license)	Included
2	**3D Slicer™** The Slicer Community	https://slicer.org	Microsoft Windows; Linux; Mac OS	Open Source	Free	Free	Included
3	**Amira®** Thermo Fisher Scientific	https://www.thermofisher.com	Microsoft Windows; Linux; Mac OS	Proprietary	< R357K (per annum)	> R235K (per annum)	Excluded
4	**Analyze** Analyze Direct™	https://analyzedirect.com	Microsoft Windows; Linux; Mac OS	Proprietary	< R72K	-	Included
5	**Avizo** Thermo Fisher Scientific	https://www.fei.com/software/avizo/?LangType=2052	Microsoft Windows; Linux; Mac OS	Proprietary	< R357K (per annum)	> R235K (per annum)	Excluded
6	**Dolphin 3D** Dolphin Imaging (Simulation software)	https://www.dolphinimaging.com	Microsoft Windows; Linux; Mac OS	Proprietary	Available for North America only	Available for North America only	Excluded
7	**EasyCrania** Microsoft®	Developed under the platform of Microsoft Visual Studio 2010 - https://academic.microsoft.com/	Microsoft Windows; Linux; Mac OS	Proprietary	On Request	On Request	Excluded
8	**ImLib3D** ImLib3D	https://imlib3d.soft112.com/	Microsoft Windows; Linux; Mac OS	Open Source	Free	Free	Included
9	**InVesalius** CTI (Renato Archer Information Technology Center, São Paulo, Brazil)	https://invesalius.github.io	Microsoft Windows; Linux; Mac OS	Open Source	Free	Free	Included
10	**iPlan® CMF™** Brainlab®	https://www.brainlab.com/radiosurgery-products/iplan-rt-treatment-planning-software/	Microsoft Windows; Linux; Mac OS	Proprietary	R150K	-	Excluded

Central University of Technology, Free State

11	**MatLab** MathWorks® CAD	https://www.mathworks.com/products/matlab.html	Microsoft Windows; Linux; Mac OS	Proprietary	> R42K (per annum)	< R10K (per annum)	Included
12	**Medical Imaging Interaction Toolkit Workbench – MITK** German Cancer Research Center	http://www.mitk.org/	Microsoft Windows; Linux; Mac OS	Open Source	Free	Free	Included
13	**Medical Image Processing and Visualisation – MIPAV** Developed by the University of Iowa	https://mipav.cit.nih.gov/	Microsoft Windows; Linux; Mac OS	Open Source	Free	Free	Included
14	**MeVisLab** MeVis Medical Solutions AG	https://www.mevislab.de/	Microsoft Windows; Linux; Mac OS	Open Source	Free	Free	Included
15	**Mimics®** Materialse® (Control Software)	https://www.materialise.com/en/medical/mimics-innovation-suite/mimics	Microsoft Windows; Linux; Mac OS	Proprietary	> R1.7M	-	Control - Included
16	**Myrian® Studio** Intrasence®	https://www.intrasense.fr/	Microsoft Windows	Proprietary	> R200K	-	Excluded
17	**Osirix** Pixmeo®	http://www.osirix-viewer.com	Mac OS	Proprietary	< R9K (per annum)	-	Excluded
18	**ProPlan CMF™** Materialse®	https://www.materialise.com/en/medical/software/proplan-cmf	Microsoft Windows; Linux; Mac OS	Proprietary	Only for Physicians	Only for Physicians	Excluded
19	**Visualisation ToolKit – VTK** Kitware, Inc.	https://vtk.org/	Microsoft Windows; UNIX; Mac OS	Open Source	Free	Free	Included
20	**Simpleware ScanIP** Synopsys®, Inc.	https://www.synopsys.com/simpleware/software/scanip.html	Microsoft Windows	Proprietary	On Request	On Request	Excluded
21	**SurgiCase®** Materialse®	https://www.materialise.com/en/medical/mimics-innovation-suite/surgicase	Microsoft Windows; Linux; Mac OS	Proprietary	Only for Physicians	Only for Physicians	Excluded

Control = MIP software highlighted in blue indicates the software that was used as the control in this study.

The MIP software, which was selected based on the operating system and cost, was further assessed for its segmentation functionality and frequency of occurrence in the sourced literature. After evaluating the software based on functionality, three software applications were excluded. Furthermore, software applications that were only mentioned once in the literature were also excluded from further evaluation. Therefore, the control software, Mimics, and five MIP software applications were selected for evaluation in process chains for prostheses manufacturing. Table 4.6 shows the outcome of the MIP software selection process.

Table 4.6 MIP software selected for further evaluation based on functionality and frequency of occurrence in the literature

	Software	Segmentation functionality	Number of appearances in literary sources	Selected software
1	Mimics® (Control)	✓	51	**Selected**
2	MatLab	×	7	Not selected
3	3D Slicer™	✓	6	**Selected**
4	InVesalius	✓	6	**Selected**
5	3D Doctor™	✓	2	**Selected**
6	MITK	✓	2	**Selected**
7	MeVisLab	✓	2	**Selected**
8	VTK	×	2	Not selected
9	Analyze	✓	1	Not selected
10	ImLib3D	✓	1	Not selected
11	MIPAV	×	1	Not selected

4.3.3 Selected CAD software

The CAD software master list included the names of software applications mentioned in the 73 literature sources. This master list comprised of 37 different CAD software applications, including the control software Geomagic Freeform by 3D Systems, Inc. After applying the first two inclusion criteria, type of operating system, and price, it was determined that 26 CAD software applications met these criteria. Thus, a total of 27 CAD software applications were listed as ‘included’ for further evaluation in process chains. Table 4.7 shows the outcome of the CAD software selection process.

Central University of Technology, Free State

Table 4.7 CAD software master list showing the included software based on the operating system and cost

	Software /Developer	Website	Operating system	License	Commercial license cost (SA Rand)	Academic license cost (SA Rand)	Software included/ excluded
1	**3D Builder** Microsoft Corporation	https://www.microsoft.com/en-za/p/3d-builder/9wzdncrfj3t6?activetab=pivot:overviewtab	Microsoft Windows; Linux; Mac OS	Open Source	Free	Free	Included
2	**3D Coat** Pilgway®	https://3dcoat.com/	Microsoft Windows; Linux; Mac OS	Proprietary	< R7K (per annum)	R825 (per annum) floating license	Included
3	**3Ds Max®** Autodesk®	https://www.autodesk.co.za/products/3ds-max/	Microsoft Windows; Linux; Mac OS	Proprietary	< R22K (per annum)	-	Included
4	**3-Matic®** Materialse®	https://www.materialise.com/en/software/3-matic	Microsoft Windows; Linux; Mac OS	Proprietary	R179 240	-	Excluded
5	**Alias®** Autodesk®	https://www.autodesk.com/products/alias-products/overview	Microsoft Windows; Linux; Mac OS	Proprietary	> R88K (per annum)	On Request	Included
6	**AutoCAD®** Autodesk®	https://www.autodesk.co.za/products/autocad/overview	Microsoft Windows; Linux; Mac OS	Proprietary	> R24K (per annum)	On Request	Included
7	**AutoCAD 123D** Autodesk®	https://www.autodesk.com/solutions/123d-apps	Microsoft Windows; Linux; Mac OS	Proprietary	Off Market	Off Market	Excluded
8	**Blender** Blender Foundation	https://www.blender.org/	Microsoft Windows; Linux; Mac OS	Open Source	Free	Free	Included
9	**CATIA®** Dassault Systèmes	https://www.3ds.com/products-services/catia/	Microsoft Windows; Linux; Mac OS	Proprietary	R120K – R875K	-	Excluded
10	**Cinema 4D Studio** Maxon	https://www.maxon.net/en/products/cinema-4d/overview/	Microsoft Windows; Linux; Mac OS	Proprietary	> R65K (per license)	< R20K (per annum)	Included
11	**FormZ Pro** AutoDesSys, Inc.	http://www.formz.com/	Microsoft Windows; Linux; Mac OS	Proprietary	> R18K (per annum)	< R6K (per annum)	Included
12	**Fusion 360®** Autodesk®	https://www.autodesk.com/products/fusion-360/students-teachers-educators	Microsoft Windows; Linux; Mac OS	Proprietary	> R9K (per annum)	On Request	Included

13	**Geomagic® Design™ X** 3D Systems®, Inc.	https://www.3dsystems.com/software/geomagic-design-x	Microsoft Windows; Linux; Mac OS	Proprietary	R250K	-	Excluded
14	**Geomagic® Freeform®** 3D Systems®, Inc.	https://www.3dsystems.com/software/geomagic-freeform	Microsoft Windows; Linux; Mac OS	Proprietary	R250K	-	Control - Included
15	**Geomagic® Sculpt™** 3D Systems®, Inc.	https://www.3dsystems.com/software/geomagic-sculpt	Microsoft Windows; Linux; Mac OS	Proprietary	R190K	-	Excluded
16	**Geomagic Studio®** SculptCAD	http://sculptcad.com/geomagic-studio/	Microsoft Windows; Linux; Mac OS	Proprietary	R290K	-	Excluded
17	**Houdini®** Side Effects Software, Inc.	https://www.sidefx.com/products/houdini/	Microsoft Windows; Linux; Mac OS	Proprietary	> R128K (per annum)	> R1K (per annum)	Excluded
18	**Inventor®** Autodesk®	https://www.autodesk.co.za/products/inventor/overview	Microsoft Windows; Linux; Mac OS	Proprietary	> R30K (per annum)	On Request	Included
19	**Lightwave 3D** NewTek, Inc.	https://www.newtek.com/lightwave/2019/	Microsoft Windows; Linux; Mac OS	Proprietary	> R18K (per annum)	< R4K (per annum)	Included
20	**Magics®** Materialse®	https://www.materialise.com/en/software/magics	Microsoft Windows; Linux; Mac OS	Proprietary	R22K	-	Included
21	**MakeHuman** The Make Human team	http://www.makehumancommunity.org	Microsoft Windows; Linux; Mac OS	Open Source	Free	Free	Included
22	**Maya®** Autodesk®	https://www.autodesk.co.za/products/maya/overview	Microsoft Windows; Linux; Mac OS	Proprietary	> R23K (per annum)	On Request	Included
23	**Meshmixer** Autodesk®	http://www.meshmixer.com/	Microsoft Windows; Linux; Mac OS	Open Source	Free	Free	Included
24	**MODO®** The Foundry Visionmongers Ltd.	https://www.foundry.com/products/modo	Microsoft Windows; Linux; Mac OS	Proprietary	> R12K (per annum)	> R12K (per annum)	Included
25	**Moment of Inspiration (MoI)** Triple Squid Software Design	http://moi3d.com/	Microsoft Windows; Linux; Mac OS	Proprietary	> R5K (per annum)	> R5K (per annum)	Included
26	**Mudbox™** Autodesk®	https://www.autodesk.com/products/mudbox/overview	Microsoft Windows; Linux; Mac OS	Proprietary	< R2K (per annum)	Free	Included

27	**Onshape** Onshape, Inc.	https://www.onshape.com/	Microsoft Windows; Linux; Mac OS	Proprietary	< R46K (per annum)	Free	Included
28	**OpenSCAD** Marius Kintel & Clifford Wolf	https://www.openscad.org/	Microsoft Windows; Linux; Mac OS	Open Source	Free	Free	Included
29	**Poser** Smith Micro Software, Inc.	https://www.posersoftware.com/	Microsoft Windows; Linux; Mac OS	Proprietary	< R3K (per annum)	-	Included
30	**RapidForm** INUS Technology, Inc.	http://www.rapidform.com	Microsoft Windows; Linux; Mac OS	Proprietary	Incorporated with Geomagic® Software, now owned by 3D Systems™, Inc. – new name Geomagic® Design™	-	Excluded
31	**Rhino3D/Rhinoceros®** Robert McNeel & Associates	https://www.rhino3d.com/	Microsoft Windows; Linux; Mac OS	Proprietary	> R18K (per annum)	< R4K (per annum)	Included
32	**Sculptris** Pixilogic®, Inc.	https://pixologic.com/sculptris/	Microsoft Windows; Linux; Mac OS	Open Source	Free	Free	Included
33	**Siemens NX** Siemens PLM Software	https://www.plm.automation.siemens.com/global/en/products/nx/	Microsoft Windows; Linux; Mac OS	Proprietary	> R180K (per annum)	Specialised Use Only	Excluded
34	**Simplify3D®** Simplify3D®	https://www.simplify3d.com/	Microsoft Windows; Linux; Mac OS	Proprietary	< R3K (per annum)	< R3K (per annum)	Included
35	**SketchUP** Trimble, Inc.	https://www.sketchup.com/	Microsoft Windows; Linux; Mac OS	Open Source	Free	Free	Included
36	**Solidworks®** Dassault Systèmes	https://www.solidworks.com/	Microsoft Windows; Linux; Mac OS	Proprietary	<R126K (per license)	-	Excluded
37	**ZBrush™** Pixilogic®, Inc.	https://pixologic.com/	Microsoft Windows; Linux; Mac OS	Proprietary	>R16K (per license)	>R8K (per license)	Included

Control = CAD software highlighted in blue indicates the software that was used as the control in this study.

The CAD software, that were selected based on their operating system and cost, was further assessed for their digital sculpting functionality and frequency of occurrence in the literary sources. After evaluating the software, 11 of the 27 software applications were found to have passed the digital sculpting functionality evaluation (Table 4.8). Additionally, one further software application was excluded because it was only mentioned once in the literature. After both rounds of exclusion, 9 CAD software applications (excluding the control Geomagic Freeform) were deemed suitable for further evaluation. In total 10 software applications (including the control software) were advanced to the next round of evaluation.

Table 4.8 CAD software selected for further evaluation based on functionality and frequency of occurrence in the literature

	Software	Digital sculpting functionality	Frequency of occurrence in literary sources	Software selected
1	Geomagic® Freeform® (Control)	✓	42	**Selected**
2	ZBrush™	✓	24	**Selected**
3	Rhino3D/Rhinoceros®	×	15	Not selected
4	3Ds Max®	×	12	Not selected
5	Maya®	✓	12	**Selected**
6	Blender	✓	9	**Selected**
7	Magics®	×	7	Not selected
8	Inventor®	×	6	Not selected
9	Meshmixer	✓	5	**Selected**
10	Mudbox™	✓	4	**Selected**
11	SketchUP	×	4	Not selected
12	3D Coat	✓	3	**Selected**
13	Cinema 4D Studio	✓	3	**Selected**
14	MODO®	✓	3	**Selected**

	Software	Digital sculpting functionality	Frequency of occurrence in literary sources	Software selected
15	Alias®	×	2	Not selected
16	AutoCAD®	×	2	Not selected
17	OpenSCAD	×	2	Not selected
18	Sculptris	✓	2	**Selected**
19	3D Builder	×	1	Not selected
20	FormZ Pro	×	1	Not selected
21	Fusion 360	×	1	Not selected
22	Lightwave 3D	✓	1	Not selected
23	MakeHuman	×	1	Not selected
24	Moment of Inspiration (MoI)	×	1	Not selected
25	Onshape	×	1	Not selected
26	Poser	×	1	Not selected
27	Simplify3D®	×	1	Not selected

4.4 Discussion and conclusion

Following a thorough examination of over 700 scholarly publications, 73 were found to be suitable for the identification of MIP and CAD software that may be suitable for evaluation in process chains. The MIP and CAD software applications were selected from master lists compiled from the literature in accordance with inclusion criteria. The selection involved a stepwise process of excluding software that did not fit the inclusion criteria. Besides the industry-benchmark software applications, which were selected to act as control applications, five MIP and nine CAD software applications were selected for further evaluation of their software functionality. This evaluation involved software feature evaluation and functionality using real-world digital data.

Chapter 5

Evaluation of Medical Image Processing Software

5.1 Introduction

After acquiring computed tomography (CT) anatomical images of a patient in need of a prosthesis, the data are processed with medical image processing (MIP) software. Medical image processing software is used to segment the region(s) of interest (ROI) from the data volume of anatomical data to create a model that is used to design a prosthesis with CAD software (Tóth et al., 2021). Accuracy is a crucial factor to consider when processing a patient's data to avoid additional scans, which come with a significant radiation dosage (Tsalafoutas et al., 2020). Therefore, precise data processing and the creation of high-quality, functional medical models are necessary (Bibb & Winder, 2010). Models should be devoid of any artefacts which could affect the accuracy of the designed prosthesis. It is, therefore, important that less expensive alternative MIP software solutions are thoroughly evaluated and compared with the industry benchmark. The MIP applications that were identified in the literature in *Phase 1* of this study, were evaluated further in *Phase 2*. This evaluation entailed an assessment of specific software features and segmentation capabilities. The sub-question addressed in this phase was:

Which MIP software can be selected and tested based on specific software features and digital segmentation functionality criteria?

Figure 5.1 presents a flow diagram of the process followed to select alternative MIP software to be tested in external maxillofacial prosthesis manufacturing process chains.

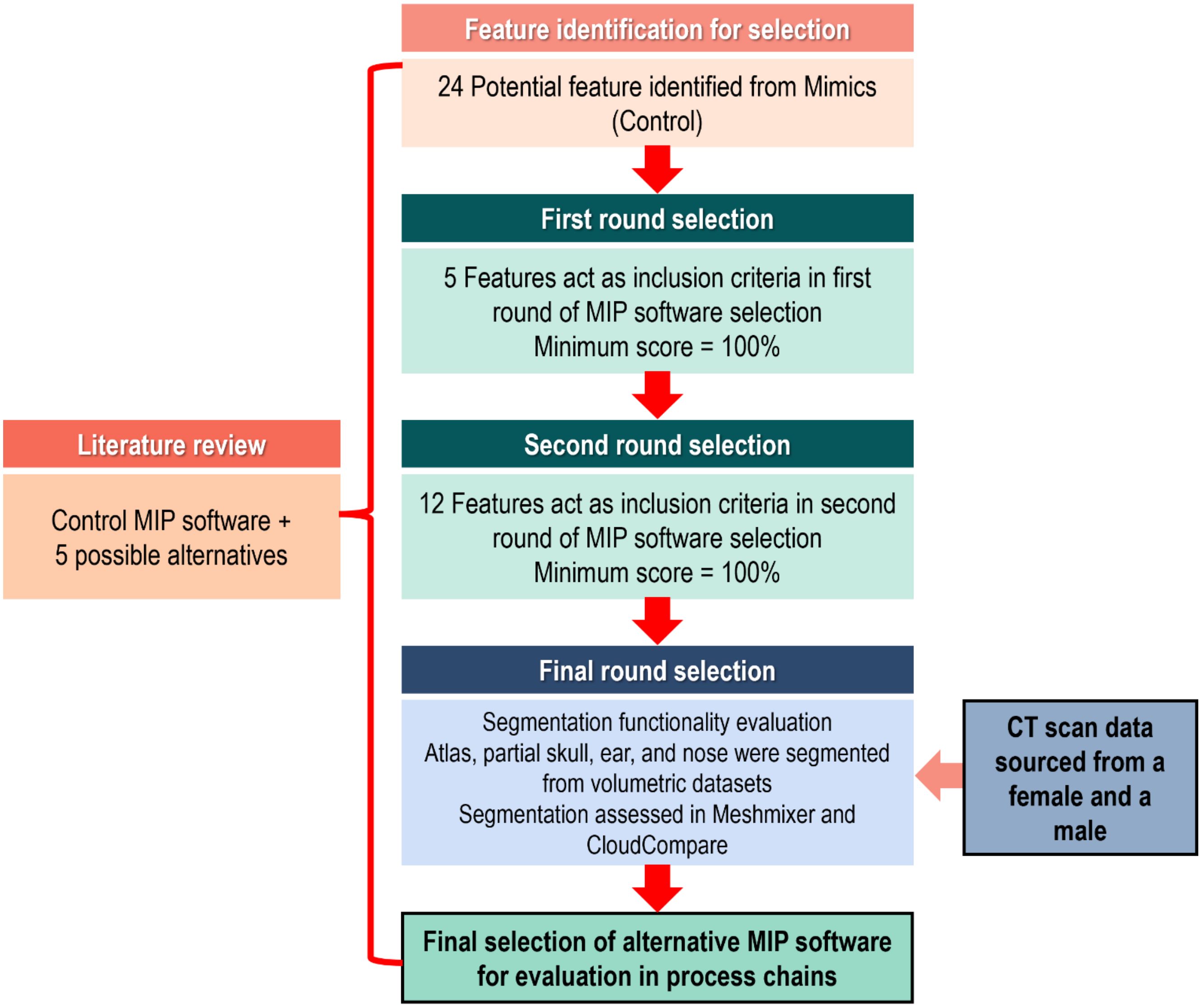

Figure 5.1 Presentation of the research process to identify alternative MIP software applications

5.2 Materials and methods

Following the identification of MIP software in the literature (3D Slicer, InVesalius, 3D Doctor, MITK, and MeVisLab), a stepwise approach was followed to compile a selection of alternative MIP software applications that could be evaluated in prosthesis manufacturing process chains. The MIP software applications identified in *Phase 1* were evaluated in two rounds based, firstly, on specific software features, and secondly, on their digital segmentation functionality.

5.2.1 Identification and description of potential software evaluation features

An evaluation guide was necessary for the first two rounds of MIP software evaluation. Using the Mimics software (control) and the Mimics manual as a guide, a list of potential software evaluation features, belonging to four categories, was identified, and described. This resulted in 24 potential evaluation features. Mimics was selected because it is FDA-approved and widely used in the medical industry and various academic institutions. It offers a comprehensive set of tools for segmenting medical scans, performing 3D reconstruction of anatomical structures, facilitating preoperative planning, and creating patient-specific designs. Table 5.1 shows the categories of the potential features and the descriptions of the features.

Table 5.1 Potential features used for the selection of evaluation features to evaluate the selected MIP software

Category		Potential evaluation features	Feature description
Digital data input	**1**	Able to import DICOM files	An international standard storage file for the medical images with metadata collected through CT or MRI scanning technologies
	2	Able to import in CT/MRI algorithm automatically or manually	Use an automatic or manual import algorithm in CT or MRI
	3	Possesses display views	2D cross-sectional images collected through CT or MRI scanning technologies viewed in three windows. (Axial, Sagittal, and Coronal)
	4	Possesses a 3D view	2D cross-sectional images displayed in the three windows are stacked or merged to create a 3D-rendered volume
	5	Displays logical view layout and user-friendly interface.	The logical flow of the layout, icons, and views displayed
Required software features	**6**	Able to adjust the orientation of imported 2D images/slices	Anterior-posterior, right-left, top-bottom orientation adjustment of imported 2D images is essential for slices to be correct
	7	Able to move through slices	Scrolling allows for moving through 2D images/slices sequentially
	8	Able to perform versatile movements within views	Move around in 2D or 3D views using panning, rotating and/or zooming utilities
	9	Able to adjust contrast levels of images/slices	Change contrast levels using a histogram to differentiate between different anatomical structures

Category		Potential evaluation features	Feature description
	10	Segmentation: Possesses manual thresholding functions	Manually settings for selecting anatomical structures for mask creation
	11	Segmentation: Able to perform predefined thresholding	Predefined settings for selecting anatomical structures for mask creation, e.g., Bone, mandible, soft tissue presets
	12	Segmentation: Able to perform mask editing of a single slice	Creating and editing a mask on a single slice
	13	Segmentation: Able to perform mask editing of multiple slices	Creating and editing a mask on multiple slices (interpolation)
	14	Segmentation: Able to perform mask subtraction.	Creating a mask layer to subtract from the volume
	15	Segmentation: Able to perform region-growing	Create 3D surface volumes from the mask selections
	16	Segmentation: Able to perform 3D volume rendering	Create a 3D rendering of the 3D surface volume of the ROI model
	17	Able to perform mesh repair	Removing small holes and noise (clean-up mesh)
	18	Able optimise mesh or to re-mesh	Reduce the number of triangles on the surface automatically
Digital data output	19	Able to create a 3D model for direct 3D printing	Design/Direct Engineering of models for 3D printing
	20	Able to export an *STL* file	Export 3D model as a Stereolithography, or Standard Triangle Language, or Standard Tessellation Language (*STL*) file for 3D printing. File format captures surface texture and shape without colour information
	21	Able to export an *OBJ* file	Export 3D model as an *OBJ* file for 3D printing developed by Wavefront Technologies. File format captures surface texture, shape, and colour
Software support and other features	22	Provides support, bug fixes, and regular updates	Software developers provide regular updates, bug fixes, and high-quality support to users
	23	Provides training videos and tutorials	Software websites provide training tutorials, support, and videos that are regularly updated to match their software updates
	24	Recommend actions for medicine and research	Software is frequently used in research studies, and developers provide links to these research articles and recommendations on how their software can be applied in different medical case studies

5.2.2 Identification of evaluation features and feature evaluation

From the 24 potential features several evaluation features were selected to evaluate the five MIP software applications. To determine which of the 24 potential features were crucial for this evaluation, a focus group of three designers was convened. These expert designers were chosen for the focus groups due to their practical experience and extensive knowledge in prosthesis manufacturing, the process chain, and alternative software programs. Following an in-depth discussion, the panel reached a consensus and suggested that the MIP software should be evaluated in two rounds. The panel suggested that in the first round, the five features of the category *Digital data input* should be used as inclusion criteria, and that a perfect score of 100% was required for a software application to advance to the next round of evaluation. The panel further recommended that twelve of the potential features should be considered in the second round of evaluation. To pass this round and to be considered for the digital segmentation functionality evaluation, a software application had to achieve a score of at least 10 out of 12 (Table 5.2).

Table 5.2 Evaluation features used as inclusion criteria in the second round of MIP software evaluation

Number	Inclusion criterion	Task description
1	Orientation adjustment of imported 2D images/slices	To perform anterior-posterior, right-left, and top-bottom orientation adjustments of imported 2D images
2	Movement through slices	To scroll to move through 2D images/slices sequentially
3	Contrast level of images/slices	To change contrast levels using a histogram to differentiate between different anatomical structures
4	Manual thresholding	To manually select settings for selecting anatomical structures for mask creation
5	Predefined thresholding	To select predefined settings for selecting anatomical structures for mask creation
6	Mask editing (a single slice)	To create and edit a mask on a single slice
7	Region growing	To create 3D surface volumes from the mask selections
8	3D Volume rendering (calculate 3D)	To create a 3D rendering of the 3D surface volume of the ROI model
9	Mesh repair	To remove small holes and noise (mesh clean-up)
10	Remeshing	To reduce the number of triangles on the surface automatic

Number	Inclusion criterion	Task description
11	Design/direct engineering of models for 3D printing	To design/direct engineering of models for 3D printing
12	Export as *STL* file	To export a 3D model as a Stereolithography, Standard Triangle Language, or Standard Tessellation Language (*STL*) file for 3D printing

5.2.3 Evaluation of digital segmentation functionality

Acquisition of real-world volumetric datasets

After selecting the MIP software applications based on the evaluation of software features, their effectiveness in segmenting real-world volumetric datasets was assessed. To perform this evaluation, it was necessary to acquire CT volumetric datasets. Therefore, on the 25th of January 2019, two real-world volumetric datasets were collected at the National District Hospital in Bloemfontein, Free State, Department of Health, South Africa. These datasets were referred to as Research Test Volumes (RTVs). A Siemens Computed Tomography (CT) scanner was used to collect the RTVs, one from a female subject (Subject 1) and one from a male subject (Subject 2). Table 5.3 describes the two RTVs.

Table 5.3 Description of the acquisition information of the two RTVs used to evaluate software segmentation

Subject 1	
Test research subject information	
Gender	Female
Age	35 (at the time of data collection)
RTV	Partial Head
Metal implants or dental amalgam fillings present	No
CT scanner and parameters	
Data collection	Siemens Computed Tomography Scanner
Medical Facility	National District Hospital in Bloemfontein, Free State Department of Health in South Africa

Subject 1	
Modality/algorithm	CT
Patient position	+0.0
Data quality	Grayscale 16 bit
Number of CT scan slices	187 (partial head scan)
Slice thickness (mm)	0.5
Slice increment (mm)	No increment
Voxel size (mm)	0.468 × 0.468 × 0.5
Resolution (pixels)	512 × 512
Subject 2	
Test research subject information	
Gender	Male
Age	52 (at the time of data collection)
RTV	Entire Head
Metal implants or dental amalgam fillings present	Yes
CT scanner and parameters	
Data collection	Siemens Computed Tomography Scanner
Medical Facility	National District Hospital in Bloemfontein, Free State Department of Health in South Africa
Modality/algorithm	CT
Patient position	HFS
Data quality	Grayscale 16 bit
Number of CT scan slices	488 (partial head scan)
Gantry/detector tilt	+0.0
Slice thickness (mm)	0.5
Slice increment (mm)	No increment
Voxel size (mm)	0.468 × 0.468 × 0.5
Resolution (pixels)	512 × 512

Identification of regions of interest

To assess the segmentation functionality of the MIP software applications, regions of interest (ROIs) for segmentation had to be identified. This involved reviewing the RTVs to identify suitable ROIs. To identify the ROIs, the RTVs were imported into Mimics software and inspected. The RTV of Subject 1 had no artefacts; however, the dental amalgam material in Subject 2's mouth introduced streak artefacts in the form of digital noise into his RTV, limiting the potential for identifying ROIs. Consequently, three ROIs were identified in Subject 1's RTV, while one was identified in Subject 2's RTV (Table 5.4). These ROIs comprised of two bony ROIs, the C1 vertebra (referred to as atlas), half skull (referred to as partial skull), and two soft tissue ROIs, an ear, and a nose. These ROIs were chosen because of their precise borders, shapes, and curves that resembled ears and noses, which were used as test geometries in further evaluations of the software and prosthesis manufacturing process chains.

Table 5.4 Description of test geometries that were segmented from the RTVs with the selected software and used to evaluate segmentation

Subject	Test geometry ROI
1	1: C1 Vertebra (Atlas)
1	2: Partial Skull
1	3: Ear
2	4: Nose

Evaluation of segmentation functionality

The segmentation functionality of the MIP software applications was evaluated if the software had passed the first two rounds of software feature evaluation. Before segmentation could commence, the RTVs were imported into the MIP software applications, including the control software, Mimics. The segmentation functionality of the software applications was evaluated by segmenting the ROIs in the RTVs, creating four test geometries of the ROIs for each software application. These test geometries were then assessed to evaluate the segmentation functionality of the software used for the segmentation. If a software application passed the segmentation evaluation, it was included in the evaluation of prostheses manufacturing process chains. Segmentation involved multiple processes in which segmentation masks, such as *Thresholding*, *Region Growing*, and *Mask Editing*, were applied. After the completion of segmentation, an *STL* file was created for each test geometry. These test geometries underwent two key evaluations. First, an error detection evaluation was performed in Meshmixer. This involved analysing discrepancies in the geometries. Second, the geometries that were produced in the MIP software were then compared to those produced with the control using CloudCompare.

Error detection using Meshmixer

Once the test geometries were generated by the selected MIP software applications, they were exported as 3D models in *STL* file format. The 3D models were then imported into Meshmixer software to assess any errors introduced during the segmentation process. The Inspector tool of Meshmixer was used to identify the errors in the mesh of the 3D models. The Inspector tool is an error detector and repair tool, which also generates measurements of the assessment indicators (Autodesk Inc. Meshmixer Manual, n.d.; Autodesk Inc. Meshmixer Overview, n.d.; Prusa3D Meshmixer Tutorial for 3D Printing Beginners, n.d.). The Inspector tool highlights the issues in the mesh with colour-coded stick/ball. The key errors that Meshmixer can identify include:

1. *Non-manifold edges*:
   Edges that do not adhere to the manifold condition, meaning they are shared by more than two faces or are not shared by any faces at all.
2. *Holes*:
   Gaps or missing faces in the mesh that create an open rather than a closed volume.
3. *Self-intersections*:
   Faces of the mesh that intersect with each other, causing geometric inconsistencies.
4. *Flipped normals*:
   Faces that are oriented incorrectly, which can cause rendering and printing issues.
5. *Duplicate faces and vertices*:
   Overlapping faces or vertices that are redundant and can cause complications in the mesh structure.

The error analysis was performed on the test geometries produced with the selected MIP software and the control software using the Inspector tool of Meshmixer. The following steps were followed to perform the error analysis (which included the repair process to ensure that the measurements are generated):

1. *Import the model:*
   - After opening Meshmixer, the 3D model was loaded into the workspace by clicking on Import.
2. *Perform an initial inspection:*
   - Obvious errors such as holes, non-manifold edges, and disconnected components were inspected by selecting the Select tool to highlight areas of interest, which were visually inspected by rotating, panning, and zooming into the model.
3. *Analysis:*
   - An analysis was performed by selecting the Inspector tool. The Inspector tool automatically detected various types of errors in the mesh, such as holes, disconnected vertices, and non-manifold edges. Detected errors are marked with coloured spheres.
4. *Repairing the model:*
   - After the Inspector tool had identified the errors, the Auto Repair All button can be selected.
   - Alternatively, specific errors can be repaired by clicking on individual spheres.
   - The holes can be closed by selecting the Simple or Smooth Fill options. Smooth Fill provides a smoother surface after closing a hole, while Simple provides a flat fill.
5. *Advanced repairs:*
   - For more complex repairs, additional tools can be used:
     - *Make Solid:* Converts the mesh to a solid model, which can sometimes fix difficult errors. Select Edit > Make Solid.
     - *Bridge*: Connects gaps or holes by creating new geometry. Select the Edit tool, then use Bridge.
     - *Erase and Fill:* Select an area around the error, then go to Edit > Erase and Fill to cleanly remove and fill in the area.
6. *Validation:*
   - After repairing, the Inspector tool was run again to ensure all errors had been fixed.
   - The geometries were checked, and if errors had persisted, the process was repeated.
7. *Export the repaired model:*
   - After fixing the errors, the model was exported by selecting File > Export and choosing the appropriate format (e.g., *STL*, *OBJ*).

Table 5.5 presents the error and repair analysis information that is supplied by Meshmixer's Inspector tool.

Table 5.5 Error and repair analysis output produced by Meshmixer's Inspector tool

Analysis Inspector	Total number of errors (starburst)	After eliminating floating pixels around the mesh model (residual data)	After errors repaired, hole filling, overlapping vertices	Number of vertices	Number of triangles

A Multivariate Analysis of Variance (MANOVA) was performed on the error analyses produced with Meshmixer. MANOVA compared means across multiple dependent variables simultaneously to ascertain if changes in independent variables (Software applications) had significant effects on a combination of dependent variables (number of errors, number of triangles). The online calculator of Statistics Kingdom was used to perform these calculations (https://www.statskingdom.com/manova-calculator.html). A 5% level of significance was used in the calculation.

Geometry comparison using CloudCompare

The geometries produced with the alternative MIP software that passed the two feature evaluation rounds were also compared to the control model using CloudCompare. The comparison entailed the evaluation of the mesh discrepancies between two 3D models to determine the suitability of the MIP software for further evaluation of performance in process chains. The *STL* files of the 3D models were first imported into CloudCompare to perform the comparisons. For each MIP software, four pairwise comparisons were performed; for example, each test model produced with software was compared to the control model.

CloudCompare is an open-source software used for identifying and correcting errors in 3D models. The most important CloudCompare attributes are: point cloud processing, mesh processing, alignment and registration, distance computation, visualisation, and analysis tools, advanced analysis, measurement tools, filtering, and noise reduction (CloudCompare User Manual Version 2.6.1, n.d.). The following steps were followed to perform the CloudCompare comparisons:

1. *Align the geometries:*
   - The two models were initially aligned using the ICP (Iterative Closest Point) algorithm to ensure optimal overlapping.
   - Alignment was achieved using Edit > Register > Align (point pairs picking) or the ICP (Iterative Closest Point) algorithm (Edit > Register > ICP).
2. *Compute distance (Cloud-to-Mesh):*
   - The Cloud-to-Cloud Distance (C2C) tool was used to quantify the geometric differences between the two models by selecting the two-point clouds or a point cloud and a mesh. This was achieved by selecting Tools > Distances > Cloud/Cloud Dist.
     - Alternatively, for Cloud-to-Mesh distance, Tools > Distances > Cloud/Mesh Dist. can be used.
     - The parameters were set (such as the maximum distance), and the distance was computed.
3. *Analyse the results:*
   - Once the computation had been completed, CloudCompare generates a scalar field with the distances.
     - The distances were visualised by activating the scalar field display in the properties window.
     - The colour scale can be adjusted to highlight areas of interest by selecting Tools > Scalar fields > Display parameters.
4. *Extract statistical information:*
   - The statistical information about the distances was obtained using Tools > Scalar fields > Compute stat. params.
     - Heat maps use colours to represent the magnitude of differences between two aligned models. This provides an intuitive visual representation of where the models differ most significantly. Blue areas show regions of minimal deviation, indicating that both geometries are highly consistent in these areas. Red areas show regions with significant deviation, suggesting discrepancies between the geometries are possibly due to scanning angles, occlusions, or alignment issues. Gradient areas are areas with a gradient from blue to red, indicate a transition in deviation, which can help to identify the direction and nature of the differences.
     - Mean distance (MD) is defined as the average distance between corresponding points on the two geometries. A lower mean distance indicates better alignment and similarity. A MD of 0.2 mm indicates that, on average, the points are very close, and a standard deviation (SD) of 0.05 mm implies that the distances are consistent.
     - Root Mean Square (RMS) distance is defined as the square root of the average of the squared distances. It gives more weight to larger deviations, providing an overall measure of the difference magnitude. An RMS distance of 0.22 mm suggests that most of the points are well-aligned with some minor deviations. An RMS = 0 indicates that the histograms are identical; RMS ~ 1 indicates that both histograms are obtained from the same parent distribution; RMS >> 1 indicates histograms are obtained from different parent distributions.

- The Gauss Chi[2] distance measures how well the distribution of distances between these two datasets fits a normal (Gaussian) distribution. It essentially tests the hypothesis that the observed distance distribution follows a Gaussian distribution. A large Chi[2] distance could be an indication that the differences between the meshes are not normally distributed and could warrant further investigation. It could suggest issues such as outliers, significant deviations, or other abnormal behaviours in the data.
- A histogram shows the frequency distribution of the distances between points. This helps visualise how distances are spread and identify any outliers.

5.2.4 Selection of alternative MIP software

A systematic approach was followed to identify the most suitable alternative MIP software that should be evaluated in process chains. The evaluations performed with Meshmixer and CloudCompare were carefully analysed using the following steps:

Meshmixer output evaluation:

- The Starburst output of the colour-coded stick/ball indicators produced by Meshmixer's Inspector tool was compared across the groups of ROI models, including the atlas, partial skull, ear, and nose.
- The number of errors within each group of models was also assessed and compared to evaluate software performance.

CloudCompare output evaluation:

- The heat maps generated by CloudCompare for different the groups of ROI models, including atlas, partial skull, ear, and nose, were examined.
- The histograms were analysed to assess the distribution of distances, identify patterns, and detect outliers within the data.
- The statistical outputs from CloudCompare were finally reviewed to identify trends and patterns that could influence software selection.

5.3 Results

5.3.1 MIP software features evaluation

During the initial phase of evaluating the five alternative MIP software applications chosen in *Phase 1*, the software's capabilities and attributes that related to *Digital data input* were evaluated. Three software applications, in addition to the control software, received perfect scores of 100% and were chosen for the second evaluation round. In this stage of the evaluation, MeVislab and MITK were eliminated, because their scores were less than 100%. Table 5.6 presents the evaluation of the *Digital data input* features.

Table 5.6 First round of alternative MIP software evaluation based on the *Digital data input* features

Evaluation feature	MIP software evaluation					
	Mimics (C)	3D Slicer	InVesalius	MeVislab	MITK	3D Doctor
Import DICOM files	✓	✓	✓	✓	✓	✓
Import in CT/MRI algorithm	✓	✓	✓	✓	✓	✓
Possesses display views	✓	✓	✓	×	✓	✓
Possesses a 3D view	✓	✓	✓	✓	✓	✓
Displays logical view layout and user-friendly interface.	✓	✓	✓	×	×	✓
Total score	5	5	5	3	4	5
% score	100	100	100	60	80	100

C = control software application

The 12 selected software features were evaluated in the second round of the evaluation of the MIP software. Aside from the control software, the software applications, 3D Slicer and InVesalius, were selected for evaluation of segmentation functionality based on their satisfactory scores in the first round, which were greater than 80%. In this round, 3D Doctor was eliminated, because it scored less than 80%. Table 5.7 shows the outcome of the second round of MIP software evaluation using the 12 inclusion software features.

Table 5.7 Second round of alternative MIP software evaluation based on the twelve inclusion software criteria

Inclusion criterion	MIP software			
	Mimics (C)	3D Slicer	InVesalius	3D Doctor
Orientation adjustment of imported 2D images/slices	✓	✓	✓	×
Movement through slices	✓	✓	✓	✓
Contrast level of images/slices	✓	✓	✓	✓
Manual thresholding	✓	✓	✓	✓
Predefined thresholding	✓	✓	✓	×
Mask editing (a single slice)	✓	✓	✓	✓
Region growing	✓	✓	✓	✓
3D Volume rendering (calculate 3D)	✓	✓	✓	✓
Mesh repair	✓	×	✓	×
Remeshing	✓	×	×	×
Design/Direct engineering of models for 3D printing	✓	✓	✓	✓
Export as *STL* file	✓	✓	✓	✓
Total score	12	10	11	8
% score	100	83.3	91.7	66.7

C = control software application

5.3.2 MIP software digital segmentation functionality

Besides the control software, Mimics, 3D Slicer, and InVesalius successfully passed the software features evaluation. These software applications were thus subjected to an assessment of their digital segmentation functionality. Table 5.8 presents photographs of the 3D models of the four ROIs produced by the three MIP software applications. It was challenging to objectively evaluate the quality of the models based solely on their visual appearance. Therefore, the models of the different MIP software applications were subjected to further assessments.

Table 5.8 Photographs of the 3D models produced by Mimics, 3D Slicer, and InVesalius

Mimics	
Atlas	Partial skull
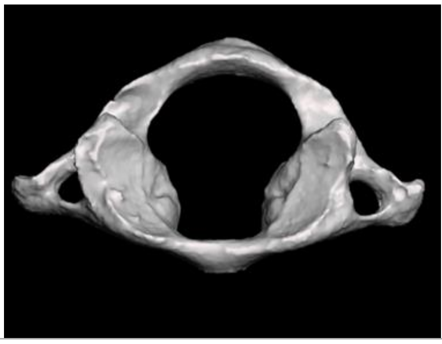	
Ear	Nose
	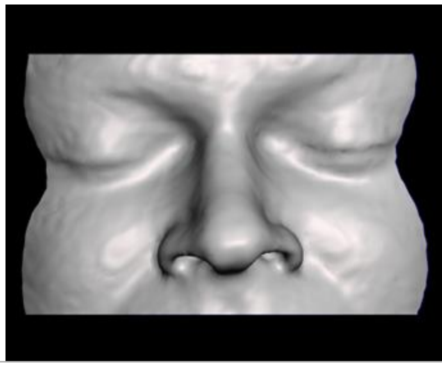
3D Slicer	
Atlas	Partial skull
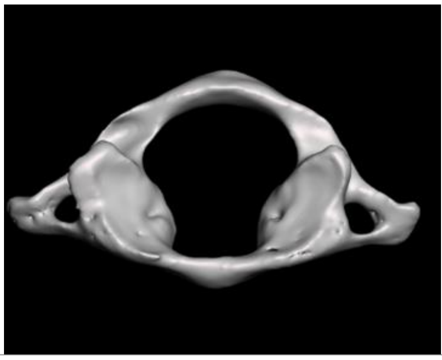	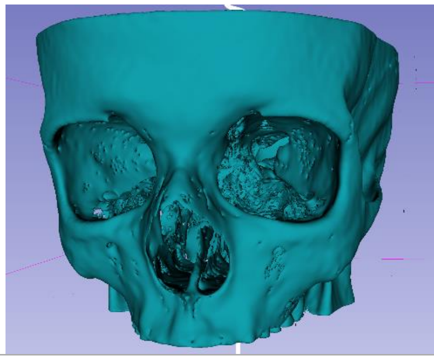
Ear	Nose
	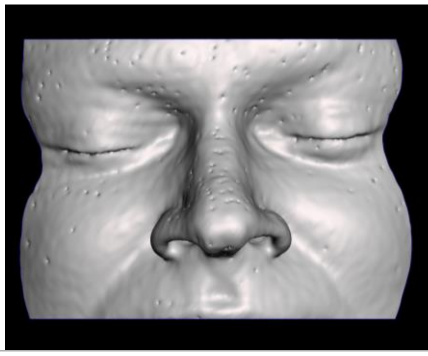

InVesalius	
Atlas	Partial skull
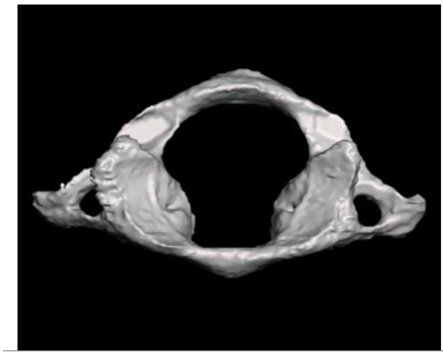	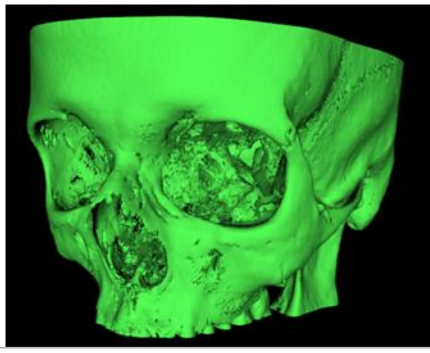
Ear	Nose
	

5.3.3 Error detection using Meshmixer

To achieve a greater understanding of how the segmentation functionality of the three MIP software compared, the error density of the segmented 3D models was assessed in Meshmixer. For three of the models, atlas, ear, and nose, the control software introduced the least number of errors, which was also evident in the starbursts (Table 5.9). When comparing the models produced with 3D Slicer and InVesalius, no clear distinction between the software applications could be made based on the introduction of errors. Therefore, a MANOVA was performed to statistically assess the differences across multiple dependent variables simultaneously. The MANOVA test indicated that there was a non-significant small difference in the software applications between the different groups, $F(4, 18) = 1.09$, $p = .391$, Pillai's V = 0.39, partial $\eta^2 = .2$. The error assessment thus revealed that none of the alternative MIP software consistently outperformed the other software. It could, therefore, be concluded that it was not feasible to identify alternative MIP software at this stage of the evaluation, which suggested that further testing was necessary.

Table 5.9 Meshmixer Inspector error analysis of the atlas, partial skull, ear, and nose models of Mimics, 3D Slicer, and InVesalius

Atlas

Mimics

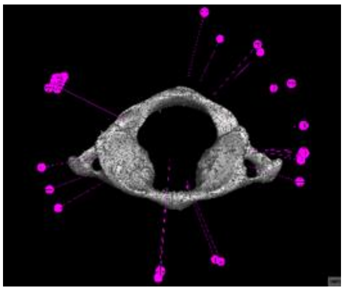

3D Slicer

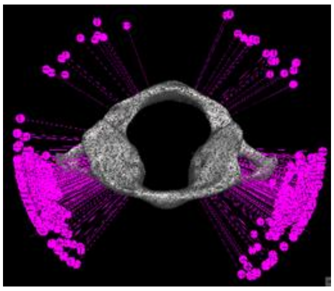

InVesalius

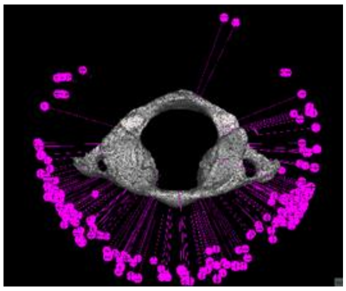

Software	Number of errors	Number of vertices	Number of triangles
Mimics (C)	32	30423	60854
3D Slicer	359	40552	79796
InVesalius	173	20743	40768

Partial skull

Mimics

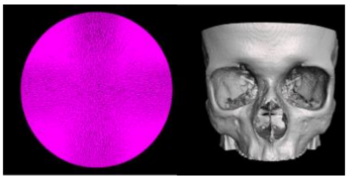

3D Slicer

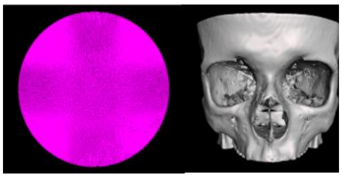

InVesalius

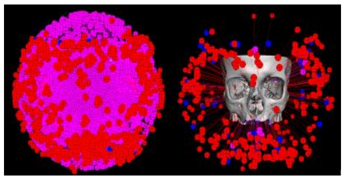

Software	Number of errors	Number of vertices	Number of triangles
Mimics (C)	70207	2119210	4016908
3D Slicer	46799	2049121	3722416
InVesalius	12725	1068640	2144335

Ear

Mimics

3D Slicer

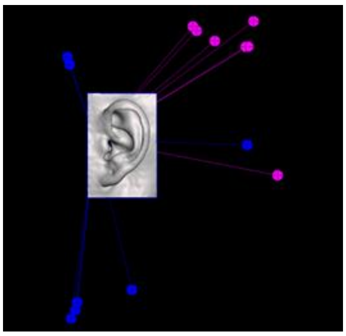

InVesalius

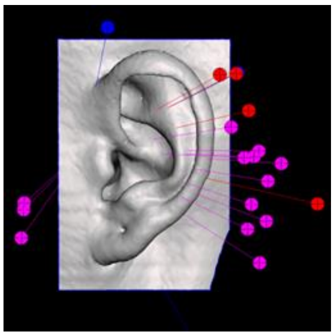

Software	Number of errors	Number of vertices	Number of triangles
Mimics (C)	0	19008	38020
3D Slicer	14	454712	292905
InVesalius	20	20699	40170

Nose		
Mimics	3D Slicer	InVesalius
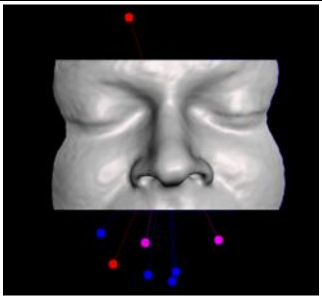	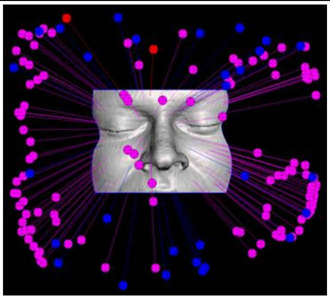	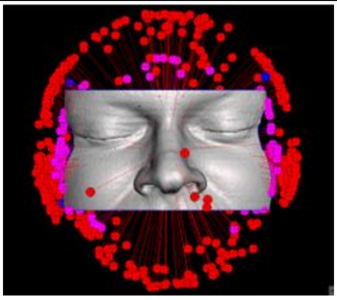

Software	**Number of errors**	**Number of vertices**	**Number of triangles**
Mimics (C)	7	19942	38490
3D Slicer	146	1263292	1183675
InVesalius	511	144340	292340

5.3.4 MIP software model comparison with control model

Several analyses, using CloudCompare, were performed to further assess how the segmentation functionality of the MIP software compared with the control software (Mimics). These analyses included the visual inspection of the heat maps and the inspection of several statistics.

Heat map of atlas comparison

The heat maps generated in CloudCompare revealed noticeable visual differences when the atlas 3D models of the alternative MIP software were compared to the models of the control software. For the 3D Slicer model, most of the discrepancies with the control atlas model fell within the mid-range of the heat map, with a few larger deviations highlighted in red (Table 5.10). In contrast, the heat map of the comparison between the InVesalius atlas model and the control model showed differences predominantly in the blue-green range, indicating that many discrepancies between these models were relatively minor.

Table 5.10 Visual comparisons of Mimics segmented atlas model and the 3D Slicer and InVesalius models

3D Slicer

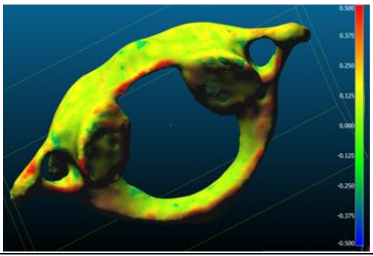
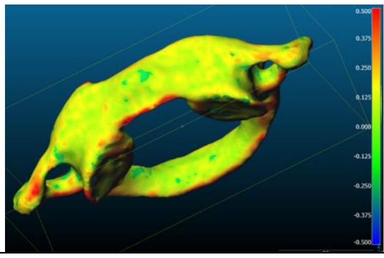
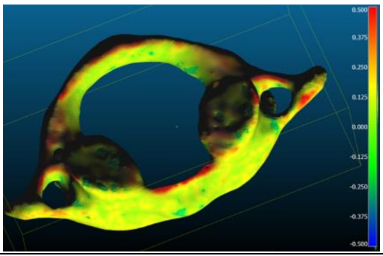

InVesalius

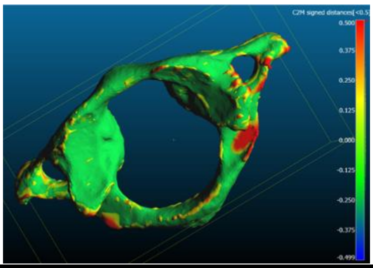
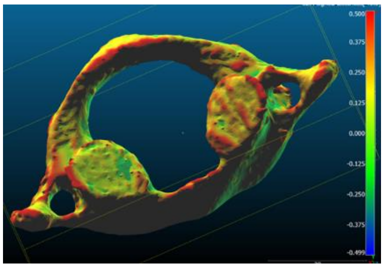
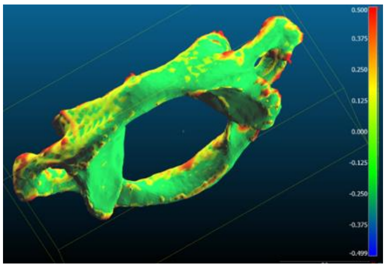

Heat map of partial skull comparison

The heat maps of the comparison between the segmented models of the partial skull produced with 3D Slicer and InVesalius with the control model revealed noticeable visual differences. These differences contrasted the findings for the atlas. For the 3D Slicer model, most discrepancies with the control skull model fell within the mid-range of the heat map, with a few significant deviations highlighted in red (Table 5.11). In contrast, the heat map comparing the InVesalius model to the control partial skull model showed differences predominantly in the yellow-red range, indicating that many of the discrepancies between these models were relatively large.

Table 5.11 Visual comparisons of Mimics segmented partial skull model with 3D Slicer and InVesalius models

3D Slicer		
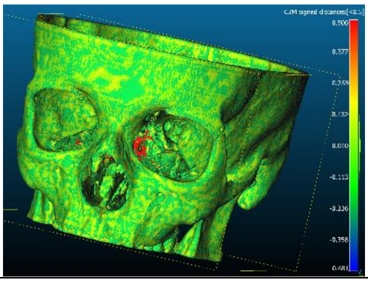	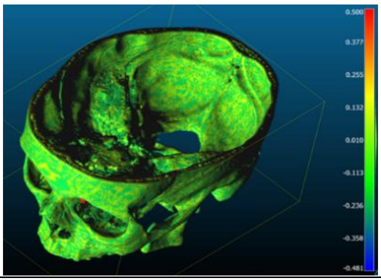	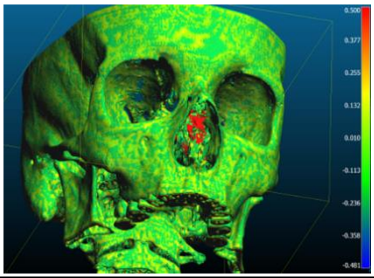
InVesalius		
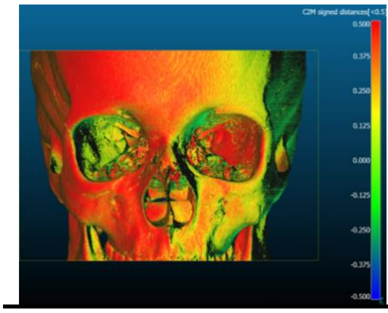	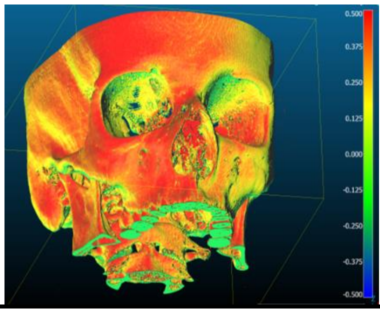	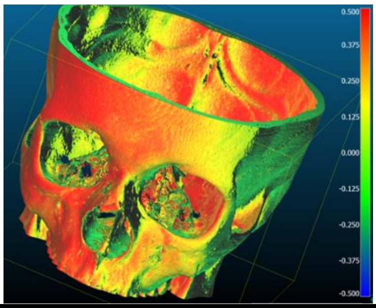

Heat map of ear comparison

The heat maps comparing the 3D Slicer and InVesalius segmented ears with the Mimics segmented ear were largely similar. For both the 3D Slicer and InVesalius models, most discrepancies with the Mimics ear model fell within the mid-range of the heat map, with a few significant deviations highlighted in red (Table 5.12). However, the heat map of the InVesalius model displayed noticeably more significant discrepancies, highlighted in red, than the 3D Slicer model.

Table 5.12 Visual comparisons of Mimics segmented ear model with 3D Slicer and InVesalius models

3D Slicer		
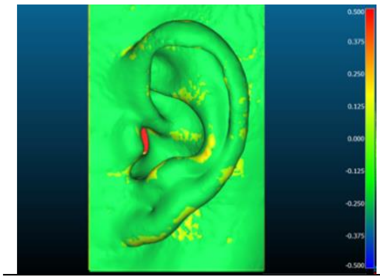	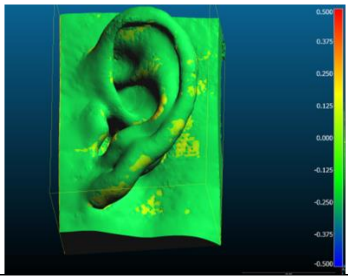	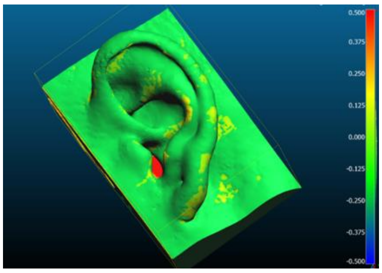
InVesalius		
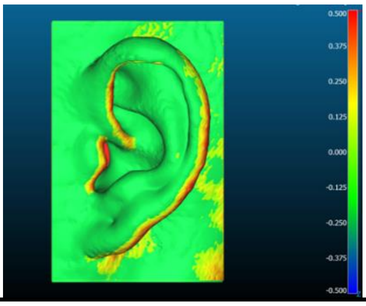	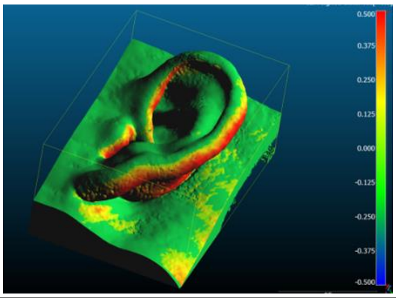	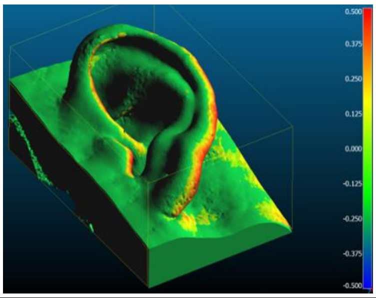

Heat map of nose comparison

When the heat maps of the 3D Slicer and InVesalius nose models were compared with the Mimics nose model, distinct visual differences were found. In the 3D Slicer model, most discrepancies with the Mimics nose model were distributed across the upper mid-range to the red spectrum, indicating a range of minor to substantial differences (Table 5.13). Conversely, the InVesalius nose model exhibited large regions with relatively minor discrepancies highlighted in green alongside substantial areas with significant discrepancies highlighted in dark red.

Table 5.13 Visual comparisons of Mimics segmented nose model with 3D Slicer and InVesalius models

3D Slicer

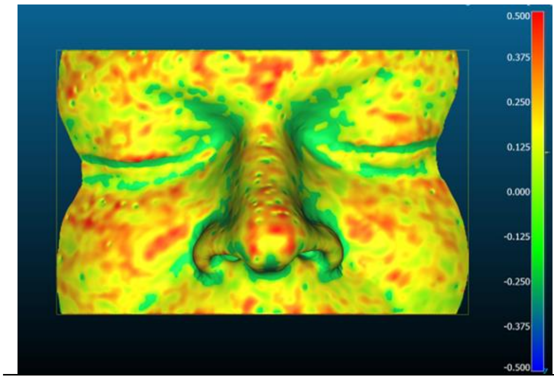

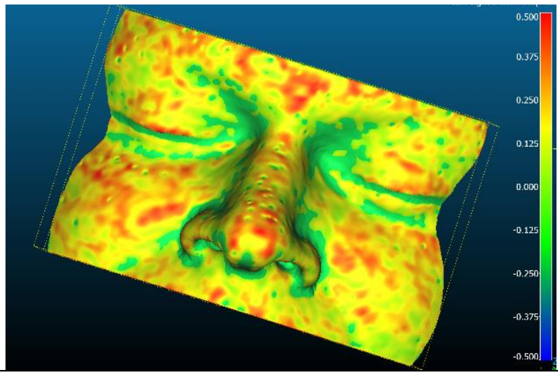

InVesalius

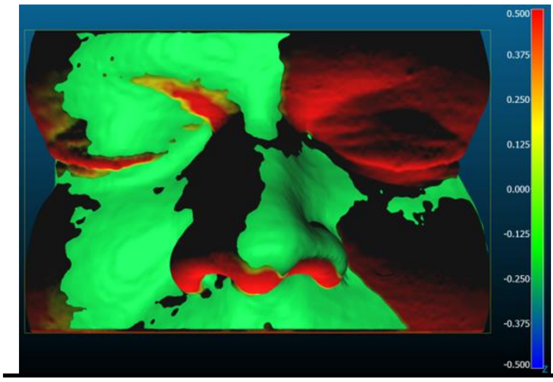

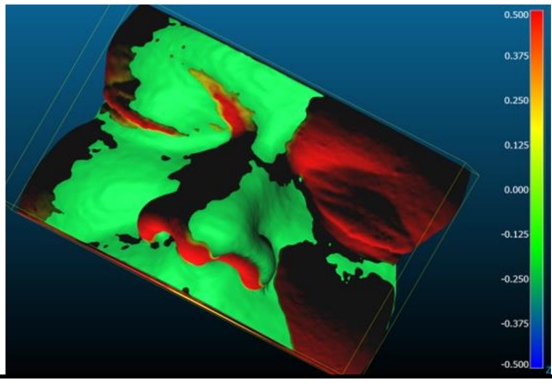

Comparative statistics

The statistical analyses with CloudCompare contributed to a better understanding of the general agreement or divergence between the models produced with the control software and the models produced with 3D Slicer and InVesalius. The analyses supported the visual inspection of the heat maps, highlighting deviations in the segmentation models produced by 3D Slicer and InVesalius when compared to the Mimics model. The histograms and Gaussian Chi^2 distance values indicated that none of the distance distributions followed a Gaussian pattern, which suggested that the differences between the two datasets were not random but probably followed systematic patterns or contained outliers. The histograms also showed an overrepresentation of extreme distance measurements at the far right of most distributions, while some histograms displayed peaks within the distributions, which indicated an overrepresentation of certain distance measurements. The mean distance and RMS values verified that the discrepancies in the 3D Slicer models were slightly less pronounced than the InVesalius models of the partial skull, ear, and nose, although this trend was not true for the atlas. Table 5.14 lists the statistics of the CloudCompare comparisons between the models of the control software Mimics and the models produced with 3D Slicer and InVesalius.

Table 5.14 Statistics of the CloudCompare comparison of the 3D Slicer and InVesalius models with the Mimics models

ROI	Geometry comparison	CloudCompare distance comparison statistics				
		Mean distance	**RMS distance**	**Gauss Chi² distance**	**Differences histogram**	**Remark**
Atlas	Mimics + 3D Slicer	0.166 (SD = 0.169) Value is less than 0.2 mm, which indicates that on average, the points are close.	0.237 Value suggests that most of the points are well-aligned with some deviations.	362308	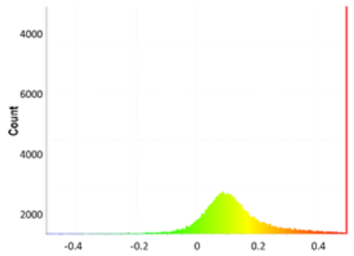	Mimics geometry slightly smaller than the 3D Slicer geometry. Similarly, between geometries are relatively high.
Atlas	Mimics + InVesalius	0.088 (SD = 0.212) Value is much less than 0.2 mm, which indicates that on average, the points are very close.	0.230 Value suggests that most of the points are well-aligned with some deviations.	42255.2	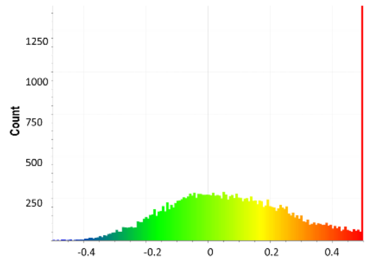	Mimics mesh is a little smaller on the X-axis and the Z-axis.
Skull	Mimics + 3D Slicer	0.020 (SD = 0.129) Value is much less than 0.2 mm, which indicates that on average, the points are very close.	0.131 Value suggests that most of the points are well-aligned with some minor deviations.	1×10^7	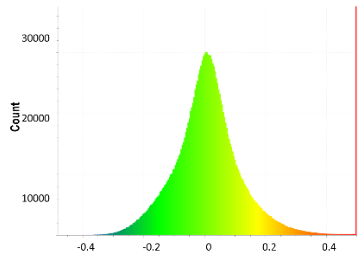	Both geometries are very similar in size. The Mimics mesh is a little larger on the Y-axis, however on the Z-axis just a little smaller. The Mimics mesh also consists of slightly more faces.

Central University of Technology, Free State

Skull	Mimics + InVesalius	0.050 (SD = 0.300) Value is much less than 0.2 mm, which indicates that on average, the points are very close.	0.300 Value suggests that the points are reasonably well-aligned with some deviations.	1×10^7	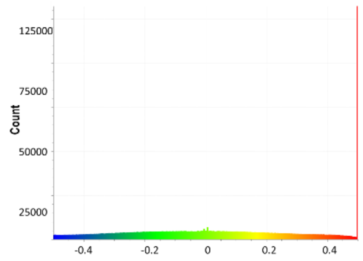	The Mimics mesh is smaller on the X-axis as well as little smaller on the Y-axis and the same size on the Z-axis.
Ear	Mimics + 3D Slicer	-0.042 (SD = 0.164) Value is less than 0.2 mm, which indicates that on average, the points are close.	0.169 Value suggests that most of the points are well-aligned with some minor deviations.	1.305×10^6	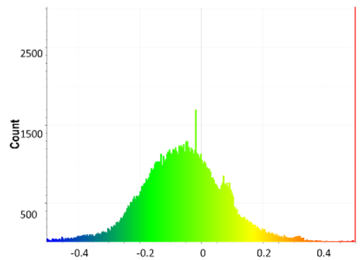	Both geometries are similar in size.
Ear	Mimics + InVesalius	0.122 (SD = 0.336) Value is less than 0.2 mm, which indicates that on average, the points are close.	0.357 Value suggests that the points are reasonably well-aligned with some deviations.	577598	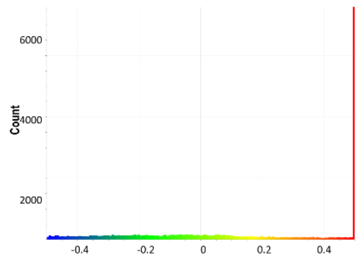	Mimics mesh is slightly larger on the X-axis and the Z-axis and almost the same size on the Y-axis.

Nose	Mimics + 3D Slicer	0.140 (SD = 0.190) Value is less than 0.2 mm, which indicates that on average, the points are close.	0.236 Value suggests that most of the points are well-aligned with some deviations.	1 × 10^7	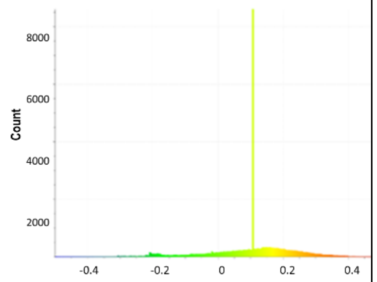	Both meshes are similar in size.
Nose	Mimics + InVesalius	0.288 (SD = 0.300) Value is greater than 0.2 mm, which indicates that on average, the points are not so close.	0.416 Value suggests that the points are not so well-aligned with some large deviations.	1 × 10^7	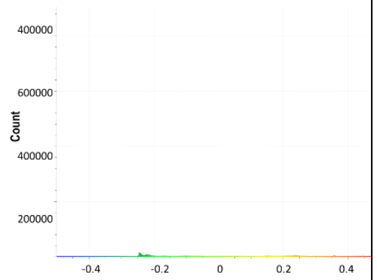	Mimics mesh is a little smaller on the X-axis and the Z-axis, and larger on the Y-axis.

RMS = Root mean square; SD = Standard deviation

5.4 Discussion and conclusion

After completing the Meshmixer and CloudCompare evaluations, it became evident that there was no clear distinction in the digital segmentation performance between 3D Slicer and InVesalius. Although 3D Slicer demonstrated slightly better segmentation accuracy in terms of deviations from the control software Mimics, the differences were not substantial enough to warrant the exclusion of either software application. According to Yap Abdullah et al. (2024) and Mandolini et al. (2022), 3D Slicer slightly outperformed InVesalius in terms of 3D reconstructions and geometric accuracy. Consequently, it was decided that the performance of both 3D Slicer and InVesalius would be evaluated in process chains for the manufacturing of external maxillofacial prostheses. Both 3D Slicer and InVesalius are open-source software, which makes them particularly well-suited for integration into more cost-effective process chains. 3D Slicer offers extensive modules for image segmentation, 3D modelling, and surgical planning, which are critical components in prosthesis design (Fedorov et al., 2012). The application is also known for its precision in anatomical replication (Pieper et al., 2004). InVesalius, on the other hand, excels in the visualisation and reconstruction of anatomical structures from DICOM files, with strong segmentation tools that facilitates precise delineation of anatomical regions (Amorim et al., 2015; Kamio et al., 2020). Both software applications support various file formats, which are of value in CAD processing (Jardini et al., 2014; Durisetti et al., 2022) and highlight their potential use in prosthesis manufacturing process chains.

Chapter 6

Evaluation of Computer-aided Design Software

6.1 Introduction

The computer-aided design (CAD) software applications that were found in the literature in *Phase 1*, were further evaluated in *Phase 2*. CAD software allows for the design of highly accurate three-dimensional (3D) models of a patient's facial anatomy, using detailed scans to ensure the prosthesis fits seamlessly and looks natural. Designers use CAD software to design and sculpt digital prosthetic models, changing textures and shapes to better fit the patient's distinct facial features. This procedure not only makes the prosthesis more aesthetically pleasing and practical, but it also expedites manufacture and makes designs more repeatable. Access to advanced CAD software allows healthcare providers to customise facial prostheses, thereby greatly enhancing the quality of life for those who need these devices. Therefore, in *Phase 3* a comprehensive assessment of the CAD software chosen from the literature was undertaken following a systematic approach. The sub-question addressed in this phase was:

Which CAD software can be selected and tested based on specific software features and digital sculpting capability criteria?

Figure 6.1 Presents a flow diagram of the process followed to select alternative CAD software to be tested in external maxillofacial prosthesis manufacturing process chains.

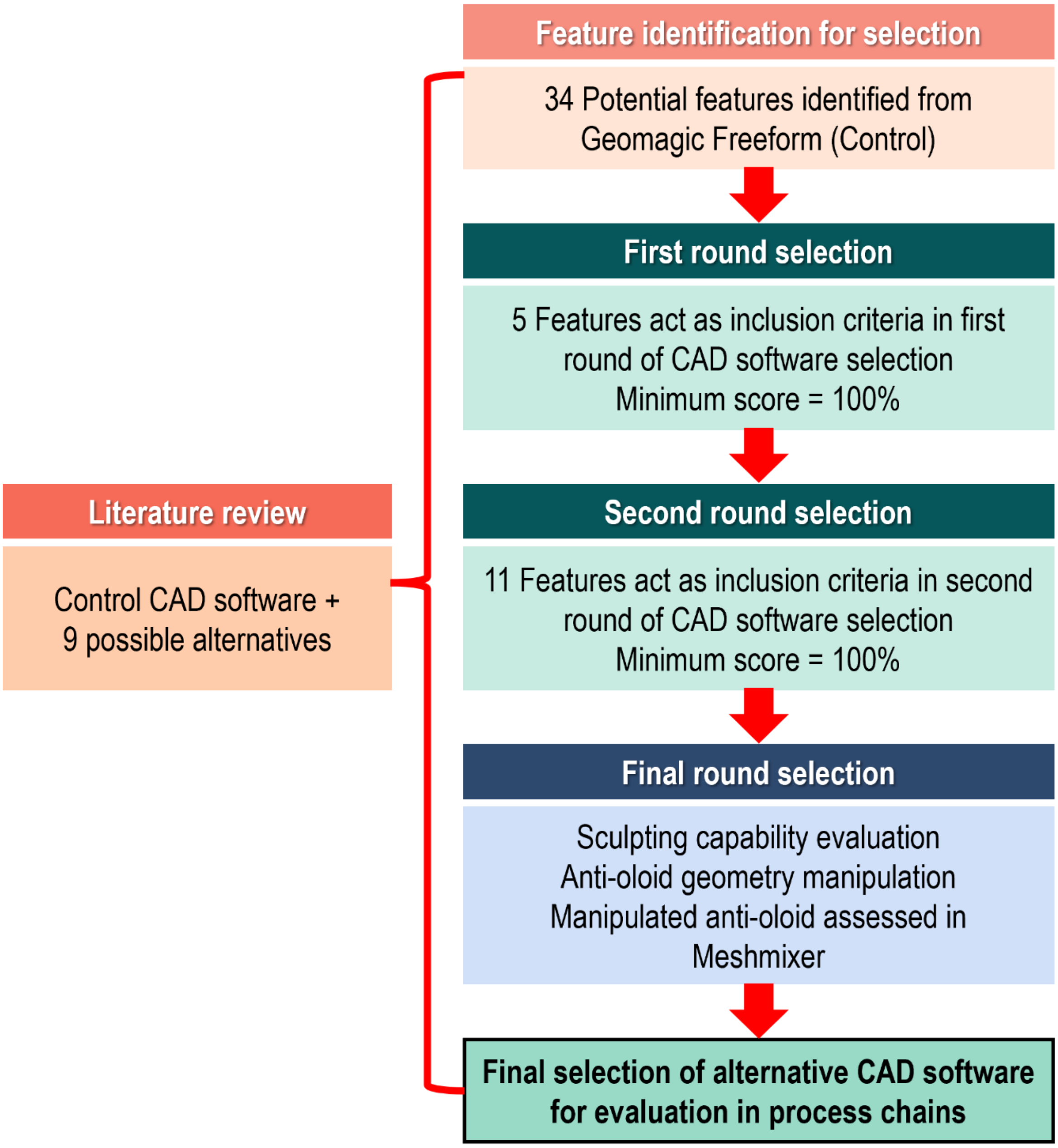

Figure 6.1 Presentation of the research process to identify alternative CAD software applications

6.2 Materials and methods

The selection of CAD software was consistent with the assessment of medical image processing (MIP) software. In the first two rounds, the evaluation was based on key software features as inclusion criteria. The subsequent evaluation focused on the digital sculpting capabilities of the software. Nine

CAD software applications, chosen from the literature, were included in this evaluation in addition to the control software, Geomagic Freeform from 3D Systems, Inc.

6.2.1 Identification and description of potential software evaluation features

Similarly to the evaluation of the MIP software, an evaluation guide was required for the two rounds of CAD software feature assessment. Potential evaluation software features were identified by examining the control software, Geomagic Freeform, and the manual as a guide. This examination resulted in 33 potential features that could be used in the first two rounds of software feature evaluation. Table 6.1 presents the potential evaluation features along with their descriptions.

Table 6.1 Potential features used for the selection of evaluation features to evaluate the selected CAD software

	Software feature	Description
1	Haptic device interface	A haptic interface is a 3D virtual tool accompanying the software Geomagic Freeform. A haptic device provides precision positioning input, and high-fidelity force-feedback output used for digital sculpting can define and manipulate more organic and anatomical models.
2	Digital sculpting interface	A digital sculpting software interface facilitates the design of organic features and models. It uses a brush-based and carving-tool user interface, allowing digital sculpting of 3D virtual clay.
3	Import 3D file formats	Import 3D file formats, such as *STL* and *OBJ*.
4	Possesses workspace	A 3D virtual workspace to sculpt 3D virtual clay digitally.
5	Coordinate system	XYZ coordinates (Cartesian coordinate system).
6	Triad/gizmo indicator	XYZ coordinates displayed in the workspace, indicating the positioning of the 3D virtual clay model.
7	Additional view for orientation in spatial virtual space	A 3D virtual clay model is displayed in an additional view/window to assist sculpting and positioning in spatial 3D virtual space.
8	Software user interface	The logical flow of the layout, icons, and views displayed.
9	Sculpting and modelling tools	Sculpting and modelling tools to apply on a 3D virtual clay model.
10	Navigation	Move around the workspace and navigate a 3D virtual clay model using panning, rotating, and zooming utilities.

11	Layer system	A layering system is required to separate each of the different activities.
12	Buck setting	Locking a 3D virtual clay model to protect it from any changes.
13	Planes	Planes to assist during alignment, cutting/slicing, and drawing on a curve.
14	Viewing the virtual model	Transparent or mesh or clay.
15	Drawing/sketching and curve tools	Drawing and sketching tools to draw a design before sculpting a 3D virtual clay model from the 2D drawing.
16	2D and 3D curve editing	Changing 2D and 3D curves.
17	Measurements	Measurement tools for determining the accurate measurements of a 3D virtual clay model created digitally to match it with real-world measurements: 3D Ruler, 3D geometry mass properties, and surface and volume mass properties.
18	Add and subtract clay	Adding and subtracting or removing clay from the primary virtual clay model.
19	Smoothing	Smoothing functions to smooth out the surface of a 3D virtual clay model.
20	Tugging and pulling (extrusion) functions	Tugging and pulling to transform a virtual clay model.
21	Interactive mirroring techniques	Using different interactive mirroring techniques.
22	Subdivide meshes	Subdividing meshes for smoother surface sculpting.
23	Boolean operations	*Union:* uniting two or more 3D virtual objects resulting in a single object; *Intersect:* intersecting two or more objects resulting in an overlapping object outcome; *Difference:* subtracting one object from another; and *Symmetric difference:* unifying two or more objects that result in an object outcome that excludes the overlapping intersecting parts.
24	Detailing and texturing virtual clay	Embossing, engraving, and texturing a virtual clay model using different digital tools to create realistic detail.
25	Photorealistic results	A style of painting that resembles photography in its meticulous attention to realistic detail.
26	Hyperrealistic results	Hyperrealism is a genre of painting and sculpture resembling a high-resolution photograph. Hyperrealism is considered an advancement of Photorealism by the methods used to create the resulting paintings or sculptures with meticulous attention to realistic detail.
27	Mask layer	Creating a mask layer to subtract, move, or pull a section from the larger volume. Masking also protects certain areas from being altered.
28	Cropping of 3D volume	Cropping the 3D virtual clay volume to delete unwanted structures.
29	Invert data selection	Select the inverse of a virtual clay model.
30	Remesh/retopolise	Applying remeshing techniques to reduce the number of triangles of the surface and volume mesh.
31	Mould generation	Mould generation is important for the 3D printing process and can be achieved using the parting line curve, shell a model function, and create a split joint.

32	Export an *STL* file	Export a 3D virtual clay model as a Stereolithography, Standard Triangle Language, or Standard Tessellation Language (*STL*) file for 3D printing.
33	Export an *OBJ* file	Export a 3D virtual clay model as an *OBJ* file for 3D printing developed by Wavefront Technologies. This file format captures surface texture, shape, and colour.

6.2.2 Identification of evaluation features and feature evaluation

To establish which of the 33 potential software features were essential for the evaluation of the CAD software, a focus group of three designers was constituted. The expert designers were selected for the focus groups based on their substantial practical experience, comprehensive knowledge of prosthesis design and manufacturing, and knowledge of various alternative software programs. After an in-depth discussion, the panel reached a consensus that 16 of the potential features should be used as evaluation features of the CAD software. These evaluation features belonged to the four categories; *Digital data input*, *Required software features*, *Digital output data, Software support and other features.* The panel further suggested that a similar evaluation approach as in *Phase 2* should be followed. They suggested that features 1 to 5 should be evaluated in the first round and the remainder in the second round. For software to pass the first round required a perfect score of 100%, and those that passed in the first round should also obtain a perfect score in the second round to then be evaluated for their digital sculpting capabilities. Table 6.2 presents the 16 evaluation software features used in the two rounds of CAD software selection.

Table 6.2 Evaluation features used as inclusion criteria used in the first and second rounds of the CAD software evaluation

Category		Inclusion criterion	Task description
Digital data input	**1**	Able to import 3D file format	Importing 3D file formats, such as *STL* and *OBJ*, is required.
	2	Have an advanced digital sculpting interface	An advanced digital sculpting interface that facilitates the design of the organic features of external maxillofacial prostheses.

	3	Contain measurement tools	Measuring tools are required to determine how accurately the 3D virtual clay model scale is created digitally to match it with real-world measurements.
	4	Able to perform actions to mimic human anatomy using a large variety of sculpting tools (>20)	Creating overhangs, undercuts, and holes by adding and removing clay and tugging and pulling clay.
	5	Sculpting highly detailed models	Able to create own surface texture tools to add advanced surface detailing and texturing.
	6	Able to perform interactive mirroring techniques	Using different interactive mirroring techniques to, for example, mirror an ear from one side to the opposite side to replace missing anatomy.
Required software features	7	Able to perform Boolean operations	*Union* - uniting two or more objects resulting in a single object; *Intersect* - intersecting two or more objects resulting in an overlapping object outcome; *Difference* - subtracting one object from another; and *Symmetric difference* - unifying two or more objects that result in an object outcome that excludes the overlapping intersecting parts.
	8	Able to perform advanced smoothing	Smoothing out the surface without losing detail and reducing the geometry size.
	9	Painting and rendering functions	Hyperrealism is a genre of painting and sculpture that resembles high-resolution photographs. It advances photorealism through methods that achieve meticulous, realistic detail in the resulting artworks.
	10	Transformations using a mask	Creating a mask layer to subtract, move, or pull a section from the larger volume.
	11	Subdivide mesh/tessellation	Subdividing meshes allows for smoother surface sculpting by adding more polygons. This is important to display fine skin texture on a model.
	12	Remeshing 3D model/retopologise	Applying remeshing techniques reduces the number of triangles on the surface and the entire mesh volume, ultimately decreasing the file size while redistributing the triangles more evenly.
Digital output data	13	Able to export a *STL* file	Export 3D geometry as an *STL* file for 3D printing.
	14	Able to export an *OBJ* file	Export 3D model as an *OBJ* file capturing surface texture, shape, and colour.
Software support and other features	15	Support, bug fixes, and regular updates	Software developers provide regular updates, bug fixes, and high-quality support to users.
	16	Training videos and tutorials	Software websites provide training tutorials, support, and videos regularly updated to match their software updates.

First round evaluation features are highlighted in grey.

6.2.3 Evaluation of digital sculpting capabilities

After selecting CAD software applications based on their software features, their effectiveness in digital sculpting was assessed. To facilitate this process, specific digital sculpting capabilities needed to be identified for evaluation. Following an extensive discussion, the focus group decided on six crucial CAD sculpting features that were thought to be necessary for efficient prosthesis design. These capabilities are outlined in Table 6.3.

Table 6.3 CAD software digital sculpting capabilities that were evaluated

CAD software manipulation	Description of manipulation
1. Perform remeshing	Remeshing involves redefining the mesh of a 3D model to improve its structure, often making it more uniform or better suited for detailed work.
2. Perform decimation	Geometric decimation is a process used to reduce the complexity of a 3D model by removing a certain percentage of its vertices, edges, or faces.
3. Slice the geometry in half and mirror	Slicing and mirroring involves cutting a 3D model in half and then duplicating one half to create a symmetrical counterpart. This is particularly useful in designing symmetrical objects, such as facial features, ensuring both sides of the model are identical.
4. Create a thin edge	The edge refers to the boundary line where two surfaces of a 3D model meet. In CAD software, edges are crucial for defining the shape and structure of a model and are often manipulated to refine or alter the geometry to blend in seamlessly with the surrounding anatomy.
5. Make an overhang	Make and overhang refers to creating parts of the model that extend outward and create an overhanging section, resulting in an undercut. This can be important in prosthesis design for fitting purposes, where certain parts need to fit snugly under others.
6. Create skin texture	Skin texture pertains to the surface details applied to a 3D model to mimic the appearance of skin. In facial prosthesis design, skin texture is important for achieving a realistic look, including details such as pores, wrinkles, and other fine details.

It was decided to use an oloid shape to assess the digital sculpting capabilities of the CAD software. The oloid geometry was selected because the use of a single geometry makes it easier to evaluate software applications consistently, and its shape simulates the depressions and curvatures of the human anatomy of an ear and nose. Paul Schatz described the oloid in 1929, which is a three-dimensional curved geometric shape (DirnbÄock & Stachel, 1997). An oloid comprises of a convex hull of a skeletal frame made by placing two linked congruent circles in perpendicular planes so that each circle's centre is on its neighbouring circle's edge. The radius of the circles is equal to the distance between their centres. Moreover, one-third of each circle's perimeter lies inside the convex hull, so the same shape may be also formed as the convex hull of the two remaining circular arcs each span an angle of $4\pi/3$. In this study, the simplest form of the oloid was used, referred to as the anti-oloid (Figure 6.2). The anti-oloid geometry, designed by Tasnimul Hasan in Solidworks (Dassault Systèmes, SolidWorks Corporation), was sourced from the GrabCAD website (https://grabcad.com/library/anti-oloid-4). This geometry was retrieved on the 5th of October in 2020. To prepare the downloaded geometry for the sculpting evaluation, it was opened in Solidworks and then exported as a stereolithography (*STL*) file.

Figure 6.2 Images of an anti-oloid

CAD software manipulation

The evaluation of the digital sculpting capabilities of the CAD software applications was conducted in two rounds. In the first round, the software that passed the initial feature evaluation was assessed for its *remeshing* and *decimation* capabilities using the anti-oloid geometry. This involved importing the anti-oloid geometry *STL* into the software and determining whether it could effectively perform these functions. Those applications that passed the first round progressed to the second round of evaluation. In the second round, their ability to perform the remaining sculpting functions, *slice the geometry in half and mirror*, *create a thin edge*, *create an overhang*, and *create skin texture* was evaluated. Figure 6.3 highlights the areas on the anti-oloid where these sculpting tasks were applied.

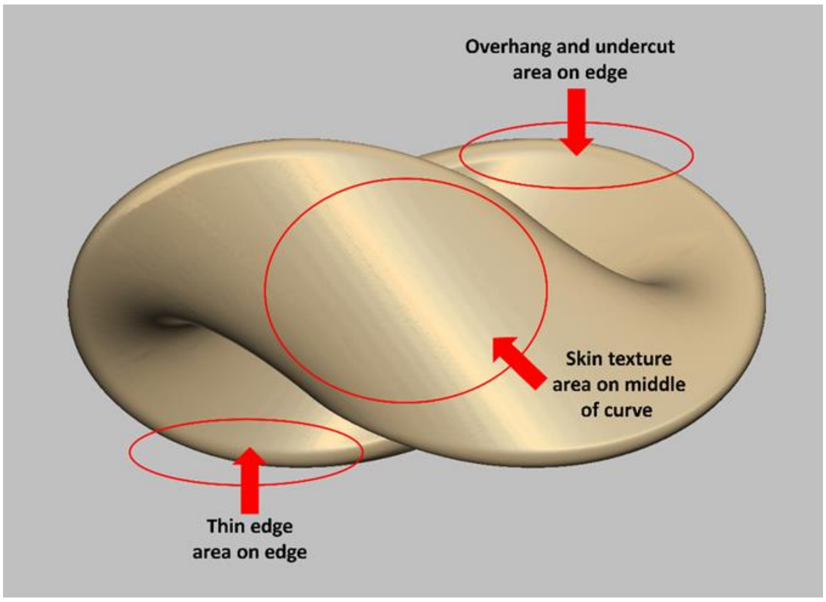

Figure 6.3 Places on the anti-oloid indicating where create a thin edge, create skin texture, and create an overhang were applied

In this study, besides the control, Geomagic Freeform, 3D Coat, and ZBrush progressed to the evaluation of digital sculpting capabilities. Each of these CAD software applications employs unique approaches and techniques for sculpting. Therefore, Table 6.4 was prepared to provide an overview of the steps involved in performing the key sculpting tasks used to evaluate the capabilities of each

CAD software. The sculpting techniques of Geomagic Freeform are also included to highlight how the software applications differ in their approaches.

Table 6.4 Methods to achieve the manipulations in Geomagic Freeform, 3D Coat and ZBrush

Manipulation	Steps
Remesh	***Geomagic Freeform*** 1. Select the Mesh tool in the Mesh tab in the toolbar. 2. Choose Remesh in the mesh tools section. 3. Set the remeshing parameters, such as the target resolution or surface detail you want to achieve. 4. After clicking on Apply, the polygons will be redistributed to smooth out the topology while maintaining the shape of the model. 5. Review the remeshed model for uniformity in topology and surface detail.
	3D Coat 1. Select the Retopo Room to start working with topology. 2. Select the Retopo menu and choose Auto-Retopo. 3. Optionally, draw strokes on your model to guide the automatic topology generation for important areas (for example, areas with more detail). 4. Adjust the parameters for polygon density and detail preservation. 5. Click Apply to generate a new mesh with optimised topology.
	ZBrush 1. Activate Dynamesh by going to Geometry panel and clicking on Dynamesh. 2. Set the Dynamesh resolution slider to control the density of the remesh. 3. Enable Dynamesh by clicking the Dynamesh button, then hold Ctrl+Drag on the canvas to remesh your model, or use ZRemesher by selecting ZRemesher. 4. Set the target polygon count and use options such as Keep Groups or Adaptive Size to maintain specific details or smooth the mesh. 5. Click ZRemesher to automatically remesh the model, optimising the topology for animation or further refinement.
Decimate	***Geomagic Freeform*** 1. Select the Mesh tool in the Mesh tab in the toolbar and select Polygon Reduction or Decimation

	2. Define the level of decimation, typically by percentage, based on how much you want to reduce the polygon count. 3. After clicking on Apply, the mesh complexity will be reduced while preserving as much detail as possible. 4. Review the model to ensure no important details were lost or distorted during the decimation process.
	3D Coat 1. Select the Sculpt Room to work on decimation. 2. Under the Voxel or Surface Mode menu, select the Decimate tool. 3. Set the decimation percentage or target polygon count. 4. Click Apply to reduce the polygon count while keeping the shape intact.
	ZBrush 1. From the Zplugin menu, select Decimation Master. 2. Click Preprocess Current to allow ZBrush to analyse the model in preparation for decimation. 3. After preprocessing, choose the percentage of decimation. 4. Click Decimate Current to reduce the polygon count while preserving the model's details.
Slice	***Geomagic Freeform*** 1. Under the Edit tab, select the Slice tool. 2. Choose the plane along which you want to slice the model (for example, X, Y, or Z plane). 3. Use the plane manipulators or input numerical values to place the slice at the desired location. 4. Once the plane is positioned, execute the slice by clicking Apply.
	3D Coat 1. Ensure you are working in Voxel Mode or Surface Mode. 2. Select the Voxels or Surface Mode menu and select the Cut Off or Split tool. 3. Use a brush, spline, or plane to define where you want to slice the model. 4. Apply the cut by pressing Enter or clicking Apply.
	ZBrush 1. Select the Slice Curve brush by pressing B, then S, then I. 2. Click and drag to define the slicing path. Hold Shift to constrain the cut to straight lines, or hold Ctrl+Shift to create a custom slicing curve.

	3. Release the mouse to execute the slice. The model will be split along the curve into separate polygroups.
Mirror	***Geomagic Freeform*** 1. Under the Edit tab, select the Mirror tool. 2. Specify the plane along which you want to mirror the model (for example, X, Y, or Z). 3. Execute the mirror operation by clicking Apply.
	3D Coat 1. Activate Symmetry by pressing S or going to the Symmetry menu. 2. Choose the axis for symmetry (X, Y, or Z) by selecting the appropriate plane for the mirror operation. 3. Once the symmetry plane is set, the mirroring will automatically occur as you sculpt or manipulate the model.
	ZBrush 1. In the Tool > Geometry menu, find the Modify Topology section. 2. Select Mirror and Weld to mirror the model across the desired axis. By default, this works across the X-axis. 3. To mirror on other axes, change the mirror direction under the Deformation menu by choosing Mirror for the X, Y, or Z axis. 4. To mirror actions during sculpting, activate Symmetry by pressing X and choosing the axis of symmetry.
Make edge	***Geomagic Freeform*** 1. Choose the Carve Tool or Knife Tool from the Sculpt menu. 2. Use these tools to sculpt sharp features along the surface where you want the edge. Adjust brush settings such as size and strength for precision. 3. If you need a cleaner edge, switch to the Trim Tool to refine the edges or use the Crease tool for sharper results. 4. Use the Smooth Tool to soften transitions around the edge, but leave the edge itself sharp.
	3***D Coat*** 1. For sharp features such as edges, use Surface Mode. 2. Select the Crease Tool from the sculpting brushes. Adjust its intensity and brush size. 3. Apply the tool along the surface where you want to create a sharp edge. For better control, use the Spline Tool for precise lines. 4. To make the edge crisper, use the Pinch Tool or Flatten Tool along the edge.

	ZBrush 1. Select the DamStandard Brush (press B, D, S) to create sharp cuts and edges. 2. Drag the brush along the surface to carve a sharp edge into the model. Adjust brush settings such as intensity to control the depth and sharpness. 3. After drawing the edge, use the Pinch Brush (press B, P, I) along the edges to tighten them and make them crisper.
Make overhang	***Geomagic Freeform*** 1. Use the Clay Tool to build up the geometry where the overhang will be. 2. Align your view to easily manage the projection of the overhang. 3. Use the Pull Tool or Drag Tool to create the overhanging geometry by stretching the material outward from the surface. 4. Use the Smooth Tool around the base of the overhang to blend it with the main structure, keeping the overhang itself intact.
	3D Coat 1. Start in Voxels Mode for ease of sculpting complex overhangs. 2. Select the Grow Tool to add material where the overhang will be. 3. Use the Move Tool to pull and shape the overhanging area. 4. If necessary, switch to Surface Mode and use the Smooth Tool to soften the base of the overhang while preserving the structure.
	ZBrush 1. Select the Move Brush (press B, M, V) to pull out parts of the model to form the overhang. 2. Use a larger brush to create broader strokes for pulling out the overhang. 3. Gently pull the geometry out from the model to form the overhang. 4. Use the Move Topological Brush for finer adjustments to the overhang and the surrounding area.
Make texture	***Geomagic Freeform*** 1. Ensure that the haptic device is connected and calibrated. This allows for tactile feedback when sculpting. 2. Select the Sculpt menu and select a tool such as the Add/Subtract tool. 3. Use a predefined stippling brush or create a custom texture brush by adjusting the pattern settings.

4. Start applying the stippling texture by gently dabbing or brushing the tool over the surface of the model. Adjust pressure and spacing to control the size and depth of the stipples.
5. Use the Smooth Tool lightly if needed to blend any rough areas without losing the stipple detail.

3D Coat

1. Ensure you are in Surface Mode for detailed sculpting.
2. Choose a Stencil or Alpha that mimics stippling. 3D Coat comes with many presets, or you can import a custom alpha texture that replicates skin pores or stippling.
3. Use the brush to apply the stippling texture across the model's surface. Adjust the intensity and brush settings to control the depth and frequency of the stipples.
4. Use the Smooth Tool to soften edges as needed, but avoid over-smoothing, which can erase stipple details.

ZBrush

1. Select the Alpha menu and select a stippling or skin texture alpha. If none is available, import a custom alpha that mimics the stippling effect.
2. Use the Standard Brush with the selected stippling alpha. Adjust the brush size and intensity as needed.
3. Gently drag or tap the brush over the surface of the model to create the stippling texture. Experiment with stroke type and drag rectangle for uniform application.
4. Fine-tune the Z Intensity slider to control the depth of the stippling. Use lower values for subtle texture and higher values for more pronounced stipples.
5. After applying the stipples, lightly use the Smooth Brush to refine any harsh transitions without losing the texture.

6.2.4 Selection of alternative CAD software

In the final stage, alternative CAD software was selected for the evaluation of their performance in prostheses manufacturing process chains. The sculpting capabilities to *slice the geometry in half and mirror*, *create a thin edge*, *create an overhang*, and *create skin texture*, were evaluated in this stage. The anti-oloid geometries that were produced after *creating an edge*, *an overhang*, and *texture* were inspected visually, followed by an analysis in Meshmixer to detect if any errors were introduced during the sculpting process. Based on the results of these assessments, the most promising alternative CAD software was selected for evaluation in the manufacturing process chains.

6.3 Results

6.3.1 CAD software features evaluation

In addition to the control software, nine alternative CAD software applications were assessed based on the evaluation of software features. Along with the control software, three of the selected CAD software applications achieved perfect scores in this first round of evaluation and were subsequently advanced to the second round of evaluation. Table 6.5 presents the software features used in the first round of evaluation and the scores awarded to the CAD software applications.

Table 6.5 First round of alternative CAD software evaluation based on the *Digital data input* features

Evaluation feature	CAD software evaluation									
	Geomagic Freeform (C)	**3D Coat**	**Blender**	**Cinema 4D**	**Maya**	**Meshmixer**	**MODO**	**Mudbox**	**Sculptris**	**ZBrush**
1. Import 3D file format	✓	✓	✓	✓	✓	✓	✓	✓	✓	✓
2. Advanced digital sculpting (clay) interface	✓	✓	×	×	×	×	×	✓	×	✓
3. Measurement tools	✓	✓	✓	✓	✓	✓	✓	✓	×	✓
4. Large variety of sculpting tools (>20)	✓	✓	×	×	×	×	×	✓	×	✓
5. Sculpting highly detailed models	✓	✓	×	×	×	×	×	✓	✓	✓
Total score	5	5	3	2	2	2	2	5	2	5
% score	100	100	60	40	40	40	40	100	40	100

Together with the control software, three alternative software applications, 3D Coat, Mudbox, and ZBrush, were evaluated in the second round. In this round, all these applications demonstrated perfect scores of 100%. Based on this result, all three alternative software applications progressed to the evaluation of their digital sculpting capabilities. The inclusion criteria and software scores are shown in Table 6.6.

Table 6.6 Second round of alternative CAD software evaluation based on the eleven inclusion software features

Inclusion criterion	CAD software			
	Geomagic Freeform (C)	3D Coat	Mudbox	ZBrush
Able to perform interactive mirroring techniques	✓	✓	✓	✓
Able to perform Boolean operations	✓	✓	✓	✓
Able to perform advanced smoothing	✓	✓	✓	✓
Painting and rendering functions	✓	✓	✓	✓
Transformations using a mask	✓	✓	✓	✓
Subdivide mesh/tessellation	✓	✓	✓	✓
Remeshing 3D model/retopologise	✓	✓	✓	✓
Able to export an *STL* file	✓	✓	✓	✓
Able to export an *OBJ* file	✓	✓	✓	✓
Support, bug fixes, and regular updates	✓	✓	✓	✓
Training videos and tutorials	✓	✓	✓	✓
Total score	11	11	11	11
% score	100	100	100	100

6.3.2 CAD software digital sculpting capabilities

Remeshing and decimation

In the first round of the sculpting capability evaluation, *remeshing* and *decimation* were assessed. Each alternative CAD software application demonstrated unique strengths in *remeshing*. 3D Coat excelled in advanced voxel-based *remeshing*, while ZBrush was distinguished by its dynamic *remeshing* through Dynamesh or ZRemesher. In contrast, Mudbox lacked sophisticated tools, providing only basic *remeshing* capabilities (Sarstedt, 2012). When considering *decimation*, both 3D Coat and ZBrush were equipped with robust *decimation* tools, whereas Mudbox's *decimation* features were comparatively limited. As a result of this evaluation, Mudbox was not advanced to the next round of evaluation, where physical sculpting capabilities were assessed on the anti-oloid geometry. Table 6.7 provides a detailed evaluation of the *remeshing* and *decimation* features of the CAD software applications.

Table 6.7 Critical evaluation of alternative CAD software remeshing and decimation capabilities

Remesh	Critique	Included in process chain evaluation
3D Coat	3D Coat possesses excellent remeshing tools, which are voxel-based, allowing for uniform manipulation of the mesh. This capability ensures that the mesh remains consistent and detailed during the sculpting process.	YES
Mudbox	Mudbox possesses remeshing tools that are limited when compared to 3D Coat and ZBrush. "Reduce" and "Rebuild" can help optimise the mesh, but they lack dynamism and flexibility.	NO
ZBrush	The "Dynamesh or ZRemesher" feature in ZBrush is a dynamic remeshing tool. It allows a designer to reshape and refine models without being concerned about stretching or distorting the mesh. This ensures that the	YES

	model can be easily refined and detailed without distortion, which is critical for accurate prosthesis creation.	
Decimate		
3D Coat	3D Coat possesses an advanced decimation tool known as "Poly Reduce." This function provides a designer with the ability to significantly lower the polygon count of a model while retaining as much detail as possible. This tool is flexible and preserves essential detail while lowering polygon counts.	YES
Mudbox	Mudbox have a "Reduce" feature that acts as its primary decimation tool. This function simplifies the mesh by reducing the number of polygons while attempting to preserve the overall shape and detail of the model. Mudbox's decimation capabilities are relatively basic compared to the more advanced tools in 3D Coat and ZBrush.	NO
ZBrush	ZBrush's decimation tool, "Decimation Master," is one of the most advanced and widely used in the industry. Decimation Master allows a designer to reduce the polygon count of a model substantially while preserving its high-resolution detail. It is a highly advanced tool, providing extensive control and maintaining high detail.	YES

6.3.3 Slice and mirror of a geometry

The haptic device of the control software Geomagic Freeform is a key component of the software that sets it apart from other CAD software. This device, often referred to as a haptic arm or haptic feedback device, allows designers to interact with 3D digital models in a tactile, hands-on manner. The intuitive control provided by the haptic device, facilitates precise slicing and mirroring. Because slicing can be highly dependent on a designer's skill, the haptic device can be a barrier for new designers. Additionally, even though mirroring is highly effective, it can occasionally be difficult to maintain alignment or symmetry across intricate organic forms without fine-tuning. Figure 6.4 shows views of slice and mirroring with Geomagic Freeform.

Geomagic Freeform

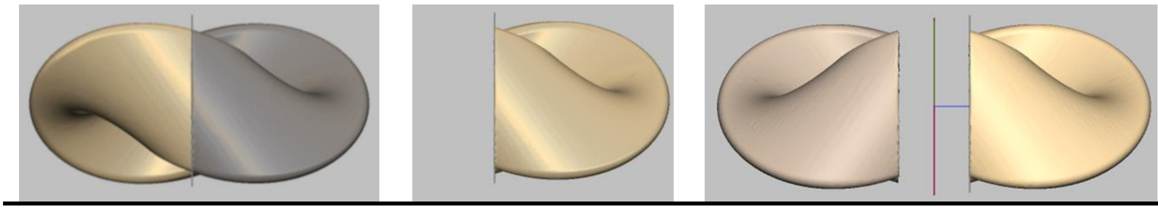

Figure 6.4 Views of the slice and mirror process in Geomagic Freeform

3D Coat offers slicing tools that allow designers to cut through voxel-based models, which is effective for creating clean slices in a model. Slicing in 3D Coat is straightforward and precise. Furthermore, 3D Coat's mirroring capabilities are also robust. Designers can mirror geometries and paint textures across a model, making it useful for symmetrical modelling tasks such as creating facial features. It should be noted that the voxel-based slicing can sometimes be challenging with very fine or intricate details, as cutting through dense voxel structures can lead to jagged edges or loss of detail. In general, mirroring goes smoothly; however, difficulties may arise when handling complex, non-uniform shapes that require additional adjustments after mirroring. Figure 6.5 shows views of slice and mirroring with 3D Coat.

3D Coat

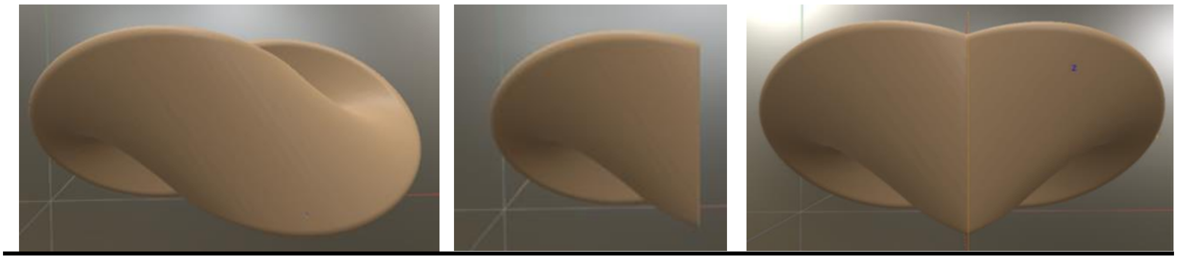

Figure 6.5 Views of the slice and mirror process in 3D Coat

ZBrush provides various advanced slice and mirroring tools. The slicing tools are powerful, but the high level of detail in models can make slicing resource-intensive. The slice tool "Slice Curve" allows designers to cut through models in a non-destructive way, and slice across complex geometries while maintaining edge sharpness and precision. Mirroring in ZBrush is effective but may sometimes require careful alignment of the pivot point to avoid unintended asymmetry, particularly with highly detailed models. The mirroring tools support both symmetrical sculpting and the mirroring of complex geometries. The "Mirror and Weld" function can mirror a geometry across any axis while maintaining high fidelity in detail. Figure 6.6 shows views of slice and mirroring with ZBrush.

ZBrush

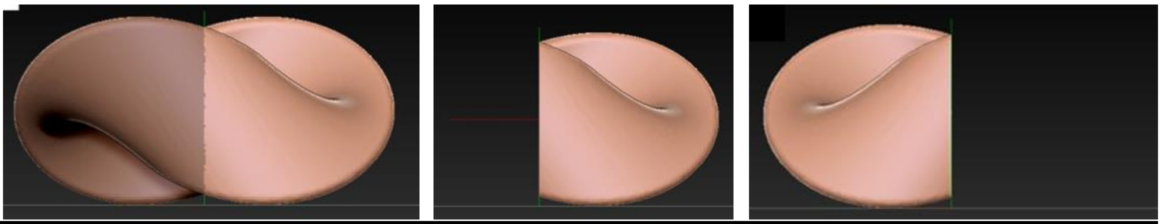

Figure 6.6 Views of the slice and mirror process in ZBrush

Edge- and overhang-making, and texture application

In the final stage of evaluating sculpting capabilities, the *creation of edges, overhangs*, and the *application of texture* were assessed. Each CAD software application demonstrated distinct advantages in executing these manipulations, while also presenting varying levels of complexity for the designer. Table 6.8 provides a critique of edge creation, overhang formation, and skin texture application across the different CAD software applications.

Table 6.8 Critical evaluation of alternative CAD software's edge-, overhang-making, and texture application capabilities

	Critique
Geomagic Freeform	• Geomagic Freeform excels in creating precise edges and overhangs, owing to its advanced haptic device that simulates the tactile experience of sculpting. The software provides superior control for intricate modelling tasks such as overhangs, allowing the designer to manipulate the model with high accuracy. Applying textures, such as stippling for skin texture is intuitive and detailed, ideal for medical applications such as maxillofacial prostheses manufacturing. • The software has a steep learning curve.

3D Coat	• 3D Coat offers robust tools for creating edges and overhangs, and its voxel-based sculpting allows for freeform alterations without concern for topology. Texture application is smooth and can be done quickly using the software's intuitive brushes. • One of the main drawbacks is the application's handling of finer details when overhangs or complex textures are involved. Challenges may be experienced with mesh quality or when adjusting finer textures.
ZBrush	• ZBrush's dynamic topology system allows for highly detailed edge creation and overhangs, making it excellent for intricate sculpting. Its vast array of brushes and customisable tools provide flexibility in creating textures such as skin stippling, ensuring high-quality results. • ZBrush's interface is rather difficult. Additionally, while the application is powerful for artistic applications, its adaptation to medical-focused workflows, such as those in maxillofacial prosthetics, might require more manual setup and customisation.

To achieve a greater understanding of the digital sculpting capabilities of the CAD software, the application of *creation of edges*, *overhangs*, and the *application of texture* to the geometries were inspected. It was visually apparent that there was not a discernible difference between the software applications. Additionally, the Meshmixer error detection revealed that relatively few mistakes were made when creating *edges*, *overhangs*, and *textures* (Table 6.9).

Table 6.9 Photographs of the manipulated anti-oloid's produced with Geomagic Freeform, 3D Coat, and ZBrush

Geomagic Freeform

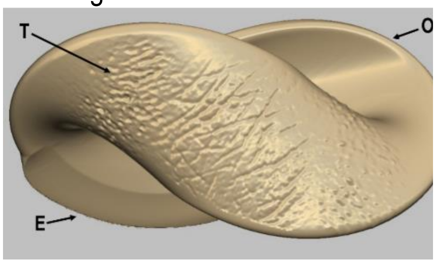

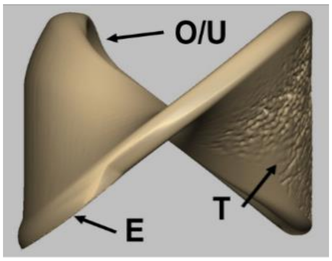

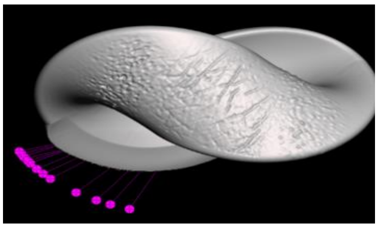

Number of errors = 13
(on edge)
Vertices = 392682
Triangles = 785312

3D Coat

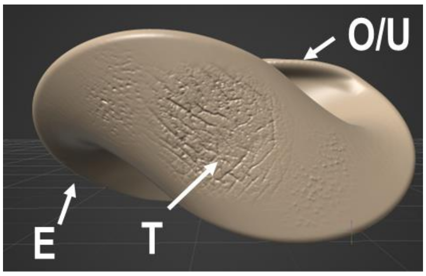

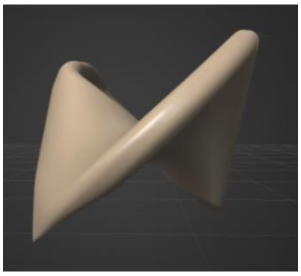

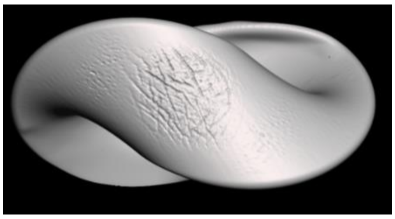

Number of errors = 0
Vertices = 1670486
Triangles = 3340972

ZBrush

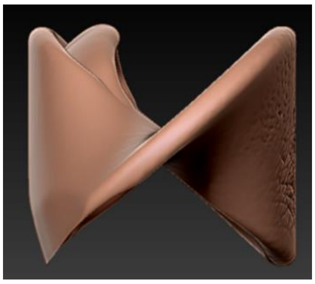

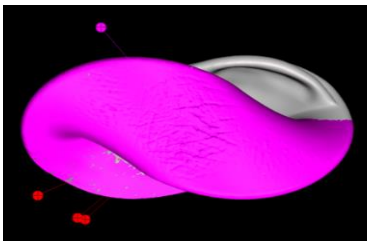

Number of errors = 4
(mostly on edge)
Vertices = 725145
Triangles = 1853608

E = edge; O/U = overhand/undercut; T = texture

6.4 Discussion and conclusion

In conclusion, the systematic evaluation of the digital sculpting capabilities of the two alternative CAD software applications 3D Coat and ZBrush revealed that they were suitable for the evaluation of their performance in prostheses manufacturing process chains. The systematic comparison of 3D Coat and ZBrush did not reveal a clear distinction in their sculpting capabilities. 3D Coat emerged as an accessible and user-friendly alternative, offering solid sculpting capabilities, though it may struggle with extremely fine details (Costello et al., 2024). On the other hand, ZBrush is more complex and challenging to navigate, but it excels in producing detailed and flexible sculpting results, with superior handling of edges and textures (Sarstedt, 2012; Erolin, 2023). However, its interface presents a steeper learning curve, and its application in the medical field requires some adaptation. These less expensive alternative CAD software applications appear to be promising for inclusion in external maxillofacial prostheses manufacturing process chains.

Chapter 7

Alternative Process Chains for External Maxillofacial Prosthesis Manufacturing

7.1 Introduction

The final phase of this research project addressed the practical implementation and evaluation of potentially cheaper alternative software for medical image processing (MIP) and computer-aided design (CAD) in the context of external maxillofacial prosthesis manufacturing. Historically, the industry-benchmarks, Mimics for MIP, and Geomagic Freeform for CAD, have set the benchmark for quality and functionality. However, their high cost poses a significant barrier, particularly to patients with limited resources, which is of major concern in South Africa.

In this study, a systematic approach was followed to identify potential cost-effective prosthesis manufacturing process chain alternatives that could deliver a comparable performance to industry-benchmark. As a result, 3D Slicer and InVesalius emerged as viable alternatives to Mimics for MIP tasks, while 3D Coat and ZBrush were identified as potential substitutes for Geomagic Freeform in CAD applications. In this final phase of the study, 3D Slicer and InVesalius were tested in combination with 3D Coat and ZBrush within test process chains. Additionally, the Artec Spider, a handheld surface scanner that uses blue light technology, as a direct data-collecting tool for CAD procedures, was also explored. Unlike traditional computed tomography (CT) scanning, the Artec Spider offers a cost-effective, radiation-free method of capturing detailed surface data, which can be directly imported into the CAD software (Costello et al., 2024). This approach not only bypasses the need for MIP software, but could potentially enhance accessibility and affordability of prosthesis manufacturing in South Africa. By including these alternatives in test process chains and systematically comparing them to the industry-benchmark could contribute to valuable insights into the feasibility of using more affordable software and scanning technologies in the production of high-quality external maxillofacial prostheses. Therefore, the sub-question addressed in this phase was:

Which alternative process chains produce external maxillofacial prostheses of comparable quality to those produced by the industry-benchmark?

Figure 7.1 presents a flow diagram of the process followed to identify alternative process chain(s) for the manufacturing of external maxillofacial prostheses.

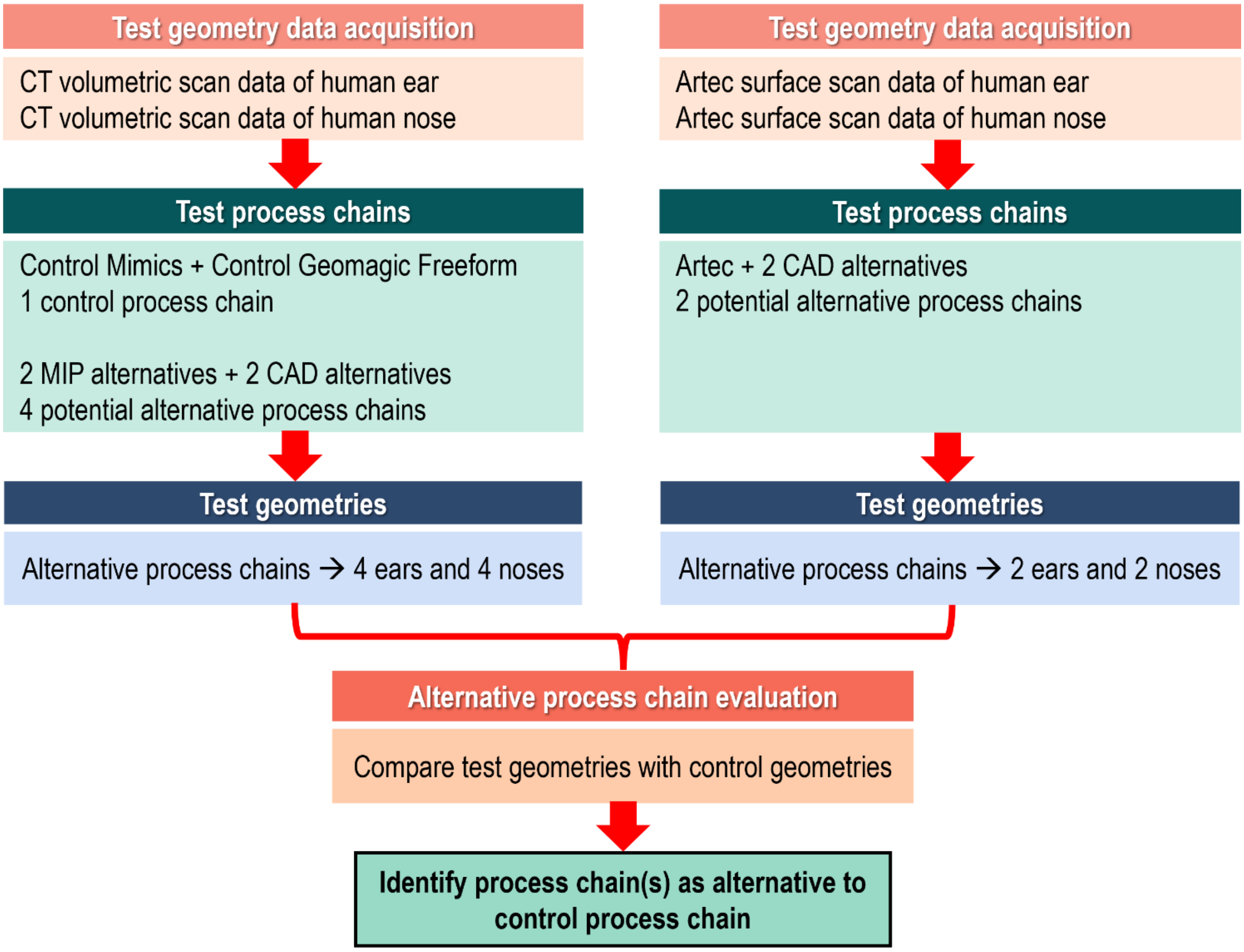

Figure 7.1 Presentation of the research process to identify alternative process chains for the manufacturing of external maxillofacial prostheses

7.2 Materials and methods

In this final phase of the study, six potential alternative process chains were rigorously tested to evaluate their efficacy in external maxillofacial prosthesis manufacturing. These process chains were based on the combination of 3D Slicer and InVesalius for MIP tasks with either 3D Coat or ZBrush for CAD tasks. Additionally, process chains using digital data sourced with the Artec Spider surface scanner, which were imported directly into 3D Coat and ZBrush, were also assessed. The primary objective was to compare the outcomes of these test process chains against a control process chain, which combined industry-benchmark software applications Mimics and Geomagic Freeform. In this study, a total of 12 test process chains were compared with two control chains. The two control chains, comprised of a combination of Mimics and Geomagic Freeform, one for producing an ear and the other for producing a nose. Eight potential alternative process chains were composed of different combinations of MIP software (3D Slicer and InVesalius) with two CAD applications (3D Coat and ZBrush). The remaining four potential alternative chains involved geometries created using the surface scan data, also paired with 3D Coat and ZBrush. Figure 7.2 illustrates the test process chains alongside the potential alternative chains together with ear and nose prostheses.

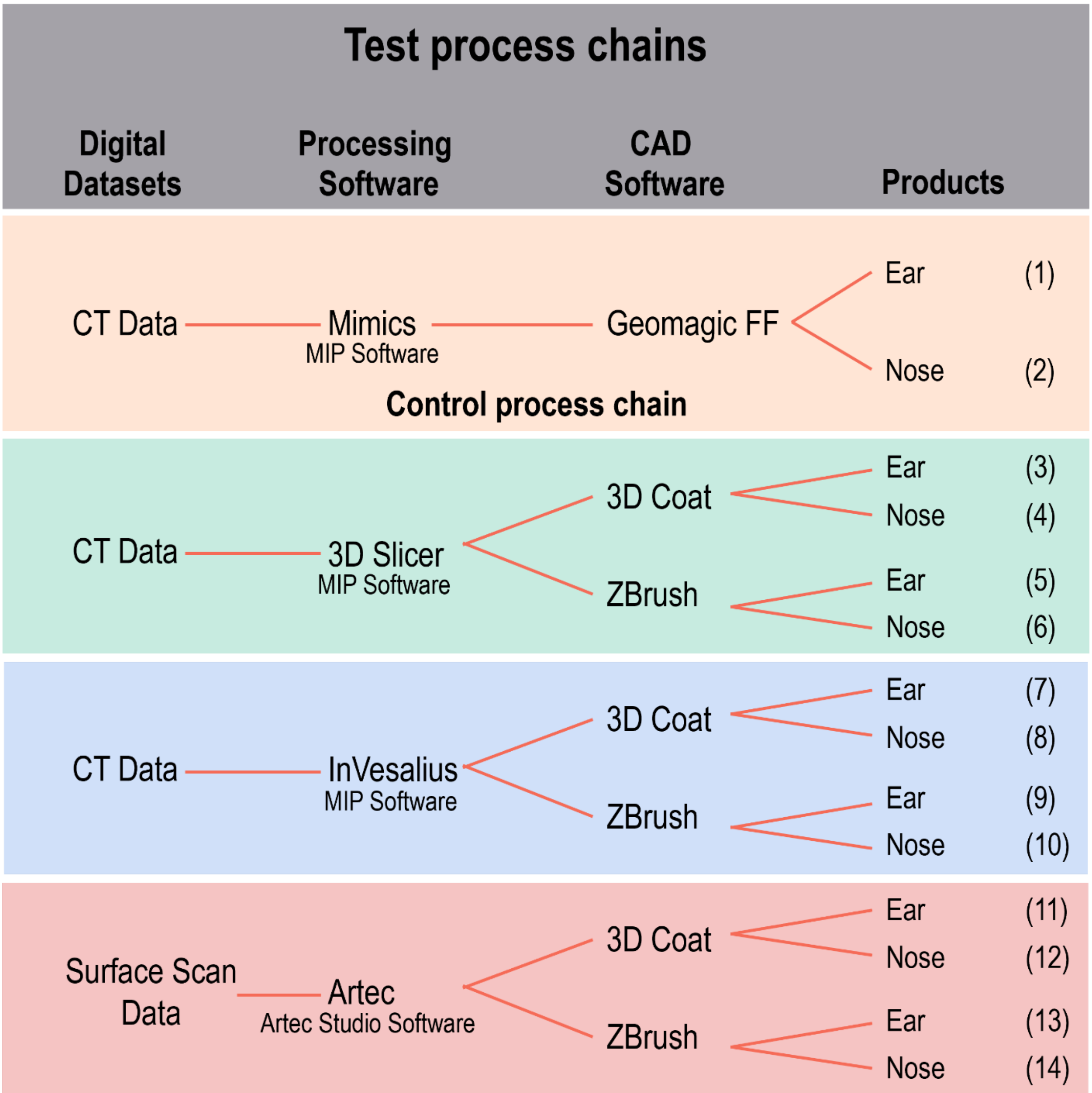

Figure 7.2 Control and test process chains tested for their potential use in external maxillofacial prosthesis manufacturing

7.2.1 Attributes of selected MIP and CAD software

3D Slicer and InVesalius are MIP software applications that are open-source and designed for reconstructing 3D medical images from Digital Imaging and Communications in Medicine (DICOM) files generated by CT or magnetic resonance imaging (MRI) scans. The 3D Slicer software platform is designed for the analysis and visualisation of medical images. It is widely used in research and clinical settings for various medical image-processing tasks. The key attributes of 3D Slicer are (Fedorov et al., 2012; 3D Slicer Website, n.d.; Kikinis et al., 2014):

1. *Multimodality imaging support:* 3D Slicer supports various imaging modalities, including MRI, CT, PET, and ultrasound, allowing for comprehensive analysis of different types of medical images.
2. *Image segmentation:* 3D Slicer offers powerful tools for segmenting anatomical structures from medical images, enabling the extraction of regions of interest (for example, organs and tumours). The segmentation can be manual, semi-automatic, or fully automatic.
3. *3D Visualisation:* 3D Slicer provides advanced 3D visualisation tools, allowing users to create detailed 3D models from 2D image data. These models can be viewed, rotated, and manipulated in real time.
4. *Volume rendering:* 3D Slicer includes volume rendering capabilities, which allow for the visualisation of entire volumes of medical images, rather than just slices. This is particularly useful for understanding complex anatomical structures.
5. *Quantitative analysis:* 3D Slicer allows for quantitative analysis of medical images, such as measuring distances, areas, and volumes of segmented structures. It can also track changes over time in longitudinal studies.
6. *Registration:* 3D Slicer provides tools for aligning images from different modalities or time points (image registration). This is essential for comparing images, planning surgeries, or monitoring disease progression.
7. *Support for custom extensions:* 3D Slicer allows users to extend functionality by developing custom modules and plugins. The software has a large community of developers who contribute new tools and features.
8. *Interactive user interface:* 3D Slicer offers an intuitive user interface that allows for easy navigation and interaction with images and 3D models. The interface is highly customizable to fit different workflows.
9. *Free and open source:* 3D Slicer is free to use and is distributed under a permissive open-source license, making it accessible to researchers, clinicians, and educators worldwide.

10. *Clinical and research applications:* 3D Slicer is used in a variety of clinical and research applications, including surgical planning, image-guided therapy, radiology, and neuroscience.
11. *Community and support:* 3D Slicer has a large and active user community, offering extensive documentation, tutorials, and forums for support and collaboration.

InVesalius is an open-source software platform designed for medical image processing and 3D reconstruction. It is particularly popular in the fields of medical research, education, and surgical planning. The key attributes of InVesalius are (InVesalius Website, n.d.):

1. *Open-Source and free*: InVesalius is freely available under an open-source license, making it accessible to various users, including researchers, healthcare professionals, and educators.
2. *Cross-platform compatibility*: InVesalius is compatible with multiple operating systems, including Windows, Linux, and macOS, providing flexibility in its usage.
3. *3D Reconstruction*: InVesalius can create high-quality 3D reconstructions from 2D DICOM images, allowing for detailed visualization and analysis of anatomical structures.
4. *User-friendly interface*: InVesalius is designed with an intuitive interface that makes it easier for users to navigate and utilize its features without extensive training.
5. *Segmentation tools*: InVesalius offers robust segmentation tools that enable users to isolate and analyse specific regions of interest (ROIs) within the medical images.
6. *Export options*: InVesalius supports exporting 3D models in various formats, such as stereolithography (*STL*) and *OBJ*, which can be used for 3D printing or further processing in other CAD software.
7. *Community and support*: InVesalius is an open-source project, benefits from a community of users and developers who contribute to its continuous improvement and provide support through forums and documentation.

3D Coat is a versatile and comprehensive CAD software widely used for digital sculpting, texturing, and 3D modelling. The key attributes of 3D Coat are (Pilgway Studio, n.d.):

1. *Voxel sculpting*: 3D Coat excels in voxel-based sculpting, allowing for the creation and manipulation of complex, highly detailed 3D models without worrying about topology.
2. *Retopology tools*: 3D Coat includes powerful automatic and manual retopology tools, enabling users to create clean and efficient meshes from high-resolution models, which is essential for animation and game design.
3. *Texturing and painting*: 3D Coat offers advanced texturing capabilities, including PBR (Physically Based Rendering) texture painting, which allows for realistic texturing with support for multiple layers and blending modes.
4. *UV mapping*: 3D Coat provides robust UV mapping tools that simplify the process of creating and editing UV maps, which is essential for applying textures accurately on 3D models.
5. *Rendering*: 3D Coat includes a built-in renderer that supports PBR, enabling users to visualise their models with realistic lighting and materials.
6. *Import and export options*: 3D Coat supports a wide range of file formats for import and export, making it compatible with other 3D software and workflows. This flexibility is crucial for integrating 3D Coat into various production pipelines.
7. *User-friendly interface*: Despite its powerful features, 3D Coat is known for its intuitive and user-friendly interface, making it accessible to both beginners and experienced users.
8. *Community and support*: 3D Coat has an active user community and extensive online resources, including tutorials, forums, and documentation, which provide valuable support and learning opportunities.

ZBrush is a premier CAD software renowned for its digital sculpting and painting capabilities. The key attributes of ZBrush are (Sarstedt, 2012; Pixologic, 2021):

1. *Advanced sculpting tools*: ZBrush offers an extensive suite of sculpting tools, including dynamic subdivision, Dynamesh, ZRemesher, and Sculptris Pro. These tools allow for the creation and manipulation of highly detailed models with millions of polygons.
2. *Dynamic tessellation*: ZBrush Dynamesh feature dynamically adjusts the topology of the model during the sculpting process, ensuring that the mesh remains optimized for detailed work without needing manual retopology.
3. *High-resolution detailing*: ZBrush supports high levels of detail, enabling artists to create intricate textures and fine details such as pores and wrinkles. The software's detailing capabilities are enhanced by features such as Alpha brushes and surface noise.
4. *Polypainting*: ZBrush allows for direct painting on the surface of 3D models without the need for UV mapping, streamlining the texturing process and providing intuitive and efficient workflows for colour application.
5. *ZRemesher*: ZBrush's automatic retopology tool helps create clean, animation-ready meshes from sculpted models. ZRemesher intelligently reduces polygon count while preserving detail, making it ideal for preparing models for animation and game development.
6. *SubTools and layers*: ZBrush enables the management of complex models through SubTools, which allows users to work on multiple elements of a model independently. Layers provide non-destructive editing, enabling artists to make changes without permanently altering the model.
7. *GoZ integration*: ZBrush integrates seamlessly with other 3D software such as Maya, 3ds Max, and Cinema 4D through the GoZ feature, facilitating a smooth workflow across different platforms.
8. *Rendering and presentation*: ZBrush includes a robust rendering engine, BPR (Best Preview Render), which supports real-time rendering with advanced lighting and material properties. This feature helps artists visualise their models with high fidelity.

9. *Community and resources*: ZBrush has a vibrant user community and extensive resources, including tutorials, forums, and documentation, providing valuable support, and learning opportunities for users at all skill levels.

7.2.2 Construction of deformity simulation models

To perform the real-world testing of the process chains, additional data was necessary to enable the tests. For the test process chains to function efficiently from the start of the chain to the product produced by the chain, it was essential to use representative models simulating ear and nose deformities. Thus, before testing the process chains, two simulation models were created from the existing data volumes of Subjects 1 and 2. First, external facial geometries, including the ears and nose, were segmented from the data volumes of Subjects 1 and 2 using Mimics (Table 7.1 A). In Geomagic Freeform, an ear deformity (ED) model was created from the model of Subject 1 (Table 7.1 B), and a nose deformity (ND) model was created from the model of Subject 2 (Table 7.1 C).

Table 7.1 Models used to produce the ear and nose deformity models and views of the ear and nose deformities

A. Facial segmentation model of Subject 1

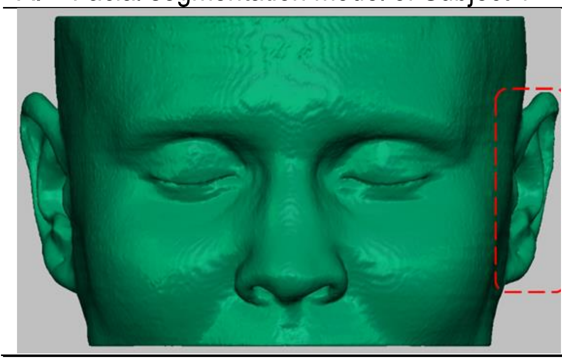

Facial segmentation model of Subject 2

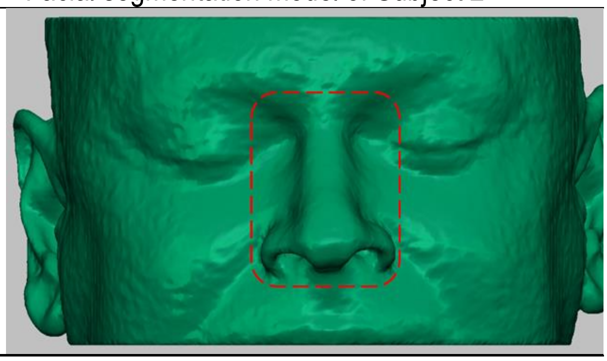

B. Views of ear deformity model

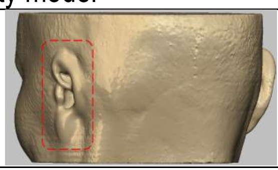

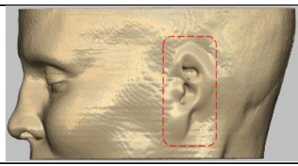

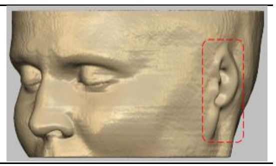

C. Views of nose deformity model

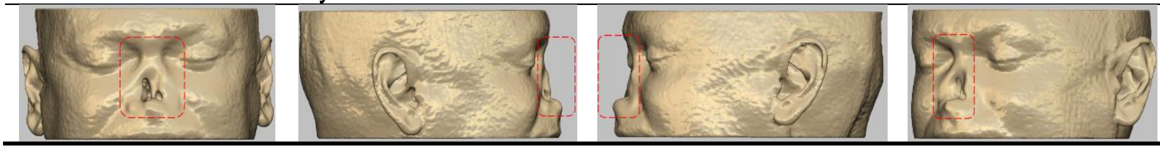

These ED and ND models served as foundational 3D models for fitting ear or nose digital prostheses. The process began by importing the ED and ND models into the CAD software applications, Geomagic Freeform, 3D Coat, and ZBrush. Thereafter, the segmented ears and noses, obtained during the evaluation of alternative MIP software (3D Slicer and InVesalius), were used to digitally "repair" the deformities in the models. After fitting an ear or nose prosthesis onto the ED and ND models, the “prosthesis” was subtracted (using Boolean operations) from the base model. The subtracted ears and noses were then further refined in the CAD software by creating thin edges and adding skin texture to enhance human likeness. For 3D printing, moulds (negative forms) were created in the CAD software, and these moulds were subsequently 3D printed. The final prostheses (positive forms) were then produced from these moulds. To demonstrate the end products of the process chains, a mould was designed in 3D Coat of the nose created in the process chain that combined 3D Slicer and 3D Coat. The model of the mould was then exported in *STL* file format and imported into the Elegoo Mars 5 Ultra 3D printer and printed in liquid resin. Finally, a silicone nose model of the mould was hand cast.

7.2.3 Acquisition of digital data for process chain testing

The surface scan data were acquired using the Artec Spider, which was available in the Centre for Rapid Prototyping and Manufacturing (CRPM), where this study was conducted. The Artec Spider is a surface scanner that is ideal for capturing high-resolution 3D geometries of complex surfaces such as a person's ear or nose (Unkovskiy et al., 2022). This 3D scanner uses blue light technology to scan surfaces and does not expose a patient to radiation (https://www.artec3d.com/portable-3d-scanners/artec). The lightweight and portable scanner can render complex geometries, sharp edges, and thin ribs. For this project, this instrument was chosen because of its plugin and point-and-scan capability, which might be an ideal alternative to CT volumetric data (Figure 7.3).

Figure 7.3 Artec Spider handheld surface scanner

To generate a geometry using the Artec Spider requires a step-by-step process. By following these steps, a 3D geometry was produced, which was then imported into CAD software for the design of a prosthesis. The following steps outline the process that was followed to generate the ear and nose geometries, which were imported into the CAD software applications, 3D Coat and ZBrush (Artec 3D, n.d.; Reichard, 2020):

1. *Preparation*:
   - The necessary Artec Spider software (Artec Studio) was installed and configured on a computer.
   - To perform a scan, a scanning environment with good lighting and a stable surface for the subject (person) to remain still was prepared.

2. *Scanning*:

    - The Artec Spider was then calibrated according to the manufacturer's instructions to ensure accurate data capture.
    - The subject was positioned comfortably, after which the target areas (ear or nose) were scanned. To scan effectively, the scanner was steadily moved around the area to capture all angles and details.

3. *Data processing:*

    - After scanning, the raw data were imported into the Artec Studio software.
    - The Artec Studio's tools were then used to clean up the scan and remove any unnecessary noise or artefacts.
    - The multiple scans were then aligned and merged to create a comprehensive 3D model.
    - The geometry was refined using the mesh optimisation tools to ensure it was smooth and accurate.

4. *Exporting the geometry:*

    - After finalising the 3D model, it was exported in *STL* file format.

5. *Import into CAD software:*

    - After opening the CAD software, the 3D model was imported.
    - At this stage, the prosthesis was fitted to the imported ED or ND model as the base.

7.2.4 Analysis of process chains

Several analyses were performed on the 3D models generated by the different process chains. During the creation of a model in a process chain, errors may be introduced. Therefore, errors were detected with the Meshmixer's Inspector tool. The methods used with Meshmixer are consistent with those mentioned in Chapter 5. The organic and complex nature of anatomical models required multiple comparisons between the control models and those from the potential alternative process chains. These comparisons were essential to reach a more comprehensive and accurate conclusion about the performance and accuracy of the different test process chains. By performing several analyses of the products of the test process chains, a better understanding of the deviations and variations across models could be achieved, ensuring that all aspects of geometric fidelity were considered.

The models created by the test process chains were compared to those from the control process chain using Materialise Magics, CloudCompare, and Geomagic Control X. Although CloudCompare and Geomagic Control X perform similar statistical analyses, they were both included in the study because of their differing analytical algorithms. The parameter control of CloudCompare is more open-ended and may result in variable outputs based on user settings, whereas parameter control in Geomagic Control X is more consistent because of standardised algorithms (CloudCompare User Manual Version 2.6.1, n.d.). Geomagic Control X often integrates enhanced noise reduction and surface smoothing, which may not be as prominent in CloudCompare's default algorithms. CloudCompare and Geomagic Control X measurements were performed at both distances set at 0.5 and 0.1. The maximum distance parameter defines the farthest distance between points in one cloud and those in another to be considered in the distance calculation. A total of six test ear and six test nose comparisons were performed against the control models. The methods used with CloudCompare are consistent with those detailed in Chapter 5. However, the following steps were followed in Magics to ensure accurate and meaningful results during these comparisons:

1. *Import models:*
   - After launching Magics, the 3D meshes of both the test and control models were imported into Materialise Magics.
2. *Align models:*
   - The alignment tools in Magics were used to position the models correctly relative to each other by the Align or Register feature found under the Alignment or Transform menu.
3. *Select comparison tool and comparison parameters:*
   - In the Analysis tab, the Compare tool was chosen.
   - Configure the parameters:
     - Reference Model**:** Select one of the models to act as the reference.
     - Comparison Model: Select the second model to compare against the reference.

- Comparison Type: Choose the type of comparison, such as geometric deviation, distance, or fit analysis.

4. *Run the comparison:*
5. *Review the heat map displayed by Magics:*
6. *Analyse statistics:*

- The statistics summary includes:
  - Maximum deviation: The largest deviation between the two models.
  - Minimum deviation: The smallest deviation between the two models.
  - Mean deviation: The average deviation across the surface.
  - Standard deviation: Measures the variability of deviations from the mean.
  - Deviation histogram: A graphical representation showing the distribution of deviations.

7. *Export results:*

Geomagic Control X, a proprietary application, was also used to compare the models. The following steps were followed in Geomagic Control X (Geomagic Control X, n.d.):

1. *Align geometries:*

- After importing the reference geometry (control model) and the test geometry (test model), they were aligned in the software's workspace.
- An initial rough alignment was performed using basic matching methods such as "Best Fit" or "3-Point Alignment."
- After the initial alignment, a follow-up alignment was performed using a finer alignment method such as "Global Registration" or "Local Alignment" to ensure that both geometries are accurately aligned for comparison.

2. *Apply comparison tools:*

- 3D Compare > Surface Comparison: The surfaces of both geometries were compared with Surface Comparison. The software then generates a colour map indicating deviations between the test model and the reference model.

3. *Set comparison parameters:*

- The maximum distance threshold for comparison was set at both 0.1 and 0.5 mm to define the acceptable range of deviations between the two geometries.
- The best-fit settings were adjusted to allow the software to optimise the comparison based on global or local alignment, depending on the precision you need.

4. *Review colour map:*

- The colour map indicated visually areas of difference between the two models:

- Green: Areas where the test model closely matches the reference model.
- Blue: Areas where the test model is smaller or has negative deviations compared to the reference.
- Red: Areas where the test model is larger or has positive deviations.

5. *Statistics generated and what they mean:*
   1. Deviation map:
      - This is the main output of the surface comparison, visually representing the deviations in the colour map.
      - Positive deviation (Red): Indicates areas where the test geometry is larger than the reference geometry.
      - Negative deviation (Blue): Indicates areas where the test geometry is smaller than the reference geometry.
      - Zero deviation (Green): Indicates areas where the two geometries match perfectly within the defined tolerance range.
   2. Maximum distance:
      - Displays the largest measured deviation between the two models. This is useful for identifying areas with significant shape or volume differences.
   3. Average deviation:
      - This provides the mean deviation across the entire surface comparison, giving an overall measure of how closely the test geometry aligns with the reference.
   4. Root Mean Square (RMS) deviation:
      - RMS deviation is a more statistically rigorous measure of the overall deviation between two geometries. It squares the individual deviations, averages them, and then takes the square root. This method is useful for minimising the impact of small deviations while emphasising larger errors.
   5. Standard deviation:
      - Indicates how spread out the deviations are from the average. A low standard deviation suggests that most points are very close to the average deviation, indicating good alignment across the geometry.
   6. Tolerance range:
      - Displays the percentage of points that fall within the predefined tolerance range (e.g., ±0.1 mm). Higher percentages indicate better overall conformity between the test and reference models.
   7. Histogram:
      - A graphical representation of the deviation data, showing the distribution of points based on their deviation values. The histogram helps in identifying how the deviations are spread across the model.

6. *Generate report:*

- Detailed reports were then generated with Geomagic Control X that includes statistical data, deviation maps, and annotated views of the comparison results. This report can be saved in various formats (PDF, HTML, etc.).

Pinpoint anatomical comparison

To perform a more precise comparison (pinpoint comparison) between the models produced by the control process chains and the models produced with the potential alternative chains, focused site deviation analyses were conducted using Geomagic Control X. These analyses were performed at specific sites on the models to facilitate a more thorough comparison across the different models. To perform these analyses of geometric accuracy, six distinct anatomical points on the ear models were chosen based on Purkait (2016), and six on the nose models based on Trieu and Thinh (2023) (Figure 7.4).

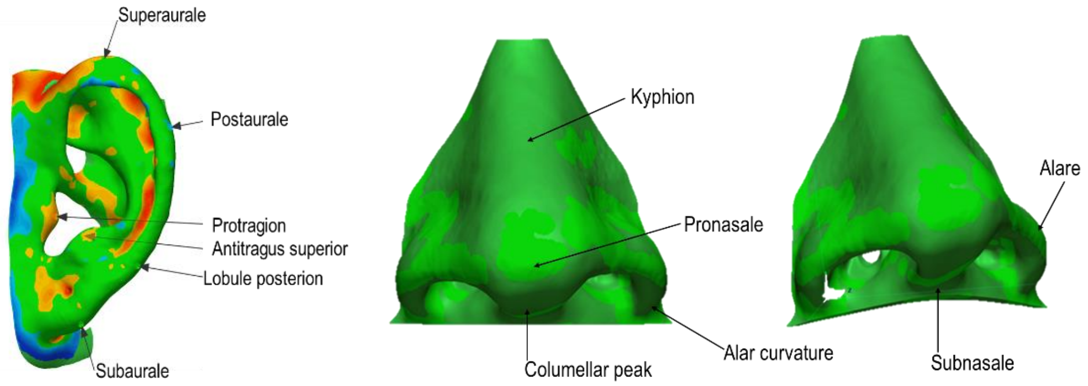

A. B.

Figure 7.4 Anatomic regions where pinpoint deviations were measured. A. Ear B. Nose

Comparative performance analysis of process chains

In the final process chain performance analysis, a more focused comparison of the test process chains was conducted to better assess their performance relative to the control chain. Statistical analyses of the test process chain outcomes (ear and nose models) were used to rank the performance of the chains, with a ranking of "1" representing the best alignment with the control process chain model. The statistical analyses employed for these comparisons included Magics histograms, CloudCompare histograms, Geomagic Control X histograms, and the pinpoint deviations in specific anatomical regions. To facilitate comparison across the different sets of ratings, the values were standardised using the following formula:

Standardised Rating (SR): $SR = \left(\frac{x_i}{\sum_i^n x_i}\right)$ (1)

Where:

x = rating value of a statistical analysis performance of the i^{th} process chain

n = total number of process chains

i = i^{th} process chain

After standardising the ratings, they were used to calculate an Unweighted Standardised Rating Index (USRI). The USRI values were calculated using the following formula:

$USRI = \left(\frac{\sum_j^m SR}{m}\right)$ (2)

Where:

SR = standardised rating value of a process chain of the j^{th} statistical analysis performance

m = total number of statistical analysis performances

j^{th} = statistical analysis performance

The USRI values were finally used to rank the performance of the various test process chains in comparison to the control process chain. Lower USRI values indicated a stronger alignment of the models produced by the alternative process chains with the control model and, thus, a higher ranking in terms of performance relative to the control chain.

Comparative cost analysis of process chains

After completing the Meshmixer, Magics, CloudCompare, and Geomagic Control X analyses, and comparative analyses, all the process chains were compared in terms of cost. Estimates were obtained for the relevant components of the process chains. These estimates were then used to rank the process chains in terms of cost.

7.2.5 Creation of an ear/nose geometry resource

The CRPM is a leading facility in South Africa specialising in the production of both internal and external facial prostheses. Given the CRPM's significant role in advancing prosthetic technology, this project has been developed with its support, underscoring the centre’s commitment to innovation. As part of the study, a repository of geometric models of ears and noses was established. This repository will serve as a valuable resource, providing pre-designed geometries that can be used in future prosthetic applications, ensuring rapid and accurate responses to patient needs. The ears and noses of willing participants were scanned with the Artec Spider after signing a letter of consent (Copy provided in Appendix C). These participants were mostly from the CRPM and the Faculty of Engineering, Built Environment and Information Technology, Central University of Technology, Free State, where the CRPM resides. The number of people scanned will increase in the future to expand the resource.

7.2.6 Illustration of the use of the resource

To illustrate the application of the resource, an ear and nose were selected from the ear/nose data repository and used to "digitally repair" the ED and ND models. The surface-scanned meshes were first exported as *STL* files using Artec Spider's Artec Studio software, and then imported into

Meshmixer for further processing. In Meshmixer, the Plane Cut function was employed to precisely slice the 3D model along a customisable plane (Autodesk Inc., n.d., 2021). The following steps detail the process of slicing the ear and nose from the edited mesh model.

1 *Cutting*:

The Plane Cut tool was used to position a virtual plane across the mesh at any angle or position. Then, by adjusting the plane, the slice area was selected. This was achieved using the following option:

- Keep Both Parts: This option retains both the top and bottom portions of the mesh after the cut, effectively splitting the model into two separate parts.
- Discard One Part: Users can choose to remove either the upper or lower part of the mesh, depending on the direction of the cut. This is useful for trimming or refining a model.

2. *Customising the plane*:

The plane used for cutting was adjusted by applying the following actions as needed:

- Translation: The plane was moved along the X, Y, or Z axis to define the exact location of the cut.
- Rotation: The plane was rotated to slice the model at specific angles, allowing for precision in making angled cuts.
- Interactive handles: The easy-to-use handles were used to manipulate the position and angle of the cutting plane in real-time.

3. *Smooth and fill options*:

After cutting, the open surface that resulted from the cut was automatically filled. This ensured that the mesh remains closed, which is important for other applications.

4. Finally, the ear or nose mesh 3D model was exported in *STL* file format.
5. After importing the EN model into 3D Coat, the ear or nose mesh model was also imported.
6. The ear or nose mesh was then used to “repair” the deformity of the EN or ND model, as detailed in section 7.2.2.

7.3 Results

7.3.1 Process chain output models

In the final stage of the study, the potential alternative process chains were evaluated by producing 3D models that represent real-world structures of external facial features. Six ear and six nose models were generated using the test process chains, each combining MIP software (3D Slicer and

InVesalius) and CAD software (3D Coat and ZBrush), and combining Artec scans and CAD software (3D Coat and ZBrush). These models were then visually inspected and compared to those produced by the control chain.

The six ear models generated through the test process chains were visually compared to the control chain's ear model. Visually, the test 3D ear models closely resembled the control ear model produced using the control process chain. Table 7.2 provides side, frontal, and back views of the ear models created through the test process chains and the control chain.

Table 7.2 Views (side, front, and back) of the ear models produced with the control process chain and the potential alternative chain

Process chain ear model	
Mimics + Geomagic Freeform (Control)	
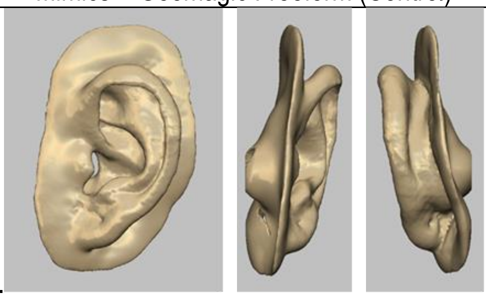	
3D Slicer + 3D Coat	3D Slicer + 3D ZBrush
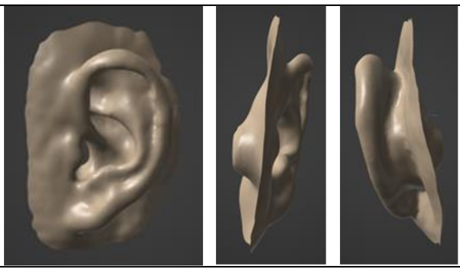	
InVesalius + 3D Coat	InVesalius + ZBrush
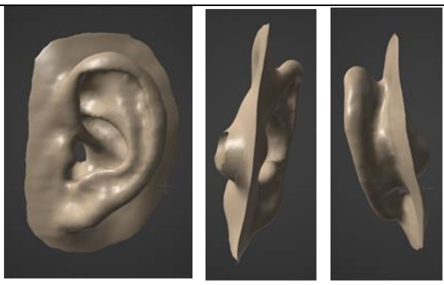	

Artec + 3D Coat	Artec + ZBrush
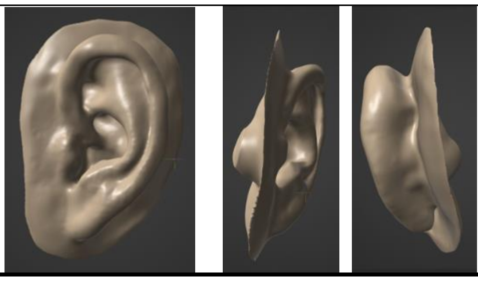	

A visual comparison was also made between the six nose models produced by the potential alternative process chains and the nose model of the control chain. The 3D models generated by the control chain and the test models matched closely. Table 7.3 provides frontal and bottom views of the nose models created through the various process chains.

Table 7.3 Views (front and bottom) of the nose models produced with the control process chain and the potential alternative chain

Process chain nose model	
Mimics + Geomagic Freeform (Control)	
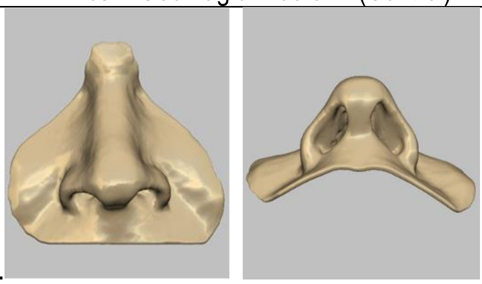	
3D Slicer + 3D Coat	3D Slicer + 3D ZBrush
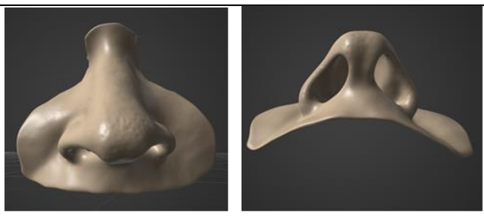	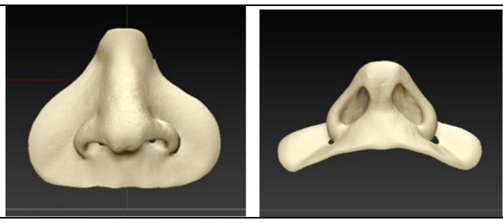

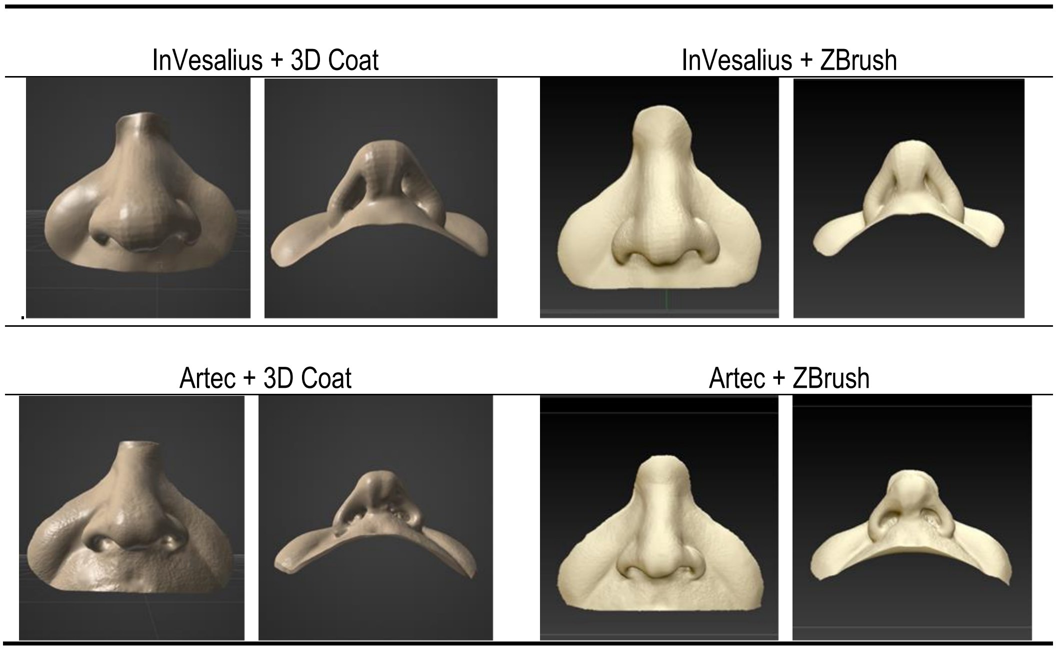

7.3.2 Analysis of process chain ear models

Error detection in models using Meshmixer

The error density of the ear 3D models was measured using the Inspector tool in Meshmixer to determine to what extent errors were introduced into the models produced with the different process chains. An analysis of the starbursts of the different ear models, along with the error statistics generated by Meshmixer, revealed that only a minimal number of errors were introduced into the models (Table 7.4). Interestingly, the two models produced with the process chain that started with 3D Slicer had the least number of errors, whereas the models produced with the two chains starting with InVesalius had the most errors.

Table 7.4 Meshmixer Inspector error analysis of process chain ear models

Process chain		
Mimics + Geomagic Freeform (Control)	3D Slicer + 3D Coat	3D Slicer + ZBrush
		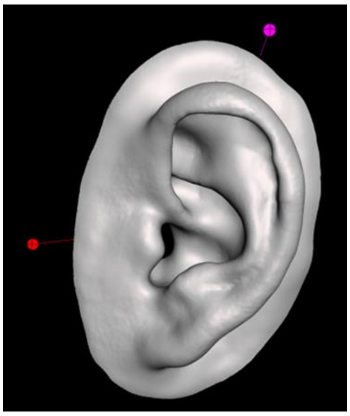
Errors = 6	Errors = 1	Errors = 2
	InVesalius + 3D Coat	InVesalius + ZBrush
	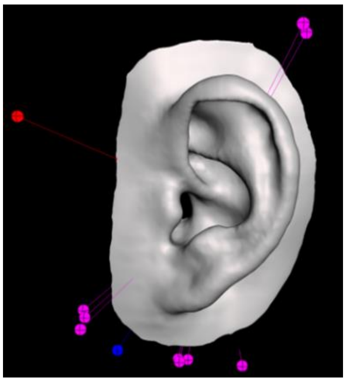	
	Errors = 11	Errors = 12
	Artec + 3D Coat	Artec + ZBrush
	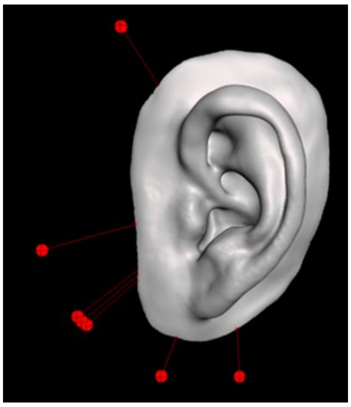	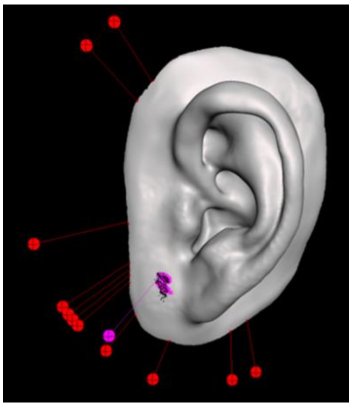
	Errors = 7	Errors = 12

Model heat map and statistical comparisons using Magics

In the comparison of ear models produced by the potential alternative process chains to the control chain in Magics, the heat maps and histograms revealed noticeable differences. The test ear model produced with 3D Slicer combined with ZBrush was the only model where most of the deviation values were concentrated around zero on the histogram, indicating a close match to the control model (Table 7.5). This was further supported by the heat map, showing mostly green areas, indicating minimal deviations between the test model and the control model. In contrast, the ear model produced using InVesalius combined with ZBrush showed a significant number of positive deviation values, represented by warm red and yellow tones on the heat map. This suggested that the test model had excess material compared to the control model. The other models showed deviations largely within the blue-green range of the heat map and histogram, with most values centred around zero or small negative deviations. This implied that these test ear models were slightly smaller than the control model, as indicated by the cooler colours.

Table 7.5 Statistics, heat maps, and histograms showing comparisons between ear models from test process chains with the model from the control process chain using Magics

Process chain	Statistics, heat map, and histogram					
	Min	Max	Range	Heat map	Histogram	Remark
3D Slicer + 3D Coat	-3.233	6.628	9.861	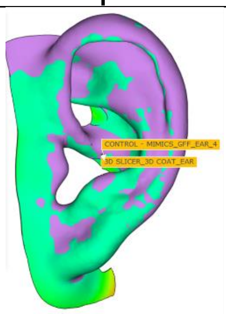	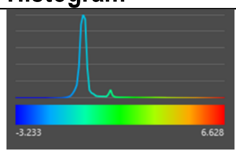	Green = Control

3D Slicer + ZBrush	-5.715	6.604	12.319	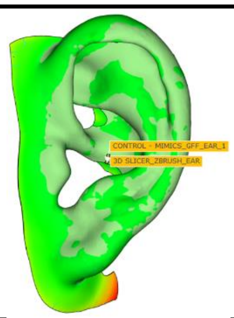	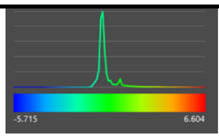	Bright green = Control
InVesalius + 3D Coat	-1.909	6.341	8.25	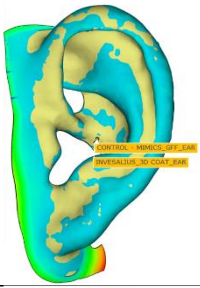	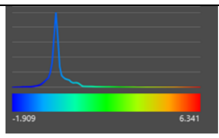	Grey = Control
InVesalius + ZBrush	-3.273	1.288	4.561	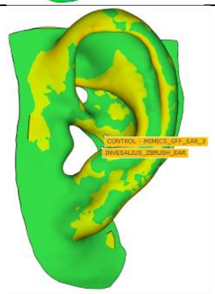	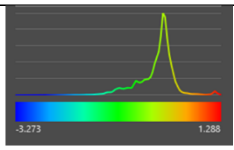	Yellow green = Control
Artec + 3D Coat	-4.852	8.981	13.833	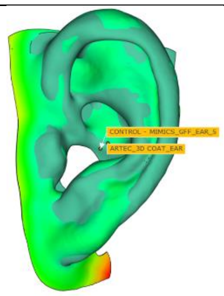	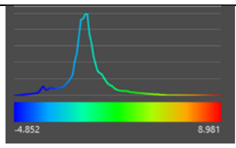	Brighter green = Control
Artec + ZBrush	-4.979	7.567	12.546	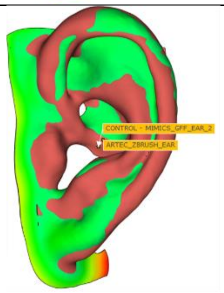	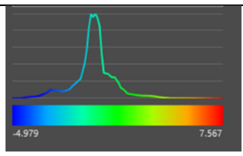	Green = Control

Min = Minimum distance; Max = maximum distance

Model heat map comparisons using CloudCompare

The heat maps generated by CloudCompare, comparing the test ear models to the control chain model, revealed noticeable differences between the models. However, these variations were generally consistent across all models, with similar patterns emerging between the test ear models and the control (Table 7.6). For all models, mid-range differences (yellow) were less pronounced when using a maximum distance of 0.1 compared to 0.5. Furthermore, the 0.1 maximum distance displayed visibly more large-range differences (red) than the 0.5 distance.

Table 7.6 Heat maps showing visual comparisons between ear models from test process chains with the model from the control process chain using CloudCompare

Heat map	
Maximum distance = 0.5	**Maximum distance = 0.1**
3D Slicer + 3D Coat with control	
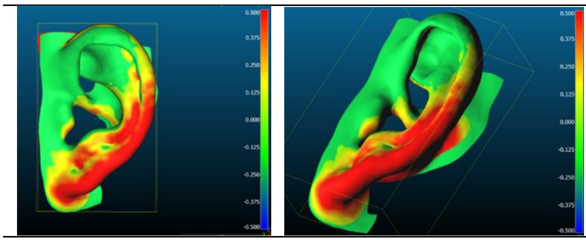	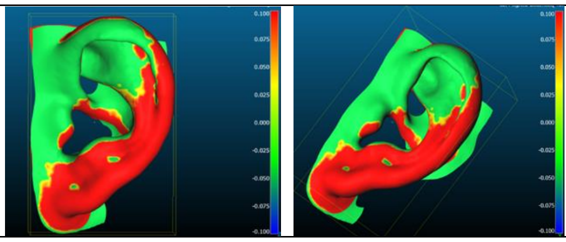
3D Slicer + ZBrush with control	
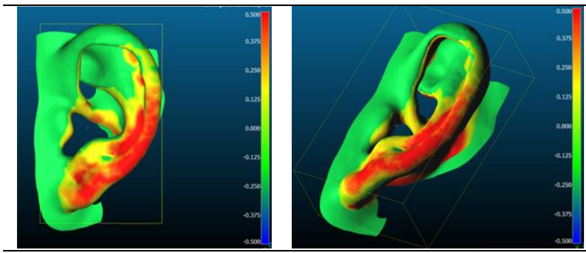	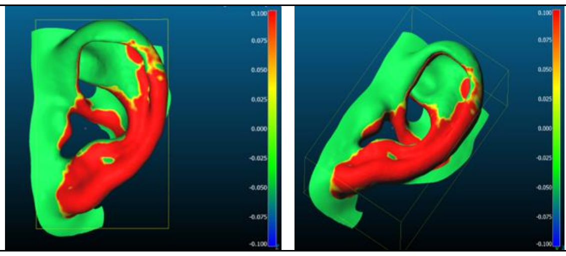
InVesalius + 3D Coat with control	
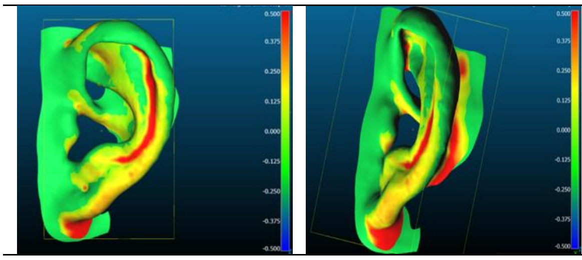	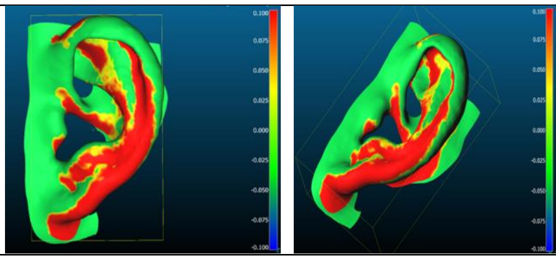

InVesalius + ZBrush with control

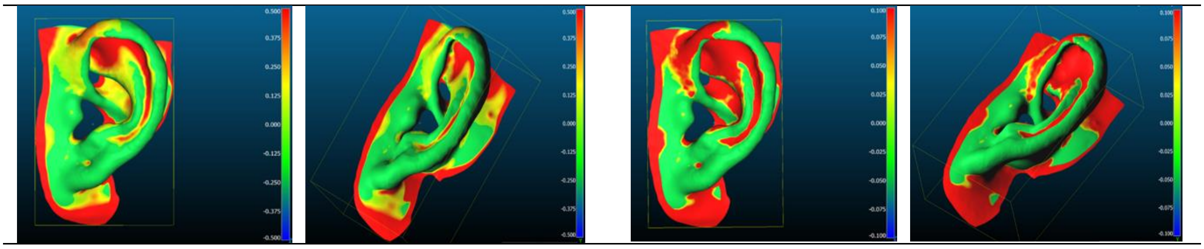

Artec + 3D Coat with control

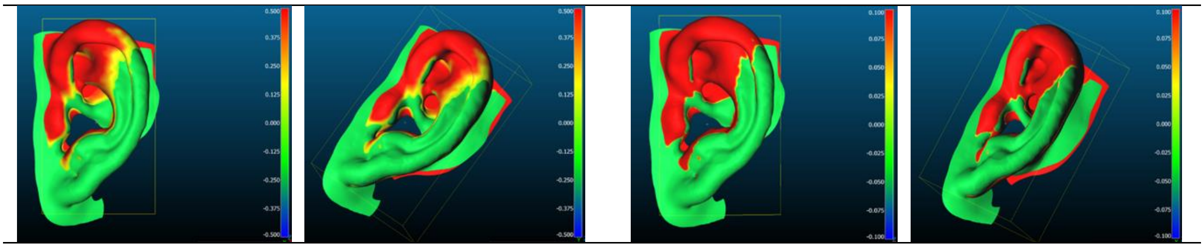

Artec + ZBrush with control

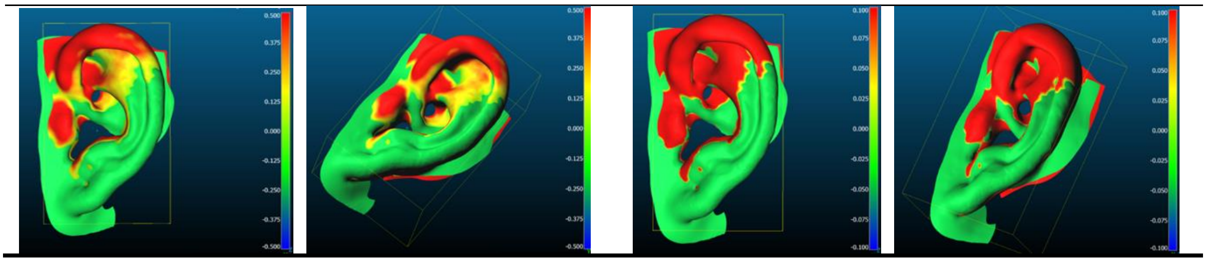

Model heat map comparisons using Geomagic Control X

Heat maps were also generated using Geomagic Control X to provide a visual comparison between the test ear models and the control ear model. The heat maps, using a maximum deviation threshold of 0.5, displayed a gradient of deviations ranging from cool blue (indicating smaller deviations) to warm red (indicating larger deviations) (Table 7.7). Notably, the ear models created with process chains incorporating Artec Spider scan data exhibited significant deviations at both extremes of the range, with distinct areas marked in blue and red. When a smaller maximum deviation of 0.1 was applied, all test models showed more consistent mid-range deviations, indicating that at this tighter tolerance, the models aligned more closely with the control model.

Table 7.7 Heat maps showing visual comparisons between ear models from test process chains with the model from the control process chain using Geomagic Control X

Heat map	
Maximum distance = 0.5	**Maximum distance = 0.1**
3D Slicer + 3D Coat with control	
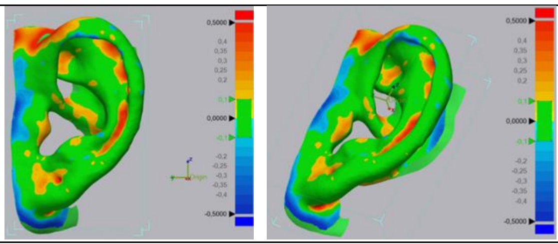	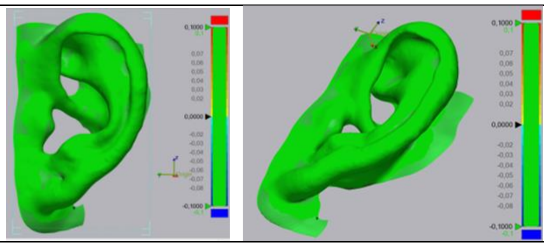
3D Slicer + ZBrush with control	
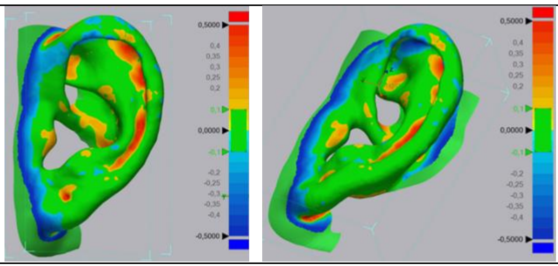	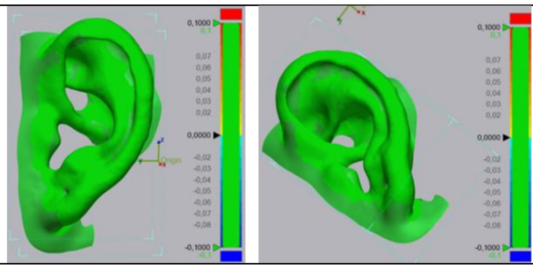
InVesalius + 3D Coat with control	
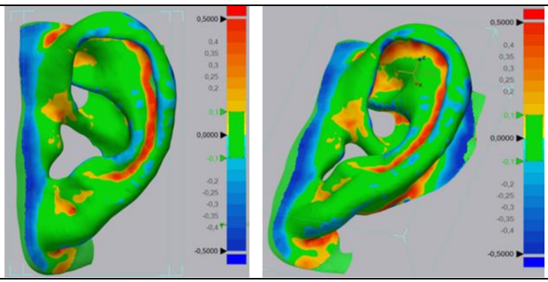	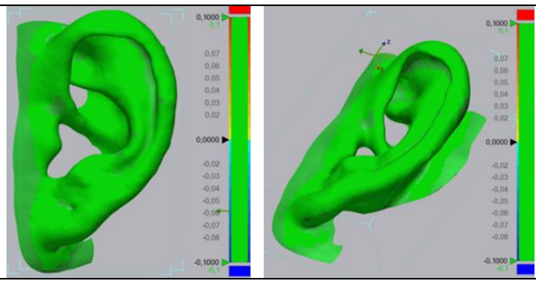
InVesalius + ZBrush with control	
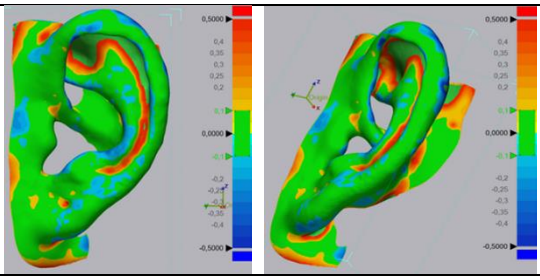	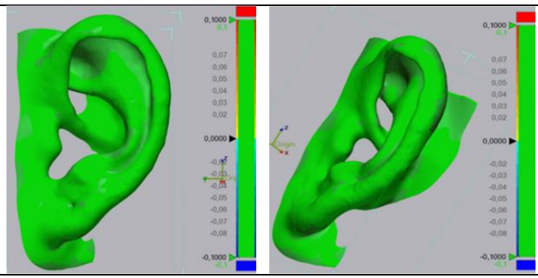

Artec + 3D Coat with control

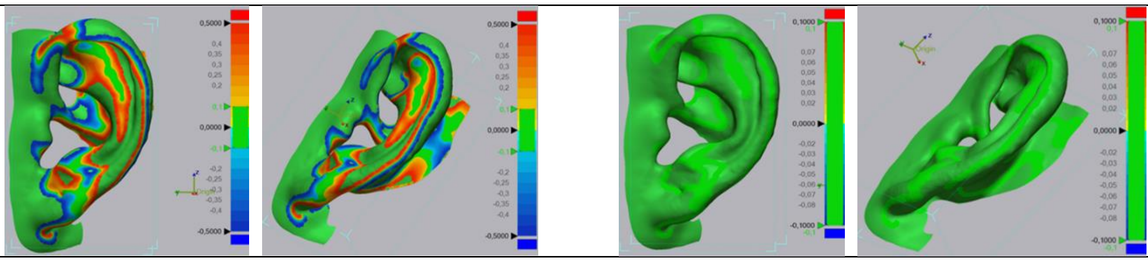

Artec + ZBrush with control

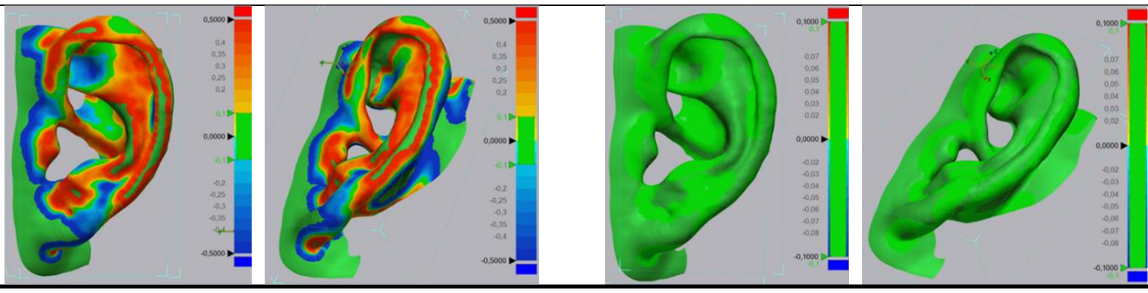

Model statistical comparison using CloudCompare

Distance statistics were calculated using CloudCompare to evaluate how closely the ear models from potential alternative process chains aligned with the control chain model. With the maximum distance set to 0.1, the statistics revealed that the points were, on average, very close, indicating that the test ear models closely resembled the control model within this range (Table 7.8). However, when the maximum distance was increased to 0.5, the statistics showed that the points remained relatively close only for comparisons that did not involve the Artec Spider scanner. For these process chains, the measurements at the 0.5 setting indicated that the alignments were less accurate.

Table 7.8 CloudCompare statistics of comparisons between ear models from test process chains with the model from the control process chain

Process chain	CloudCompare distance comparison statistics						
	Maximum distance = 0.5			Maximum distance = 0.1			
	Mean distance	RMS distance	Gauss Chi² distance	Mean distance	RMS distance	Gauss Chi² distance	Remark
3D Slicer + 3D Coat	0.157 (SD = 0.303) Value is less than 0.2 mm, which indicates that on average, the points are close.	0.341 Value suggests that the points are not well-aligned with some large deviations.	961323	0.082 (SD = 0.045) Value is close to zero mm, which indicates that on average, the points are very close.	0.093 Value suggests that the points are very well aligned with very little deviations.	4.106×10^6	Mimics and Geomagic Freeform mesh was slightly larger on the X-axis and Z- axis, and very similar in size on the Y- axis.
3D Slicer + ZBrush	0.104 (SD = 0.290) Value is less than 0.2 mm, which indicates that on average, the points are close.	0.308 Value suggests that the points are not well-aligned with some large deviations.	1.515×10^6	0.078 (SD = 0.049) Value is close to zero mm, which indicates that on average, the points are very close.	0.092 Value suggests that the points are very well aligned with very little deviations.	1×10^7	Mimics and Geomagic Freeform mesh was slightly larger on the X-axis, Z- axis, and on the Y- axis.
InVesalius + 3D Coat	0.049 (SD = 0.256) Value is less than 0.2 mm, which indicates that on average, the points are close.	0.260 Value suggests that most of the points are well-aligned with some deviations.	303508	0.070 (SD = 0.055) Value is close to zero mm, which indicates that on average, the points are very close.	0.089 Value suggests that the points are very well aligned with very little deviations.	2.838×10^6	Mimics and Geomagic Freeform mesh was slightly larger on the X-axis and Z- axis, and also larger in size on the Y- axis.

InVesalius + ZBrush	0.156 (SD = 0.305) Value is less than 0.2 mm, which indicates that on average, the points are close.	0.342 Value suggests that the points are not well-aligned with some large deviations.	1×10^{7}	0.079 (SD = 0.049) Value is close to zero mm, which indicates that on average, the points are very close.	0.093 Value suggests that the points are very well aligned with very little deviations.	1×10^{7}	Mimics and Geomagic Freeform mesh was slightly smaller on the X-axis, and also smaller on the Z- axis and on the Y- axis.
Artec + 3D Coat	0.337 (SD = 0.280) Value is greater than 0.2 mm, which indicates that on average, the points are not close.	0.438 Value suggests that the points are not well-aligned with some large deviations.	1×10^{7}	0.093 (SD = 0.030) Value is close to zero mm, which indicates that on average, the points are very close.	0.098 Value suggests that the points are very well aligned with very little deviations.	1×10^{7}	Mimics and Geomagic Freeform mesh was slightly larger on the X-axis and Z-axis, and also larger in size on the Y-axis.
Artec + ZBrush	0.314 (SD = 0.282) Value is greater than 0.2 mm, which indicates that on average, the points are not close.	0.422 Value suggests that the points are not well-aligned with some large deviations.	3.758×10^{6}	0.092 (SD = 0.032) Value is close to zero mm, which indicates that on average, the points are very close.	0.097 Value suggests that the points are very well aligned with very little deviations.	4.549×10^{6}	Mimics and Geomagic Freeform mesh was slightly larger on the X-axis and Z-axis, and also larger in size on the Y-axis.

SD = Standard deviation

Model statistical comparison using Geomagic Control X

Distance statistics were also calculated using Geomagic Control X to evaluate how closely the ear models from the potential alternative process chains resembled the control model. When the maximum distances were set at 0.1 and 0.5, the results showed that most points were relatively close. However, upon inspecting the RMS values, which is a more statistically robust measure of overall deviation between two geometries, the comparison revealed that the RMS values for models from process chains involving Artec Spider scan data were significantly larger than those models from chains combining MIP with CAD software. This indicated that the deviations in the ear models generated from the Artec Spider process chains were notably larger compared to the other chains, highlighting the higher accuracy of the chains comprising of MIP and CAD software. Table 7.9 shows comparative statistics of the ear model produced by the control process chain and the ear models produced by the test process chains.

Table 7.9 Geomagic Control X statistics of comparisons between ear models from test process chains with the model from the control process chain

Process chain	Geomagic Control X distance comparison statistics								
	Maximum distance = 0.5				Maximum distance = 0.1				
	Mean distance	RMS distance	Min	Max	Mean distance	RMS distance	Min	Max	Remark
3D Slicer + 3D Coat	0.083 (SD = 0.115)	0.142	-0.144	0.267	0.015 (SD = 0.046)	0.048	-0.1	0.1	Mimics and Geomagic Freeform mesh was slightly larger on the X-axis and Z- axis, and very similar in size on the Y- axis.
3D Slicer + ZBrush	0.0003 (SD = 0.144)	0.144	-0.5	0.499	-0.002 (SD = 0.053)	0.053	-0.1	0.1	Mimics and Geomagic Freeform mesh was slightly larger on the X-axis, Z- axis, and on the Y- axis.
InVesalius + 3D Coat	-0.009 (SD = 0.166)	0.166	-0.499	0.499	-0.009 (SD = 0.053)	0.054	-0.1	0.1	Mimics and Geomagic Freeform mesh was slightly larger on the X-axis and Z- axis, and also larger in size on the Y- axis.
InVesalius + ZBrush	0.012 (SD = 0.158)	0.159	-0.499	0.500	-0.016 (SD = 0.052)	0.055	-0.1	0.1	Mimics and Geomagic Freeform mesh was slightly smaller on the X-axis, and also smaller on the Z- axis and on the Y- axis.
Artec + 3D Coat	0.009 (SD = 0.204)	0.204	-0.499	0.500	-0.039 (SD = 0.044)	0.059	-0.1	0.1	Mimics and Geomagic Freeform mesh was slightly larger on the X-axis and Z-axis, and also larger in size on the Y-axis.
Artec + ZBrush	0.059 (SD = 0.278)	0.284	-0.500	0.499	-0.001	0.057	-0.1	0.1	Mimics and Geomagic Freeform mesh was slightly larger on the X-axis and Z-axis, and also larger in size on the Y-axis.

SD = Standard deviation; Min = Minimum distance; Max = maximum distance

Pinpoint anatomical region deviations using Geomagic Control X

The deviations between the control ear model and the test ear models were measured at six specific anatomical points to provide comparative data. The calculation of the absolute mean deviations demonstrated that process chains that combined MIP with CAD software produced more accurate ear models than those produced using process chains reliant on Artec Spider surface scan data. This result suggested that the integration of MIP and CAD software was more effective in producing anatomically accurate models compared to the models based on surface scan data. Table 7.10 presents the deviations measured at the six pinpoint anatomical regions of the ear model comparisons.

Table 7.10 Deviation and absolute mean comparison of ear pinpoint anatomical regions

Process chain	Deviation of pinpoint anatomical region						
	Superaurale	Subaurale	Protragion	Antitragus superior	Postaurale	Lobule posterion	Absolute mean deviation
3D Slicer + 3D Coat	0.095	0.022	0.233	0.106	-0.111	0.013	0.097
3D Slicer + ZBrush	-0.096	-0.041	0.191	-0.005	-0.130	0.017	0.080
InVesalius + 3D Coat	0.062	-0.034	0.078	0.052	-0.211	-0.052	0.082
InVesalius + ZBrush	-0.034	-0.044	0.022	-0.041	-0.039	-0.027	0.035
Artec + 3D Coat	-0.454	-0.143	-0.395	-0.359	-0.349	0.455	0.359
Artec + ZBrush	0.358	-0.470	0.267	-0.109	0.453	0.483	0.357

7.3.3 Analysis of process chain nose models

Error detection in models using Meshmixer

Similarly to the starburst analysis of the various ear models, the error density analysis with Meshmixer's Inspector tool revealed that only a minimal number of errors were introduced into the nose models. Interestingly, the control process chain introduced the most errors among all the process chains (Table 7.11). Additionally, three of the test process chains did not introduce any errors into the models.

Table 7.11 Meshmixer Inspector error analysis of process chain nose models

Process chain		
Mimics + Geomagic Freeform (Control)	3D Slicer + 3D Coat	3D Slicer + ZBrush
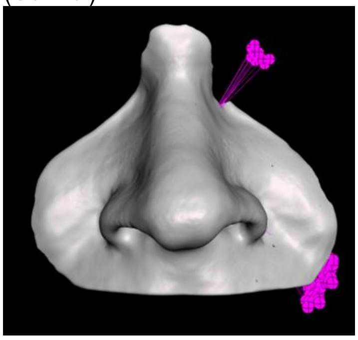	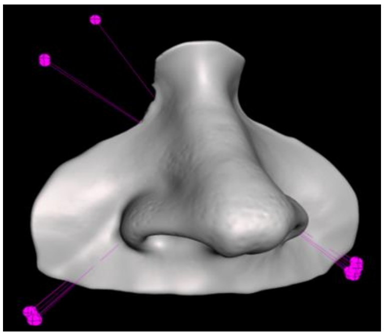	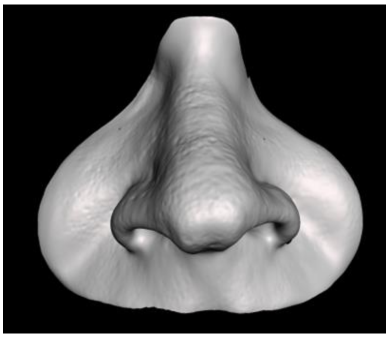
Errors = 45	Errors = 19	Errors = 0
	InVesalius + 3D Coat	InVesalius + ZBrush
	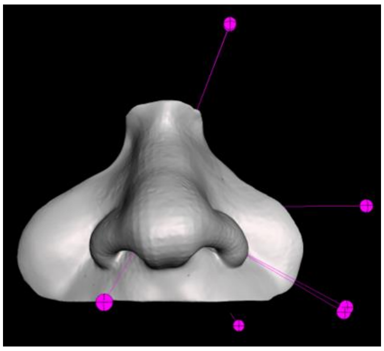	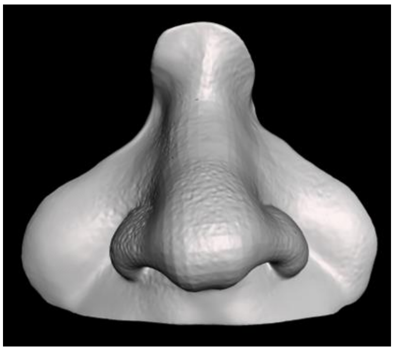
	Errors = 7	Errors = 0
	Artec + 3D Coat	Artec + ZBrush
	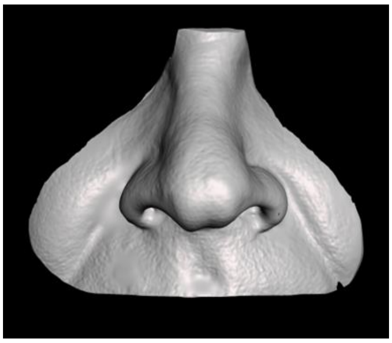	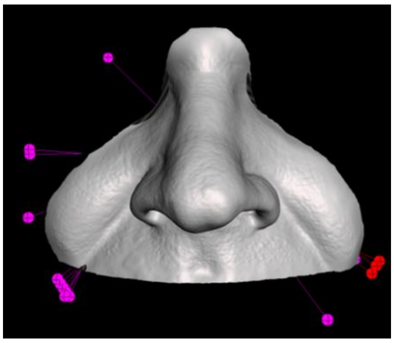
	Errors = 0	Errors = 15

Model heat map and statistical comparisons using Magics

The nose models produced by the potential alternative process chains were also compared to the control model in Magics. This comparison revealed interesting differences. The nose model analyses showed deviation values consistently exhibited as two distinct peaks (Table 7.12). Both deviation peaks fell within the green range of the histogram in the model produced using InVesalius combined with 3D Coat, indicating that the model closely resembled the control model with minimal deviations. A large deviation peak occurred in the green range, and a smaller one in the blue range in the models produced using 3D Slicer combined with 3D Coat, and 3D Slicer combined with ZBrush. These peaks suggest that these test models were largely similar to the control model, although certain areas of the model were slightly smaller than the control, as indicated by the blue deviation values. In contrast, the models produced using InVesalius combined with ZBrush, and Artec combined with 3D Coat, showed deviation peaks in the green-red zone, with a larger peak in the red range and a smaller peak in the green. These deviations imply that these two test models were substantially larger than the control model, with the red deviations indicating areas of excess material.

Table 7.12 Statistics, heat maps, and histograms showing comparisons between nose models from test process chains with the model from the control process chain using Magics

Process chain	Statistics, heat map, and histogram					
	Min	Max	Range	Heat map	Histogram	Remark
3D Slicer + 3D Coat	-3.237	3.245	6.482	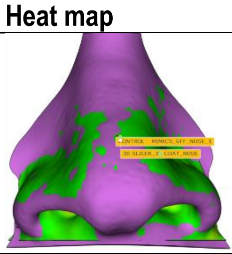	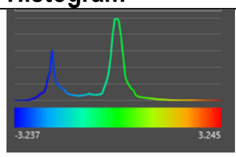	Green = Control
3D Slicer + ZBrush	-3.075	2.703	5.778	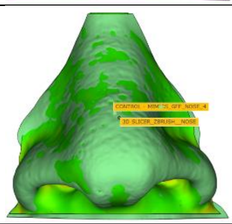	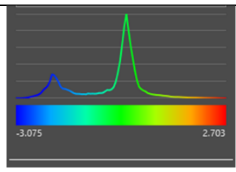	Shiny green = Control

InVesalius + 3D Coat	-9.226	6.617	15.843	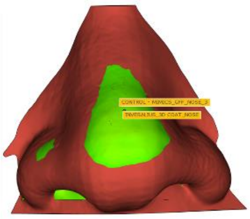	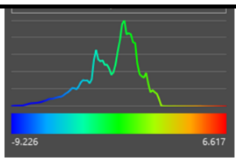	Bright green = Control
InVesalius + ZBrush	-9.197	1.568	10.765	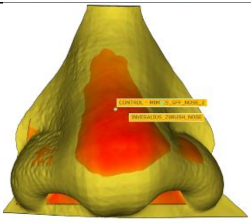	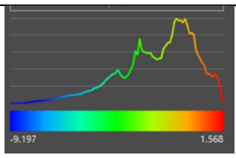	Red = Control
Artec + 3D Coat	-9.422	1.577	10.999	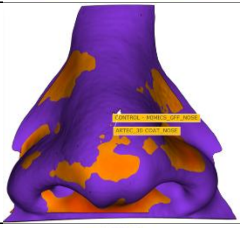	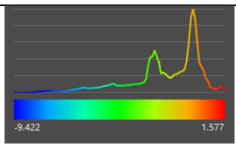	Orange = Control
Artec + ZBrush	-9.886	4.846	14.732	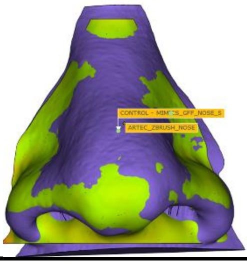	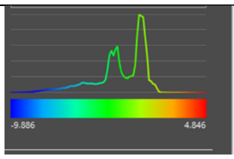	Green = Control

Min = Minimum distance; Max = maximum distance

Model heat map comparisons using CloudCompare

The CloudCompare heat maps comparing the nose models produced by the potential alternative process chains with the control chain revealed noticeable visual differences. The deviations were substantial for both maximum settings of 0.1 and 0.5, with many of the deviations lying in the red zone. The process chains using InVesalius combined with either 3D Coat or ZBrush, showed the most discrepancies, with large areas highlighted in the red spectrum, indicating substantial differences (Table 7.13). In contrast, the other models displayed extensive regions with relatively minor discrepancies, highlighted in green, alongside areas with significant discrepancies, highlighted in dark red.

Table 7.13 **Heat maps showing visual comparisons between nose models from test process chains with the model from the control process chain using CloudCompare**

Heat maps	
Maximum distance = 0.5	**Maximum distance = 0.1**
3D Slicer + 3D Coat with control	
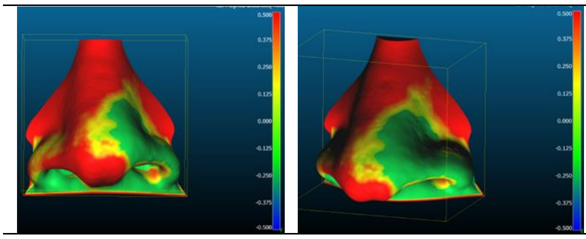	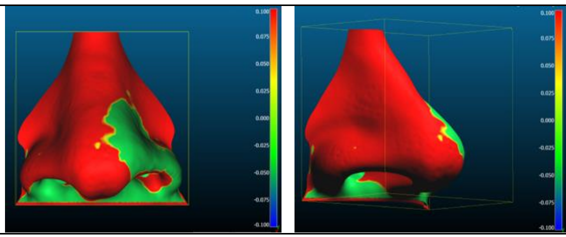
3D Slicer + ZBrush with control	
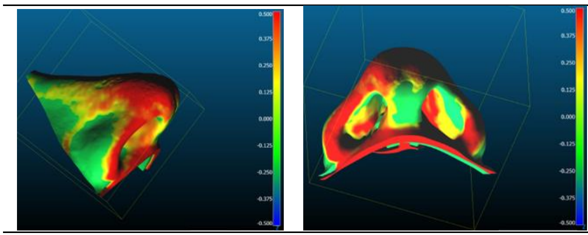	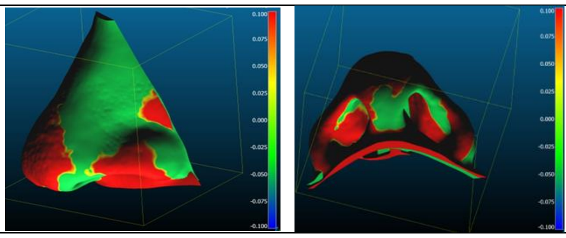
InVesalius + 3D Coat with control	
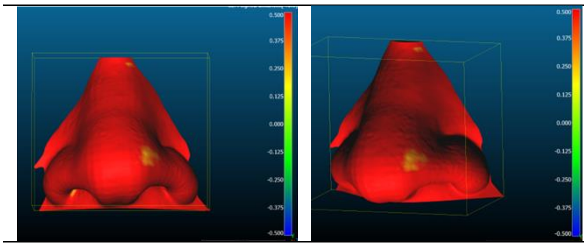	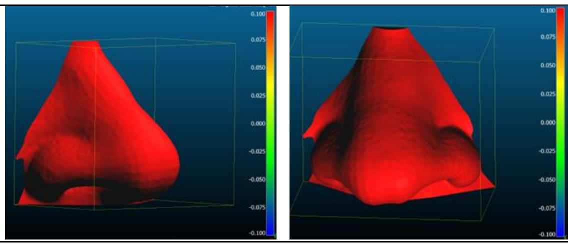
InVesalius + ZBrush with control	
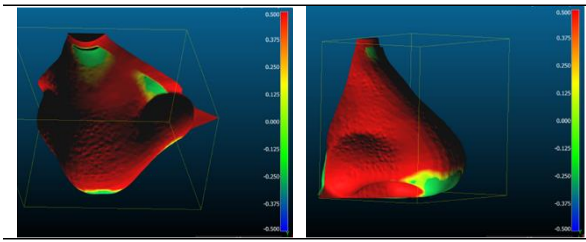	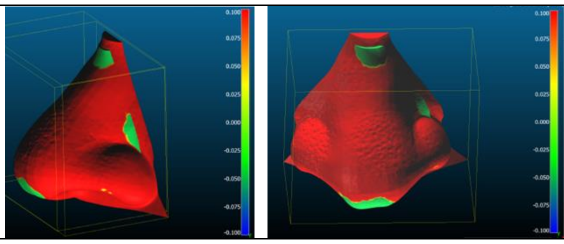
Artec + 3D Coat with control	
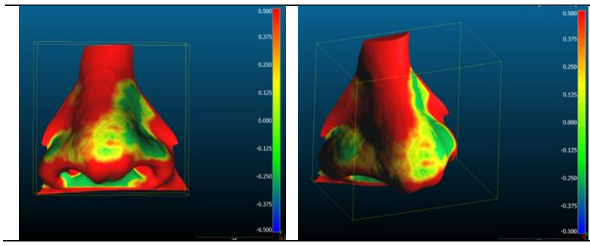	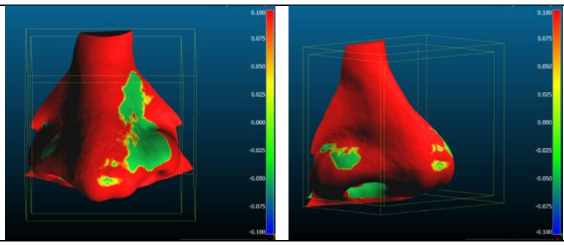

Artec + ZBrush with control

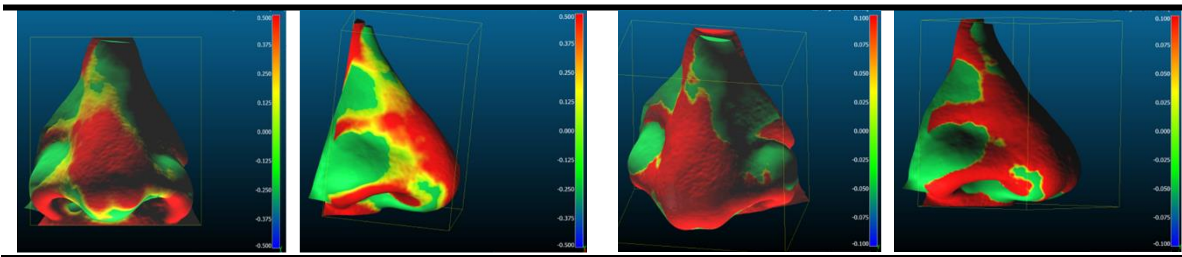

Model heat map comparisons using Geomagic Control X

The Geomagic Control X heat maps of the comparison between the alternative process chain nose models and the control model, showed a relatively wide range of deviations. All alternative process chain nose models, except for the one produced with 3D Slicer in combination with 3D Coat, exhibited deviations from the control model that ranged from the mid-range (indicating relatively minor differences) to the extreme red zone with a maximum distance set at 0.5 (Table 7.14). These deviations signified large, significant deviations between the alternative model and the control. When the maximum distance setting was adjusted to 0.1, all alternative nose models demonstrated deviations predominantly within the green spectrum from the control, indicating a closer alignment between the models, but still showing variations across the test models.

Table 7.14 **Heat maps showing visual comparisons between nose models from test process chains with the model from the control process chain using Geomagic Control X**

Heat map	
Maximum distance = 0.5	**Maximum distance = 0.1**
3D Slicer + 3D Coat with control	
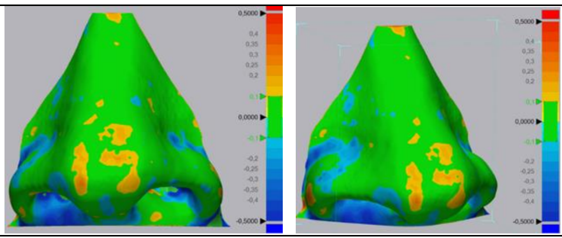	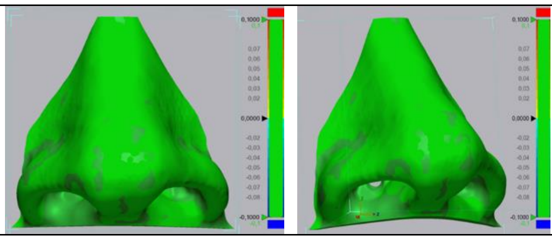
3D Slicer + ZBrush with control	
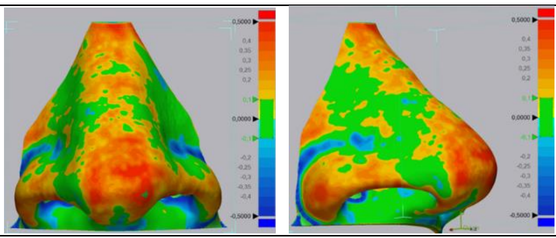	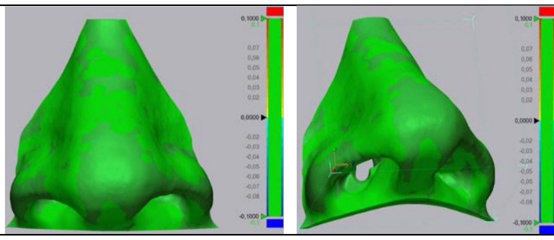
InVesalius + 3D Coat with control	
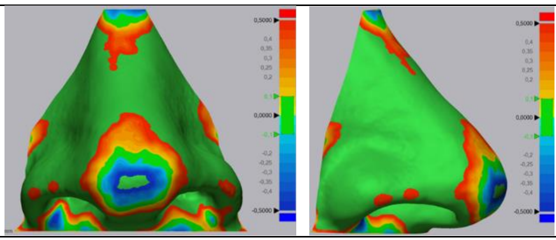	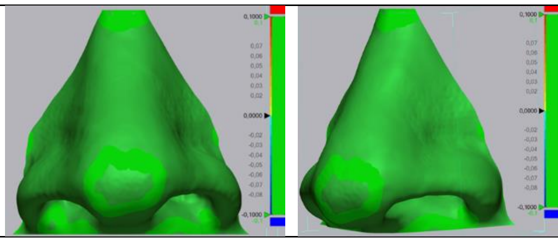
InVesalius + ZBrush with control	
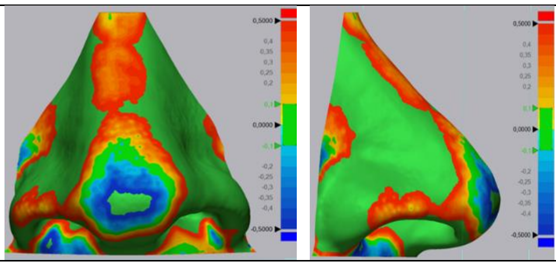	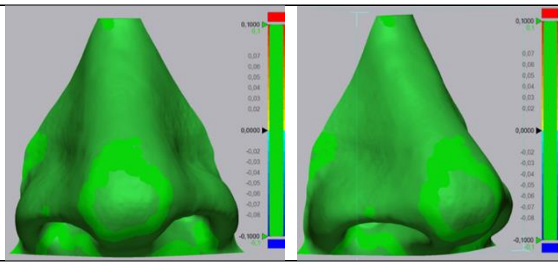

Artec + 3D Coat with control

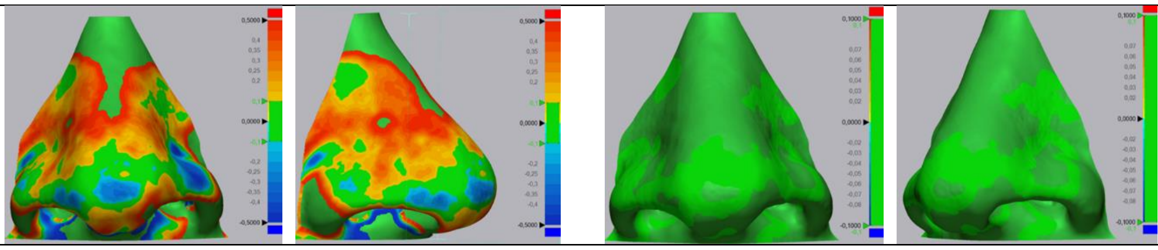

Artec + ZBrush with control

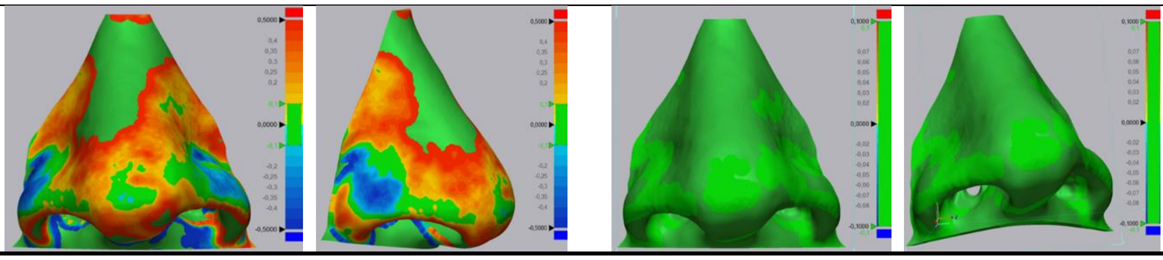

Model statistical comparison using CloudCompare

The distances statistics were also calculated to show how well the alternative process chain nose models aligned with the control nose model. When the maximum distance was set to 0.1, the statistics indicated that, on average, the points were very close, demonstrating that the test nose models closely resembled the control model in this range (Table 7.15). However, when the maximum distance was increased to 0.5, the alignment in all comparisons showed substantial deviations, as shown by the relatively high RMS values. In particular, the deviations were not close for the process chains that involved InVesalius, as well as the chain were Artec Spider nose scan data were combined with 3D Coat.

Table 7.15 CloudCompare statistics of comparisons between nose models from test process chains with the model from the control process chain

Process chain	CloudCompare distance comparison statistics						
	Maximum distance = 0.5			Maximum distance = 0.1			
	Mean distance	RMS distance	Gauss Chi² distance	Mean distance	RMS distance	Gauss Chi² distance	Remark
3D Slicer + 3D Coat	0.292 (SD = 0.297) Value is slightly greater than 0.2 mm, which indicates that on average, the points are relatively close.	0.417 Value suggests that the points are not well-aligned with some large deviations.	1×10^7	0.092 (SD = 0.032) Value is close to zero mm, which indicates that on average, the points are very close.	0.097 Value suggests that the points are very well aligned with very little deviations.	1×10^7	Mimics and Geomagic Freeform mesh was similar in size on the X-axis, and slightly smaller on the Y-axis and on the Z-axis.
3D Slicer + ZBrush	0.199 (SD = 0.330) Value is slightly less than 0.2 mm, which indicates that on average, the points are close.	0.385 Value suggests that the points are not well-aligned with some large deviations.	9.571×10^6	0.086 (SD = 0.041) Value is close to zero mm, which indicates that on average, the points are very close.	0.095 Value suggests that the points are very well aligned with very little deviations.	1×10^7	Mimics and Geomagic Freeform mesh was marginally smaller on the X-axis and significantly smaller on the Y-axis, and noticeably larger on the Z-axis.
InVesalius + 3D Coat	0.467 (SD = 0.142) Value is greater than 0.2 mm, which indicates that on average, the points are not close.	0.488 Value suggests that the points are not well-aligned with some large deviations.	1×10^7	0.099 (SD = 0.013) Value is close to zero mm, which indicates that on average, the points are very close.	0.099 Value suggests that the points are very well aligned with very little deviations.	1×10^7	Mimics and Geomagic Freeform mesh was similar in size on the X-axis, and slightly smaller on the Y-axis, and significantly smaller on the Z-axis.

InVesalius + ZBrush	0.436 (SD = 0.185) Value is greater than 0.2 mm, which indicates that on average, the points are not close.	0.474 Value suggests that the points are not well-aligned with some large deviations.	1×10^{7}	0.467 (SD = 0.142) Value is greater than 0.2 mm, which indicates that on average, the points are not close.	0.099 Value suggests that the points are very well aligned with very little deviations.	1×10^{7}	Mimics and Geomagic Freeform mesh was significantly smaller on the X-axis and on the Y-axis and noticeably larger on the Z-axis.
Artec + 3D Coat	0.467 (SD = 0.142) Value is greater than 0.2 mm, which indicates that on average, the points are not close.	0.488 Value suggests that the points are not well-aligned with some large deviations.	1×10^{7}	0.090 (SD = 0.034) Value is close to zero mm, which indicates that on average, the points are very close.	0.096 Value suggests that the points are very well aligned with very little deviations.	1×10^{7}	Mimics and Geomagic Freeform was similar in size on the X-axis, and slightly smaller on the Y-axis and on the Z-axis.
Artec + ZBrush	0.284 (SD = 0.294) Value is slightly greater than 0.2 mm, which indicates that on average, the points are relatively close.	0.409 Value suggests that the points are not well-aligned with some large deviations.	3.758×10^{6}	0.089 (SD = 0.036) Value is close to zero mm, which indicates that on average, the points are very close.	0.096 Value suggests that the points are very well aligned with very little deviations.	5.435×10^{6}	Mimics and Geomagic Freeform mesh was slightly smaller on the X-axis and significantly smaller on the Y-axis, as well as noticeably larger on the Z-axis.

SD = Standard deviation

Model statistical comparison using Geomagic Control X

The distance statistics were also calculated using Geomagic Control X to assess how closely the test nose models aligned with the control model. When the maximum deviation was set to 0.5, the results indicated that, on average, the test nose models were closely aligned with the control. In this range, the nose model produced with the process chain in which 3D Slicer was combined with 3D Coat showed the best overall fit (see Table 7.16). Similarly, at a maximum distance setting of 0.1, all test nose models exhibited minimal deviations, further highlighting their close resemblance to the control model across this tighter tolerance range.

Table 7.16 Geomagic Control X statistics of comparisons between nose models from test process chains with the model from the control process chain

Process chain	Geomagic Control X distance comparison statistics								
	Maximum distance = 0.5				Maximum distance = 0.1				
	Mean distance	RMS distance	Min	Max	Mean distance	RMS distance	Min	Max	Remark
3D Slicer + 3D Coat	0.036 (SD = 0.154)	0.158	-0.500	0.500	-0.006 (SD = 0.052)	0.052	-0.1	0.1	Mimics and Geomagic Freeform mesh was similar in size on the X-axis, and slightly smaller on the Y-axis and on the Z-axis.
3D Slicer + ZBrush	0.081 (SD = 0.189)	0.206	-0.499	0.500	0.012 (SD = 0.057)	0.058	-0.1	0.1	Mimics and Geomagic Freeform mesh was marginally smaller on the X-axis and significantly smaller on the Y-axis, and noticeably larger on the Z-axis.
InVesalius + 3D Coat	0.118 (SD = 0.280)	0.304	-0.500	0.500	0.004 (SD = 0.058)	0.058	-0.1	0.1	Mimics and Geomagic Freeform mesh was similar in size on the X-axis, and slightly smaller on the Y-axis, and significantly smaller on the Z-axis.
InVesalius + ZBrush	0.140 (SD = 0.269)	0.306	-0.499	0.500	-0.003 (SD = 0.059)	0.059	-0.1	0.1	Mimics and Geomagic Freeform mesh was similar in size on the X-axis, and slightly smaller on the Y-axis and on the Z-axis.
Artec + 3D Coat	0.113 (SD = 0.231)	0.257	-0.500	0.500	0.014 (SD = 0.057)	0.059	-0.1	0.1	Mimics and Geomagic Freeform was similar in size on the X-axis, and slightly smaller on the Y-axis and on the Z-axis.
Artec + ZBrush	0.135 (SD = 0.232)	0.268	-0.499	0.500	0.009 (SD = 0.058)	0. 059	-0.1	0.1	Mimics and Geomagic Freeform mesh was slightly smaller on the X-axis and significantly smaller on the Y-axis, as well as noticeably larger on the Z-axis.

SD = Standard deviation; Min = Minimum distance; Max = maximum distance

Pinpoint anatomical region deviations using Geomagic Control X

The deviations between the control nose model and the test nose models were measured at six specific anatomical points to provide more accurate comparative data. No distinct pattern emerged from these pinpoint deviation measurements. However, models produced from process chains involving 3D Slicer, as well as the chain combining Artec Spider scan data with ZBrush, exhibited substantially lower absolute mean deviation values compared to the other test chains (see Table 7.17). It is important to note that the alignment of the control model with the test models produced with InVesalius in combination with ZBrush, and to a lesser extent InVesalius combined with 3D Coat, proved to be challenging, which probably contributed to the higher deviation measurements in these cases.

Table 7.17 Deviation and absolute mean comparison of nose pinpoint anatomical regions

Process chain	Deviation of pinpoint anatomical region						
	Kyphion	Pronasale	Columellar peak	Subnasale	Alare	Alar curvature	Absolute mean deviation
3D Slicer + 3D Coat	-0.029	-0.034	-0.138	-0.127	0.264	-0.079	0.112
3D Slicer + ZBrush	0.228	0.255	-0.006	-0.123	0.404	0.219	0.205
InVesalius + 3D Coat	0.496	-0.486	0.489	NR	NR	0.465	0.484
InVesalius + ZBrush	0.406	-0.457	0.151	NR	NR	NR	0.338
Artec + 3D Coat	0.493	-0.279	0.225	-0.354	0.492	0.422	0.378
Artec + ZBrush	0.000	-0.087	0.372	-0.104	0.198	-0.402	0.194

NR = No result because of alignment problems

7.3.4 Best-fit ranking of potential alternative process chains

A more focused comparison of the test process chains was conducted to better understand their relative performance against the control process chain. Based on various comparative statistical analyses, the process chains were ranked, with a score of "1" indicating the best alignment with the control model. USRI values were calculated for each of the test process chains using the SRs of the initial ratings to compare the performance of the different process chains. The index values revealed that the test chains involving 3D Slicer consistently produced the most accurate models (Table 7.18). The process chain combining InVesalius with 3D Coat ranked second, while the remaining three chains demonstrated similar performances, all positioned in the third tier. Despite the slight differences among the chains, all test process chains were deemed acceptable, leading to the conclusion that each alternative process chain offers a viable substitute for the industry-benchmark chain.

Table 7.18 Best-fit ranking of test process chains based on different comparative rankings between the test models and control models

Best-fit rating, standardised rating, and USRI																	
Process chains	**Magics histogram**				**CloudCompare histogram (Max 0.5)**				**Geomagic Control X histogram (Max 0.5)**				**Pinpoint anatomical deviation**				**USRI**
	Ear		*Nose*		*Ear*		*Nose*		*Ear*		*Nose*		*Ear*		*Nose*		
3D Slicer + 3D Coat	2	0.17	2	0.13	2	0.17	2	0.14	3	0.21	1	0.06	2	0.15	1	0.07	13.8
3D Slicer + ZBrush	1	0.08	2	0.13	2	0.17	1	0.07	1	0.07	2	0.12	2	0.15	2	0.13	11.5
InVesalius + 3D Coat	2	0.17	1	0.06	1	0.08	3	0.21	2	0.14	3	0.18	2	0.15	4	0.27	15.8
InVesalius + ZBrush	3	0.25	4	0.25	2	0.17	3	0.21	3	0.21	4	0.24	1	0.08	3	0.20	20.1
Artec + 3D Coat	2	0.17	4	0.25	2	0.17	3	0.21	2	0.14	3	0.18	3	0.23	3	0.20	19.4
Artec + ZBrush	2	0.17	3	0.19	3	0.25	2	0.14	3	0.21	4	0.24	3	0.23	2	0.13	19.5

SR = Standardised Rating; USRI = Unweighted Standardised Rating Index; Max 0.5 = Statistics of maximum distance set at 0.5 used for ranking

7.3.5 Prints of nose moulds and casting of silicone models

To illustrate the final steps in the process chain for designing and manufacturing a prosthesis, a mould was created using a nose designed in the combination of 3D Slicer and 3D Coat software. This mould was then 3D printed using liquid resin material. The 3D printed mould was subsequently used to cast a silicone nose prosthesis, which was hand-painted. Table 7.19 displays various angles of the printed mould as well as the front views of the silicone nose prosthesis.

Table 7.19 Example of nose mould (negative) and silicone nose prostheses (positive)

3D Slicer combined with 3D Coat		
 Complete mould	 Mould front	 Mould back
 Silicone nose front	 Silicone nose placed on mould	

7.3.6 Estimated cost of the process chains

To gain insight into how the potential alternative process chains differed in terms of cost, they were compared using cost estimates for software investment and data generation. Although costs such as labour and equipment, specifically the CT scanner and Artec Spider, were not included, it is important to note that the initial investment for the Artec Spider surface scanner is approximately R530 000. Overall, the test process chains were found to be significantly more cost-effective when compared to the control process chain. Table 7.20 presents a comprehensive overview of the key components of the process chains under evaluation. It revealed that the process chain using surface scanned data combined with 3D Coat was the most affordable, with the two chains that combined 3D Coat with the two MIP software applications being the cheapest among the MIP and CAD process chains. This highlights that cost savings can be achieved by opting for surface scanning technology and carefully selecting software combinations.

Table 7.20 Cost-based ranking of the process chains

Process chain cost analysis							
Proposed process chain	Data acquisition	MIP software		CAD software		Total process chain cost	Proposed process chain ranking
		Initial investment	Recurring cost (license fee)	Initial investment	Recurring cost (license fee)		
Mimics + Geomagic Freeform	CT Dicom/scan R1500 – R2000	Mimics > R1.7M	Mimics R268 000 (annual license renewal fee)	Geomagic Freeform with Haptic Device R250 000	-	±R520 000	7
3D Slicer + 3D Coat	CT Dicom/scan R1500 – R2000	3D Slicer Free	3D Slicer Free	3D Coat Free	3D Coat Free	±R2 000	2
3D Slicer + ZBrush	CT Dicom/scan R1500 – R2000	3D Slicer Free	3D Slicer Free	ZBrush R15 900 (per license)	-	±R17 900	4
InVesalius + 3D Coat	CT Dicom/scan R1500 – R2000	InVesalius Free	InVesalius Free	3D Coat Free	3D Coat Free	±R2 000	2
InVesalius + ZBrush	CT Dicom/scan R1500 – R2000	InVesalius Free	InVesalius Free	ZBrush R15 900 (per license)	-	±R17 900	4
Artec Spider + 3D Coat	Artec Spider Initial investment R527 289	Artec Studio Initial investment R527 289	Artec Studio Free	3D Coat Free	3D Coat Free	R 0	1
Artec Spider + ZBrush	Artec Spider Initial investment R527 289	Artec Studio Initial investment R527 289	Artec Studio Free	ZBrush R15 900 (per license)	-	±R17 900	4

"1" = most cost effective

7.4 Ear/nose geometry resource

A dedicated ear and nose repository has been established at CRPM to produce external maxillofacial prostheses. The Artec Spider surface scanner was used to create 14 ear and 14 nose 3D geometries that make up this initial database. Without the need for CT scanning, these pre-designed, instantly available ear and nose geometries are meant to be a useful resource for medical professionals and designers. Table 7.21 outlines the steps involved in the creation of the geometries, illustrating the process from scanning to final model production. Table 7.21 A shows the raw data displayed in Artec Studio software, while Table 7.21 B shows the scanned datasets that have been “knitted” together to form surface meshes of three ears and three noses, and Table 7.21 C shows the 3D models of the ears and noses created from the surface mesh data.

Table 7.21 Examples of ear and nose geometries in the ear/nose resource

Ear			
A.		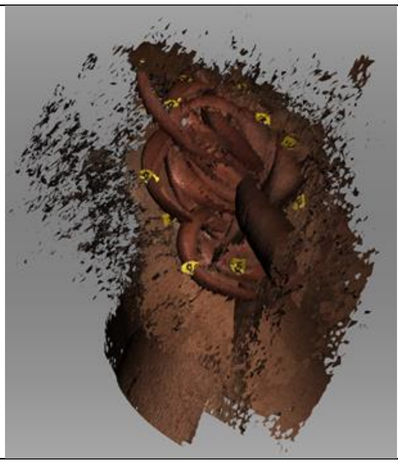	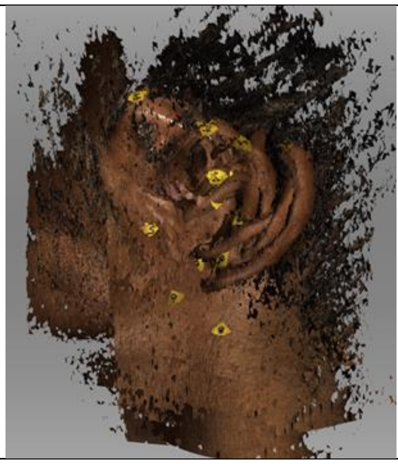

B.

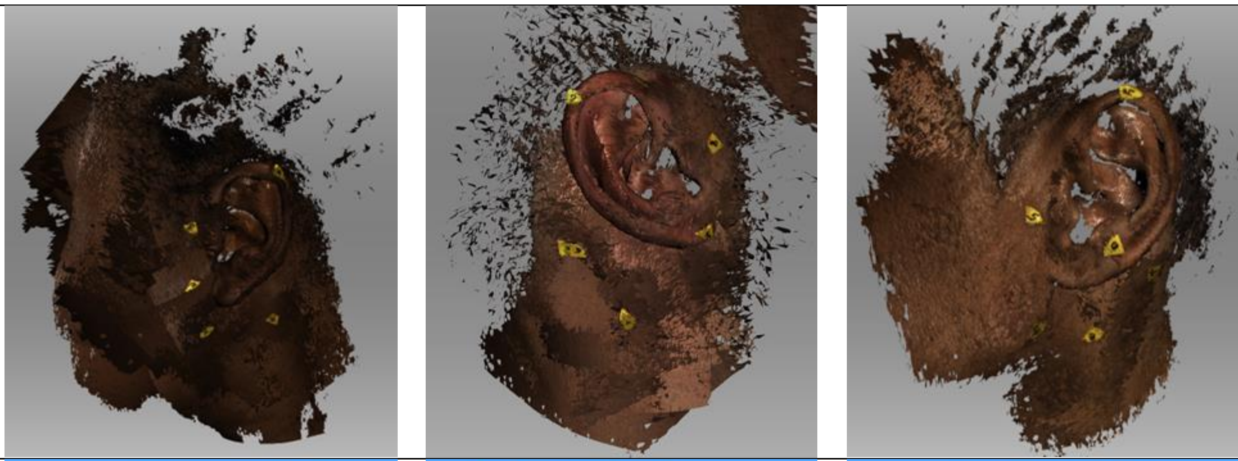

C.

Noses

A.

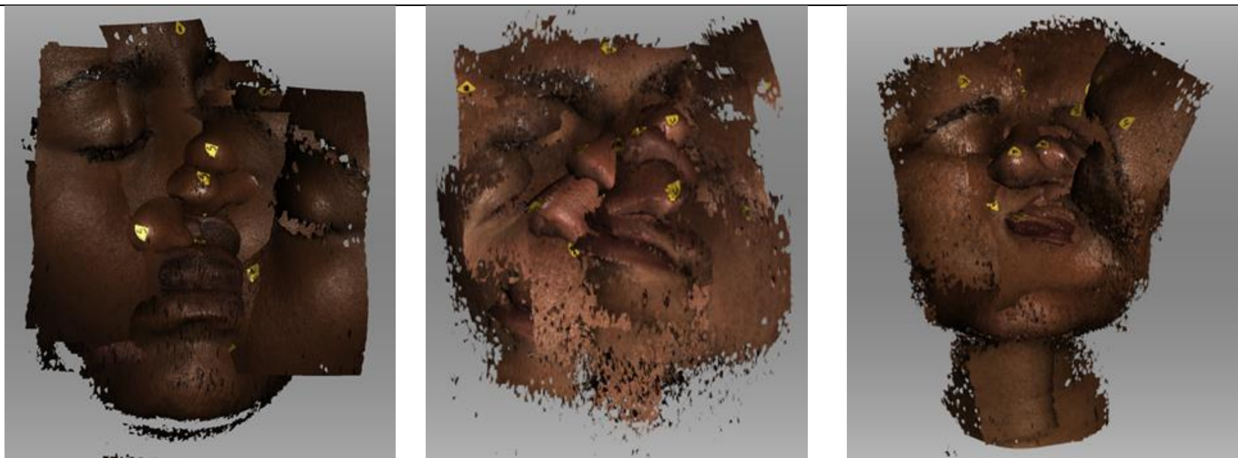

B.

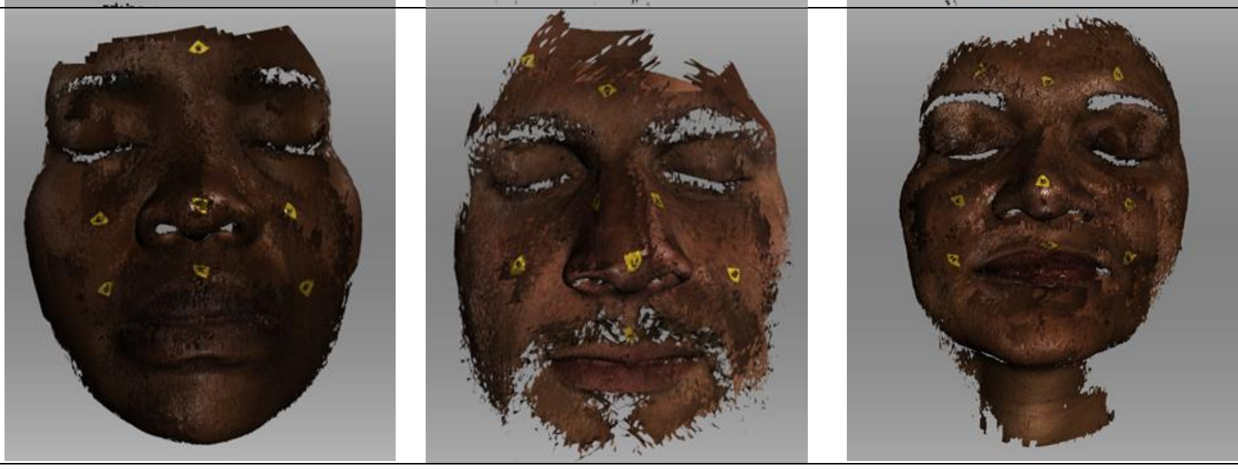

C.

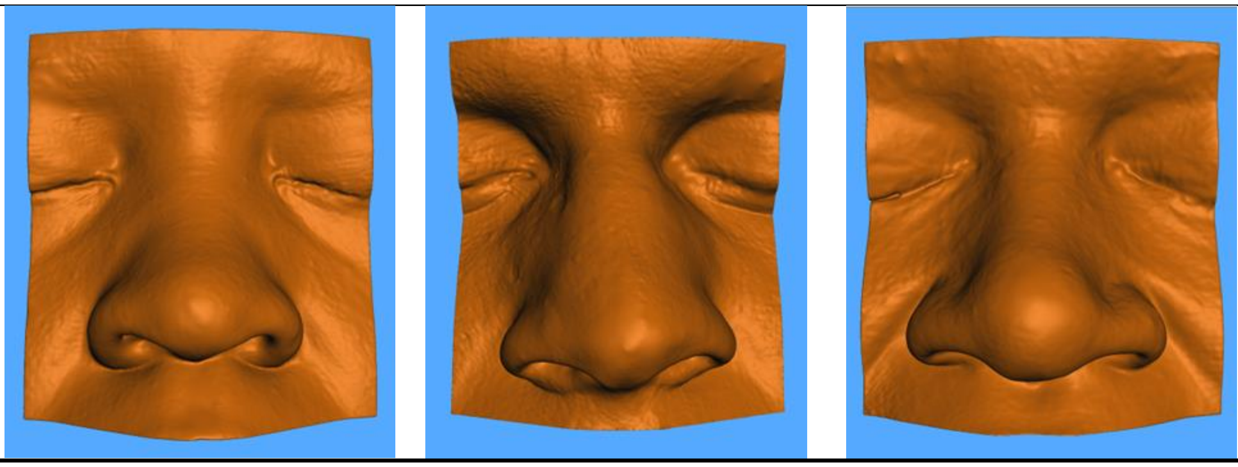

7.4.1 Deformity repair illustration using an ear from the resource

The ED model was digitally repaired to demonstrate the application of the dedicated ear and nose repository. After importing the ED model into 3D Coat, an ear selected from the database was imported into the CAD software. The ear was then positioned over the deformity to digitally repair the ED model. Once properly aligned, the ear's edges were blended and smoothed to produce a seamless fit. Table 7.22 A shows the ear used for the digital repair, while Table 7.22 B, C, and D present various views of the ear on the ED model. Table 7.22 E, F, and G illustrate the smoothed edges, and Table 7.22 H and I display the final ear, securely and seamlessly attached to the ED model.

Table 7.22 Illustration of the steps followed to digitally repair the ear deformity (ED)

Images of digital repair of ED		
A. 	B. 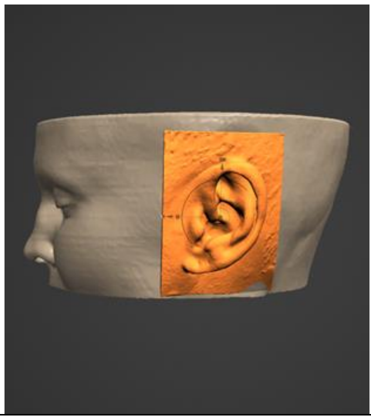	C. 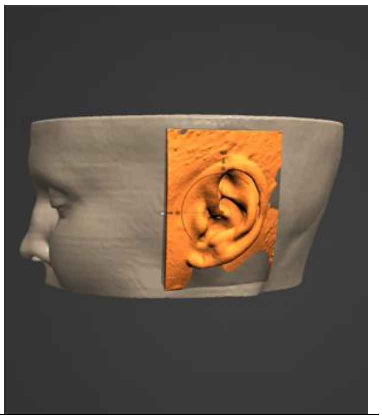

D.	E.	F.
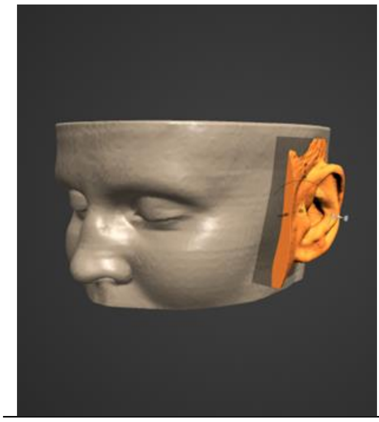	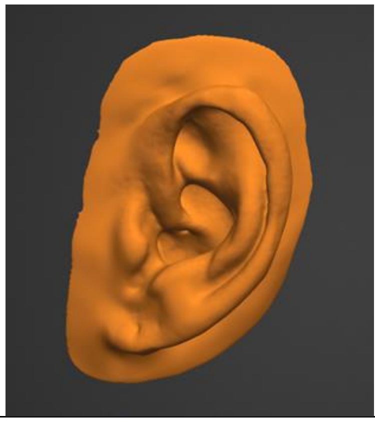	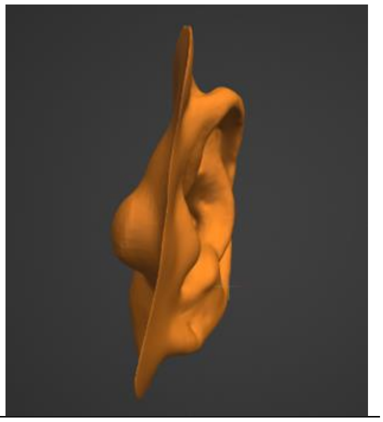
G.	H.	I.
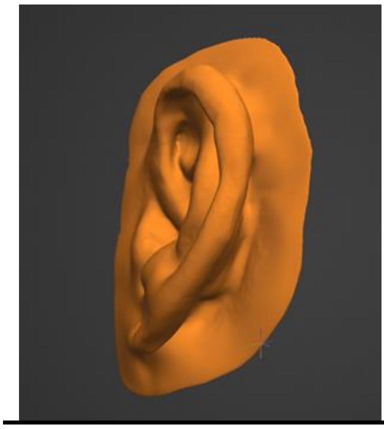	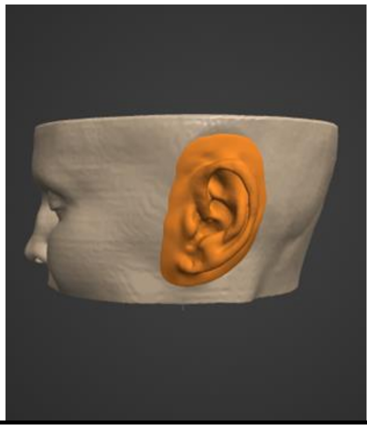	

7.4.2 Deformity repair illustration using a nose from the resource

The ND model was also digitally repaired to demonstrate the application of the repository. A nose model, selected from the database, was fitted onto the ND model using 3D Coat, illustrating the process of integrating pre-designed prosthetic components. Table 7.23 A shows the nose used for the digital repair, while Table 7.23 B, C, and D present various views of the nose on the ND model. Table 7.23 E, F, and G illustrate the smoothed edges of the nose, and Table 7.23 H and I display the final nose, securely and seamlessly attached to the ND model.

Table 7.23 Illustration of the steps followed to digitally repair the nose deformity (ND)

Images of digital repair of ND		
A. 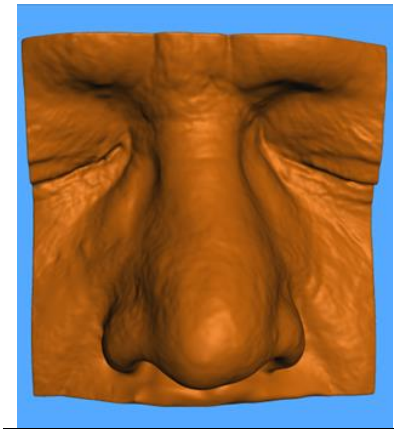	B. 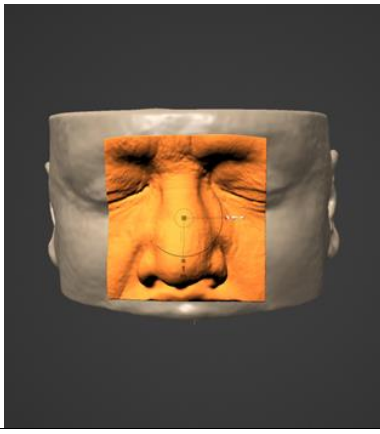	C. 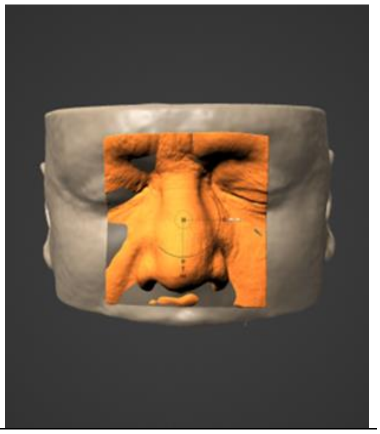
D. 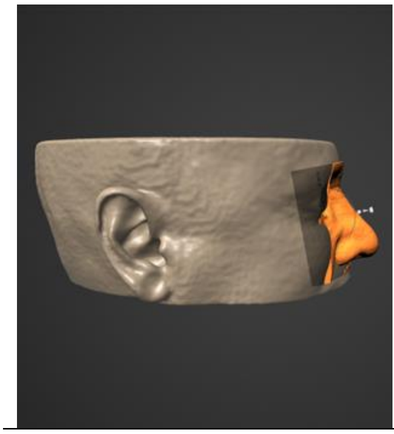	E. 	F. 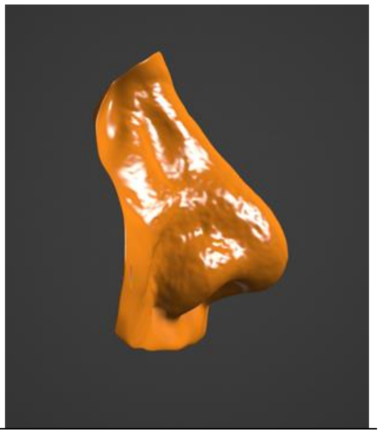
G. 	H. 	I. 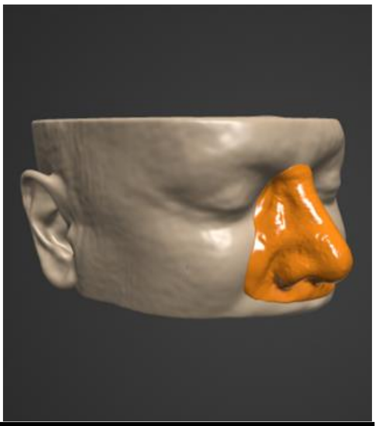

7.5 Discussion and conclusion

In the final phase of this study, several potential alternative process chains were evaluated as more cost-effective alternatives to the industry-benchmark control process chain. The results of the study showed that all six evaluated process chains were viable alternatives for the industry-benchmark, as they exhibited similar accuracy and performance. The four alternative process chains, which integrated MIP and CAD software, produced real-world models of comparable quality to those produced with the control process chain. However, it is important to highlight that ZBrush is a sophisticated software application that requires a skilled designer to operate for model design (Sarstedt, 2012; Durisetti et al., 2022). Similarly, process chains that used data from the Artec Spider scanner produced models that were similar to those of the control chain. However, a crucial difference between the two groups became apparent. The process chains that integrated MIP software mostly depended on CT volumetric data, which has a higher radiation risk and costs more because it requires specialised equipment and knowledge (Esmaeilzadeh et al., 2024). On the other hand, the process chains that used Artec Spider data provide a more economical option because it is portable, radiation-free, and cheaper (Diara, 2023). It is a more accessible choice because it does not require specialised expertise. Despite the advantages of the Artec Spider, it has limitations. When using the Artec Spider to capture surface data, it can be difficult to capture data of undercuts and holes of facial anatomy (Paxton et al., 2022; Erolin, 2023). As a result, there may be missing data that needs to be designed further in CAD software. In addition, the scanner has trouble in recognising hair and reflective surfaces, and the mesh alignment during the "knitting" process might be challenging (Paxton et al., 2022).

In summary, the results of this study showed that it was possible to identify process chains that are more cost-effective. Based on project requirements, process chains can be chosen based on overall cost, and balancing factors such as the use of surface-scanned data versus CT-generated data, software complexity, quality level, and the skill level necessary for effective implementation.

Chapter 8

Discussion and Conclusion

8.1 Introduction

Facial trauma and deformities in South Africa have significant repercussions, not only for the affected individuals but also for their families and communities. The consequences of facial trauma extend beyond physical disfigurement, and includes economic burdens such as loss of income, the need for extended care, and the emotional toll on both the individual and their caregivers (Yadav & Shrestha, 2017; Sarwer et al., 2022). These factors highlight the importance of accessible reconstructive solutions, particularly for populations with limited financial resources (Adeleke et al., 2023).

Advanced technologies have revolutionised the field of external maxillofacial prosthesis manufacturing. Digital imaging, medical image processing (MIP), computer-aided design (CAD), computer-aided manufacturing (CAM), and additive manufacturing (AM) have collectively transformed how prostheses are designed and produced (Bai et al., 2014; Cruz et al., 2020). These technologies have largely supplanted traditional, labour-intensive carving methods, offering less invasive and more efficient alternatives that are increasingly favoured in clinical practice (Petrovic et al., 2012; Sakib-Uz-Zaman & Khondoker, 2023). The ability to create custom-made prostheses that precisely match a patient's anatomy represents a significant advancement, providing patients with more personalised and effective treatment options (Cruz et al., 2020; Safali et al., 2023). Despite these advancements, the high costs associated with these advanced technologies pose a significant barrier to many South African patients who require prostheses (Olatunji et al., 2023). This study was motivated by this financial challenge to look for more reasonably priced data sources and software options that could produce results that were on the level of the industry benchmarks. Therefore, by testing the integration of surface scan data, and alternative MIP and CAD software options into prosthesis manufacturing process chains, workable solutions were identified that could make necessary medical interventions more accessible to a wider segment of the South African population.

8.2 Process chain options for maxillofacial prosthesis manufacturing

The manufacturing of prostheses is an interdisciplinary process that involves the collaboration of a range of experts to create a digital prosthesis design suitable for manufacturing. This team typically includes engineers, designers, and medical professionals, each contributing specialised knowledge to ensure that a prosthesis meets both functional and aesthetic requirements (Tack et al., 2016). The designer plays a central role in developing the digital model for a prosthesis, which often includes creating a mould for the final product, which is followed by prosthesis manufacturing using AM technologies (Cristache et al., 2021).

Traditionally, computed tomography (CT) digital volumetric data has been the standard for generating the detailed anatomical information required for prosthesis design. However, CT comes with a significant radiation burden, as it exposes patients to considerably higher levels of radiation compared to conventional radiography (Esmaeilzadeh et al., 2024). This poses health risks, especially when multiple scans are needed (Shbeer, 2024). An emerging alternative is the use of surface scan data, which implements structured light technology, offering a significant advantage by eliminating radiation exposure (Unkovskiy et al., 2022). In addition to being safer, and non-invasive, surface scanning is also more cost-effective, and does not require specialised expertise, making it a more accessible option for both healthcare providers and patients (Diara, 2023; Costello et al., 2024). This shift toward surface scan data not only reduces health risks but also helps in lowering the overall costs of prosthesis production, making these life-changing medical devices more affordable and accessible.

The traditional software used for designing prostheses typically involves expensive proprietary applications (Irshad et al., 2024), which significantly increase the overall manufacturing costs. By identifying more cost-effective alternatives for both MIP and CAD software, it is possible to reduce these costs without compromising on quality (Mandolini et al., 2022; Yap Abdullah et al., 2024). When working with CT data, MIP software is required to segment a region of interest (ROI) from the data volume, which is then imported into CAD software for the prosthesis design process (Mian et al., 2022). In contrast, surface scan data can be imported directly into CAD software, streamlining the process (Costello et al., 2024; Schipper et al., 2024). Therefore, by integrating less expensive MIP and CAD software can substantially lower costs in both CT and surface scan workflows.

8.3 Process chain choice

Although various surface scanning instruments and software applications have been compared in the literature, a comprehensive comparison of the entire process chain, comprising of different combinations of components, has not been undertaken, as far as could be determined, making this study a first of its kind. This study employed an innovative and uniquely tailored methodology to achieve its objectives. Following a pragmatic and systematic approach, and by validating each step of the process, six alternative process chain options for the manufacturing of external maxillofacial prostheses were identified. The selection of appropriate process chains involves balancing cost, quality, and patient-specific factors such as health risks and financial constraints. The most cost-effective process chain identified in this study was the combination of surface scan data from the Artec Spider scanner with the CAD software 3D Coat. Despite being one of the least expensive chains tested, the resulting 3D models exhibited notable deviations from those produced by the control process chain, highlighting a trade-off between cost and precision. Conversely, the highest quality process chains were those combining the MIP software applications 3D Slicer or InVesalius with 3D Coat. While these options delivered superior accuracy and remained more affordable than the control chain, they are still relatively costly due to their dependence on CT data. Additionally, the use of CT imaging poses significant health risks to patients, particularly because of high radiation exposure (Durisetti et al., 2022). Table 8.1 presents the proposed alternative process chains identified in this study, and their ranking by quality, cost, and associated radiation risk.

Table 8.1 Ranking of process chains based on quality and cost

Process chain			Quality ranking	Cost ranking	Radiation risk	Remark
Data type	MIP software	CAD software				
CT	3D Slicer	ZBrush	1	4	Yes	Besides the radiation risk, ZBrush is a complex software to operate and requires a skilled designer.
CT	3D Slicer	3D Coat	2	2	Yes	Besides the radiation risk, this process chain is one of the promising of the tested chains.
CT	InVesalius	3D Coat	3	2	Yes	Besides the radiation risk, this process chain is one of the promising of the tested chains.
SD		3D Coat	4	1	No	Besides the advantages of being radiation-free and cost-effective, surface scanning undercuts and holes in facial anatomy is difficult and results in missing data that may require additional designing in CAD software. Processing of scanned meshes is also challenging.
SD		ZBrush	4	4	No	Besides the advantages of being radiation-free, surface scanning undercuts and holes in facial anatomy are difficult and result in missing data that may require additional designing in CAD software. Processing of scanned meshes is also challenging. ZBrush is a complex software to operate and requires a skilled designer.
CT	InVesalius	ZBrush	6	4	Yes	Besides the radiation burden, ZBrush is a complex software to operate and requires a skilled designer.

CT = computed tomography; SD = surface scan data

It could be concluded from this study that the choice of process chain should be determined by specific needs, the designer's expertise, and the available resources. For instance, in cases where a young child may require multiple prostheses over time due to growth and development, the most cost-effective process chain could be the best option, even if it results is slightly lower quality. Given the potential health risks, it is crucial to avoid exposing young children to CT scanning, as the high radiation doses could be harmful, especially when multiple scans are needed (Chodick et al., 2009; Meulepas et al., 2019). Although CT scans have significant medical benefits, their increased use since the 1980s has raised concerns about potential cancer risks, particularly after childhood exposure (Printz, 2019). Therefore, careful consideration should be given to the use of CT scans in younger patients. Furthermore, patients facing financial constraints might prioritise affordability, accepting lower precision in exchange for access to a necessary medical device. Ultimately, the findings of this study highlight the importance of balancing cost, quality, and patient safety when selecting an appropriate process chain for the manufacturing of an external maxillofacial prosthesis.

8.4 Concluding remarks and recommendations

In conclusion, this study successfully identified alternative process chains for the manufacturing of external maxillofacial prostheses, offering cost-effective options that maintain acceptable quality. The findings emphasise the importance of balancing precision with affordability in the choice of software and data acquisition methods. While the research has successfully identified more affordable options, it also highlights the potential for further refinement. As surface scanning technology continues to advance, future studies should focus on exploring instruments with more sophisticated capabilities to enhance accuracy and reduce costs. Likewise, the ongoing evolution of 3D printing technologies and materials opens opportunities for additional research into even more accessible options. Continued innovation in these areas will be critical in expanding the availability of external maxillofacial prostheses, ensuring that more patients in South Africa can benefit from these life-enhancing medical devices at a lower cost.

References

3D Slicer Website. (n.d.). *3D Slicer Website*. Https://Www.Slicer.Org/. Retrieved November 11, 2024, from https://www.slicer.org/

Abbady, H. E. M. A., Klinkenberg, E. T. M., De Moel, L., Nicolai, N., Van Der Stelt, M., Verhulst, A. C., Maal, T. J. J., & Brouwers, L. (2022). 3D-printed prostheses in developing countries: A systematic review. *Prosthetics and Orthotics International*, *46*(1), 19–30. https://doi.org/10.1097/PXR.0000000000000057

Aburamadan, R., & Trillo, C. (2020). Applying design science approach to architectural design development. *Frontiers of Architectural Research*, *9*(1), 216–235. https://doi.org/10.1016/j.foar.2019.07.008

Adeleke, A. I., Hlongwa, M., Makhunga, S., & Ginindza, T. G. (2023). Epidemiology of maxillofacial injury among adults in sub-Saharan Africa: a scoping review. *Injury Epidemiology*, *10*(58), 1–21. https://doi.org/10.1186/s40621-023-00470-5

Al Mardini, M., Ercoli, C., & Graser, G. N. (2005). A technique to produce a mirror-image wax pattern of an ear using rapid prototyping technology. *The Journal of Prosthetic Dentistry*, *94*(2), 195–198. https://doi.org/10.1016/j.prosdent.2005.04.019

Al-Ali, M. A., Alao, D. O., & Abu-Zidan, F. M. (2022). Factors affecting mortality of hospitalized facial trauma patients in Al-Ain City, United Arab Emirates. *PLoS ONE*, *17*(11 November). https://doi.org/10.1371/journal.pone.0278381

Alemayehu, S., Afera, B., Kidanu, K., & Belete, T. (2020). Management Outcome of Burn Injury and Associated Factors among Hospitalized Children at Ayder Referral Hospital, Tigray, Ethiopia. *International Journal of Pediatrics (United Kingdom)*, *2020*. https://doi.org/10.1155/2020/9136256

AlShaibani, R., Akhtar, T., Gentle, M., Chen, P., & Liao, P. (2021). Digital Applications of Maxillofacial Reconstruction– A systematic review. *Journal of Advanced Dentistry*, *1*(1), 21–27. https://doi.org/10.52870/jad.21004

Alturkistani, R., Kavin, A., Devasahayam, S., Thomas, R., Colombini, E. L., Cifuentes, C. A., Homer-Vanniasinkam, S., Wurdemann, H. A., & Moazen, M. (2020). Affordable passive 3D-printed prosthesis for persons with partial hand amputation. *Prosthetics and Orthotics International*, *44*(2), 92–98. https://doi.org/10.1177/0309364620905220

Amaya-Rivas, J. L., Perero, B. S., Helguero, C. G., Hurel, J. L., Peralta, J. M., Flores, F. A., & Alvarado, J. D. (2024). Future trends of additive manufacturing in medical applications: An overview. *Heliyon*, *10*(5), 1–18. https://doi.org/10.1016/j.heliyon.2024.e26641

Amorim, P. H. J., de Moraes, T. F., Rezende, R. A., da Silva, J. V. L., & Pedrini, H. (2017). Medical Imaging for Three-Dimensional Computer-Aided Models. In A. Ovsianikov, J. Yoo, & V. Mironov (Eds.), *3D Printing and Biofabrication* (pp. 1–27). Springer International Publishing AG. https://doi.org/10.1007/978-3-319-40498-1_6-1

Amorim, P., Moraes, T., Silva, J., & Pedrini, H. (2015). Invesalius: An interactive rendering framework for health care support. In G. Bebis, R. Boyle, B. Parvin, D. Koracin, I. Pavlidis, R. Feris, T. McGraw, M. Elendt, R. Kopper, E. Ragan, Z. Ye, & G. Weber (Eds.), *Advances in Visual Computing. ISVC 2015. Lecture Notes in Computer Science (including subseries Lecture Notes* *in Artificial Intelligence and Lecture Notes in Bioinformatics)* (Vol. 9474, pp. 45–54). Springer, Cham. https://doi.org/10.1007/978-3-319-27857-5_5

Angelou, I. K., van Aswegen, H., Wilson, M., & Grobler, R. (2022). A profile of adult patients with major burns admitted to a Level 1 Trauma Centre and their functional outcomes at discharge: A retrospective review. *South African Journal of Physiotherapy*, *78*(1), a1543–a1550. https://doi.org/https://doi.org/10.4102/sajp. v78i1.1543

Annamma, L. M., Hattori, M., Ali, I. E., Dsouza, J., Waqar, A., Chugh, A., & Sumita, Y. I. (2024). Frequently used extraoral maxillofacial prosthetic materials and their longevity – A comprehensive review. *Japanese Dental Science Review*, *60*, 137–147. https://doi.org/10.1016/j.jdsr.2024.03.001

Artec 3D. (n.d.). *User Guide Artec Studio 11*.

Autodesk Inc. (n.d.). *Meshmixer Manual*. Https://Forums.Autodesk.Com>. Retrieved November 10, 2024, from https://www.google.com/search?q=meshmixer+manual+pdf&oq=Meshmixer+Manual&gs_lcrp=EgZjaHJvbWUqBwgBEAAYgAQyBggAEEUYOTIHCAEQABiABDIICAIQABgWGB4yCAgDEAAYFhgeMggIBBAAGBYYHjIICAUQABgWGB4yCAgGEAAYFhgeMg0IBxAAGIYDGIAEGIoFMgoICBAAGIAEGKIEMgoICRAAGIAEGKIE0gEJMTkxNDdqMGo3qAIAsAIA&sourceid=chrome&ie=UTF-8

Autodesk Inc. (2021). *Meshmixer*. Https://Www.Research.Autodesk.Com/Projects/Meshmixer/. https://www.research.autodesk.com/projects/meshmixer/

Bai, S., Feng, Z., Gao, R., Dong, Y., Bi, Y., Wu, G., & Chen, X. (2014). Development and application of a rapid rehabilitation system for reconstruction of maxillofacial soft-tissue defects related to war and traumatic injuries. *Military Medical Research*, *1*(1), 11. https://doi.org/10.1186/2054-9369-1-11

Barrios-Muriel, J., Romero-Sánchez, F., Alonso-Sánchez, F. J., & Salgado, D. R. (2020). Advances in orthotic and prosthetic manufacturing: A technology review. *Materials*, *13*(2). https://doi.org/10.3390/ma13020295

Bayazit, N. (2004). Investigating Design: A Review of Forty Years of Design Research. *Design Issues*, *20*(1), 16–29. https://doi.org/10.1162/074793604772933739

Bertolini, M., Rossoni, M., & Colombo, G. (2021). Operative workflow from CT to 3D printing of the heart: Opportunities and challenges. *Bioengineering*, *8*(10), 1–15. https://doi.org/10.3390/bioengineering8100130

Bhargava, R. (2019). The Jaipur foot and the "Jaipur Prosthesis." *Indian Journal of Orthopaedics*, *53*(1), 5–7. https://doi.org/10.4103/ortho.IJOrtho_162_18

Bibb, R., Eggbeer, D., & Paterson, A. (2015). *Medical Modelling: The Application of Advanced Design and Rapid Prototyping Techniques in Medicine* (Second Edition). Woodhead Publishing.

Bibb, R., & Winder, J. (2010). A review of the issues surrounding three-dimensional computed tomography for medical modelling using rapid prototyping techniques. *Radiography*, *16*(1), 78–83. https://doi.org/10.1016/j.radi.2009.10.005

Binhuraib, H., Alreshidi, F., Bardi, S., Alghamdi, N., Alhelali, S., Althagafi, T., Alsayegh, R., Alsalem, F., Aljathnan, A., Alshahrani, N., & Alhaqbani, M. (2023). Evaluating the efficiency of complete digital workflow in prosthodontics. *Journal of Healthcare Sciences*, *3*(12), 695–700. https://doi.org/10.52533/johs.2023.31220

Blender Foundation. (2021). *Blender*. Https://Www.Blender.Org/. https://www.blender.org/

Bogue, R. (2013). 3D printing: the dawn of a new era in manufacturing? *Assembly Automation*, *33*(4), 307–311. https://doi.org/10.1108/AA-06-2013-055

Buffinton, C. M., Baish, J. W., & Ebenstein, D. M. (2023). An Introductory Module in Medical Image Segmentation for BME Students. *Biomedical Engineering Education*, *3*(1), 95–109. https://doi.org/10.1007/s43683-022-00085-0

Buonamici, F., Mussi, E., Santarelli, C., Carrabba, N., Stefano, P., Marchionni, N., & Carfagni, M. (2022). Modelling and fabrication procedure for a 3D printed cardiac model - surgical planning of Left Ventricular Aneurysm. *MethodsX*, *9*(101822), 1–21. https://doi.org/10.1016/j.mex.2022.101822

Chander, N. G., Venkat, N., & Rizwana, A. N. (2024). Innovations and advancements in adhesives for maxillofacial prosthesis in carcinoma rehabilitated patients. *Oral Oncology Reports*, *11*(100625), 1–4. https://doi.org/10.1016/j.oor.2024.100625

Chen, K. J., Elkaseer, A., Scholz, S. G., & Hagenmeyer, V. (2024). On the correlation between pre-processing workflow and dimensional accuracy of 3D printed parts in high-precision Material Jetting. *Additive Manufacturing*, *91*. https://doi.org/10.1016/j.addma.2024.104335

Chen, J. V., Dang, A. B. C., & Dang, A. (2021). Comparing cost and print time estimates for six commercially-available 3D printers obtained through slicing software for clinically relevant anatomical models. *3D Printing in Medicine*, *7*(1), 1–14. https://doi.org/10.1186/s41205-020-00091-4

Chen, Z., Zhang, M., Xie, S., Zhang, X., Tang, S., Zhang, C., & Li, H. (2022). Global burden of thermal burns, 1990–2017: Unbalanced distributions and temporal trends assessed from the Global Burden of Disease Study 2017. *Burns*, *48*(4), 915–925. https://doi.org/10.1016/j.burns.2021.08.002

Chodick, G., Kim, K. P., Shwarz, M., Horev, G., Shalev, V., & Ron, E. (2009). Radiation Risks from Pediatric Computed Tomography Scanning. *Pediatric Endocrinology Reviews*, *7*(2), 29–36.

CloudCompare User Manual Version 2.6.1. (n.d.). *CloudCompare*. Https://Www.Cloudcompare.Org/Doc/QCC/CloudCompare%20v2.6.1%20-%20User%20manual.Pdf. Retrieved November 11, 2024, from https://www.cloudcompare.org/doc/qCC/CloudCompare%20v2.6.1%20-%20User%20manual.pdf

Coetzee, R. (2019). Towards designing an artefact evaluation strategy for human factors engineering: A lean implementation model case study. *South African Journal of Industrial Engineering*, *30*(3 Special Edition), 289–303. https://doi.org/10.7166/30-3-2244

Collins Dictionary. (2022). *Collins Dictionary* (14th ed.). HarperCollins. https://www.collinsdictionary.com/

Cookson, T. P., Fuentes, L., & Bitterly, J. (2024). Addressing gender-based violence through social protection: a scoping review. *Development in Practice*. https://doi.org/10.1080/09614524.2023.2290438

Copeland, C., Reyes, C. C., Peck, J. L., Srivastava, R., & Zuniga, J. M. (2022). Functional performance and patient satisfaction comparison between a 3D printed and a standard transradial prosthesis: a case report. *BioMedical Engineering Online*, *21*(1). https://doi.org/10.1186/s12938-022-00977-w

Costello, L. F., McMenamin, P. G., Quayle, M. R., Bertram, J. F., & Adams, J. W. (2024). Applying 3D surface scanning technology to create photorealistic three-dimensional printed replicas of human anatomy. *Future Science OA*, *10*(1). https://doi.org/10.1080/20565623.2024.2381956

Creswell, J. W., Plano Clark, V. L., Gutmann, M. L., & & Hanson, W. E. (2003). Advanced Mixed Methods Research Designs. In A. Tashakkori & C. Teddlie (Eds.), *Handbook of Mixed Methods in Social and Behavioral Research* (3rd Edition, pp. 209–240). SAGE Publications, Inc. https://doi.org/10.4135/9781506335193

Cristache, C. M., Tudor, I., Moraru, L., Cristache, G., Lanza, A., & Burlibasa, M. (2021). Digital workflow in maxillofacial prosthodontics—an update on defect data acquisition, editing and design using open-source and commercial available software. *Applied Sciences (Switzerland)*, *11*(3), 1–19. https://doi.org/10.3390/app11030973

Crotty, M. (1998). *The Foundations of Social Research: Meaning and Perspective in the Research Process. London:* (M. Crotty, Ed.; 1st ed.). SAGE Publications Inc.

Cruz, R. L. J., Ross, M. T., Powell, S. K., & Woodruff, M. A. (2020a). Advancements in Soft-Tissue Prosthetics Part A: The Art of Imitating Life. *Frontiers in Bioengineering and Biotechnology*, *8*(121), 1–20. https://doi.org/10.3389/fbioe.2020.00121

Cruz, R. L. J., Ross, M. T., Powell, S. K., & Woodruff, M. A. (2020b). Advancements in Soft-Tissue Prosthetics Part B: The Chemistry of Imitating Life. *Frontiers in Bioengineering and Biotechnology*, *8*(147), 1–23. https://doi.org/10.3389/fbioe.2020.00147

Cruz, R. L. J., Ross, M. T., Skewes, J., Allenby, M. C., Powell, S. K., & Woodruff, M. A. (2020c). An advanced prosthetic manufacturing framework for economic personalised ear prostheses. *Scientific Reports*, *10*(11453). https://doi.org/10.1038/s41598-020-67945-z

Das, A., Awasthi, P., Jain, V., & Banerjee, S. S. (2023). 3D printing of maxillofacial prosthesis materials: Challenges and opportunities. In *Bioprinting* (Vol. 32, Issue e00282). Elsevier B.V. https://doi.org/10.1016/j.bprint.2023.e00282

Davies, B., du Toit, C., & Hlela, M. B. K. M. (2024). Fire deaths in Cape Town, South Africa: A retrospective review of medico-legal and toxicological findings (2006 – 2018). *Burns*. https://doi.org/10.1016/j.burns.2024.01.001

De Caxias, F. P., Dos Santos, D. M., Bannwart, L. C., De Moraes Melo Neto, C. L., & Goiato, M. C. (2019). Classification, History, and Future Prospects of Maxillofacial Prosthesis. *International Journal of Dentistry*, *2019: 8657619*, 1–7. https://doi.org/10.1155/2019/8657619

De, M., Sagar, S., Dave, A., Kaul, R. P., & Singhal, M. (2023). Complicated Facial Lacerations: Challenges in the Repair and Management of Complications by a Facial Trauma Team. *Craniomaxillofacial Trauma & Reconstruction*, *16*(1), 39–54. https://doi.org/10.1177/19433875211064512

De Sordi, J. O., de Azevedo, M. C., Meireles, M., Pinochet, L. H. S., & Jorge, C. F. B. (2020). Design science research in practice: What can we learn from a longitudinal analysis of the development of published artifacts. *Informing Science: The International Journal of an Emerging Transdiscipline*, *23*, 1–23. https://doi.org/10.28945/4493

Diara, F. (2023). Structured-Light Scanning and Metrological Analysis for Archaeology: Quality Assessment of Artec 3D Solutions for Cuneiform Tablets. *Heritage*, *6*(9), 6016–6034. https://doi.org/10.3390/heritage6090317

DirnbÄock, H., & Stachel, H. (1997). The Development of the Oloid. *Journal for Geometry and Graphics*, *1*(2), 105–118.

Dong, C., Petrovic, M., & Davies, I. J. (2024). Applications of 3D printing in medicine: A review. *Annals of 3D Printed Medicine*, *14*(100149), 1–17. https://doi.org/10.1016/j.stlm.2024.100149

Dostalova, T., Kozak, J., Hubacek, M., Holakovsky, J., Kříž, P., Strnad, J., & Seydlova, M. (2011). *Facial Prosthesis* ((Prof) Ilser Turkyilmaz, Ed.; Implant Dentistry, p. 544). IntechOpen. www.intechopen.com

Durisetti, S., Alapati, D., Vadnala, S. K., Kotha, K., Ramesh Chandra, G., & Govindarajan, S. (2022). Evaluation of Tools Used for 3D Reconstruction of 2D Medical Images. In A. B. Reddy, B. V. Kiranmayee, R. R. Mukkamala, & K. S. Raju (Eds.), *Proceedings of Second International Conference on Advances in Computer Engineering and Communication Systems. Algorithms for Intelligent Systems.* (pp. 287–298). Springer. https://doi.org/10.1007/978-981-16-7389-4_27

Engdahl, S. M., Gonzalez, M. A., Lee, C., & Gates, D. H. (2024). Perspectives on the comparative benefits of body-powered and myoelectric upper limb prostheses. *Journal of NeuroEngineering and Rehabilitation*, *21*(1). https://doi.org/10.1186/s12984-024-01436-4

Ennion, L., & Johannesson, A. (2018). A qualitative study of the challenges of providing pre-prosthetic rehabilitation in rural South Africa. *Prosthetics and Orthotics International*, *42*(2), 179–186. https://doi.org/10.1177/0309364617698520

Erolin, C. (2023). Preparing anatomical scan data for sharing online. *Journal of Visual Communication in Medicine*, *46*(2), 105–114. https://doi.org/10.1080/17453054.2023.2216238

Esmaeilzadeh, M., Bronzlik, P., Solmaz, H., Polemikos, M., Heissler, H. E., Raab, P., Lanfermann, H., & Krauss, J. K. (2024). Reducing radiation exposure and costs: CT body scout views with an enhanced protocol versus conventional radiography after shunt surgery. *Clinical Neurology and Neurosurgery*, *240*(108281), 1–6. https://doi.org/10.1016/j.clineuro.2024.108281

Farook, T. H., Barman, A., Abdullah, J. Y., & Jamayet, N. Bin. (2021). Optimization of Prosthodontic Computer-Aided Designed Models: A Virtual Evaluation of Mesh Quality Reduction Using Open Source Software. *Journal of Prosthodontics*, *30*(5), 420–429. https://doi.org/10.1111/jopr.13286

Farook, T. H., Bin Jamayet, N., Abdullah, J. Y., Asif, J. A., Rajion, Z. A., & Alam, M. K. (2020). Designing 3D prosthetic templates for maxillofacial defect rehabilitation: A comparative analysis of different virtual workflows. *Computers in Biology and Medicine*, *118*, 103646. https://doi.org/10.1016/j.compbiomed.2020.103646

Farook, T. H., Rashid, F., Jamayet, N. Bin, Abdullah, J. Y., Dudley, J., & Alam, M. K. (2022). A virtual analysis of the precision and accuracy of 3-dimensional ear casts generated from smartphone camera images. *Journal of Prosthetic Dentistry*, *128*(4), 830–836. https://doi.org/https://doi.org/10.1016/j.prosdent.2020.12.041

Farsil, C., Amroune, S., Slamani, M., Zaoui, M., Houari, A., Zouaoui, K., Kouder, M., Zergane, S., & Nassereddine, B. (2024). Examining and Developing a Medically Relevant Component through Reverse Engineering. *Academic Journal of Manufacturing Engineering*, *22*(2), 43–49.

Faste, T., & Faste, H. (2012). *Demystifying "Design Research": Design is not Research, Research is Design*. https://www.idsa.org/wp-content/uploads/Faste.pdf

Fedorov, A., Beichel, R., Kalpathy-Cramer, J., Finet, J., Fillion-Robin, J. C., Pujol, S., Bauer, C., Jennings, D., Fennessy, F., Sonka, M., Buatti, J., Aylward, S., Miller, J. V., Pieper, S., & Kikinis, R. (2012). 3D Slicer as an image computing platform for the Quantitative Imaging Network. *Magnetic Resonance Imaging*, *30*(9), 1323–1341. https://doi.org/10.1016/j.mri.2012.05.001

Feng, Z., Dong, Y., Zhao, Y., Bai, S., Zhou, B., Bi, Y., & Wu, G. (2010). Computer-assisted technique for the design and manufacture of realistic facial prostheses. *British Journal of Oral and Maxillofacial Surgery*, *48*(2), 105–109. https://doi.org/10.1016/j.bjoms.2009.05.009

Fernández-Cedrón Bermejo, C., Sánchez Fernández, E., Costales Marcos, M., Núñez Batalla, F. J., Llorente Pendás, J. L., & Gómez Martínez, J. R. (2024). Comparison of the MIPS technique versus linear incision with tissue preservation in osseointegrated implants in the Ponto model®. *Acta Otorrinolaringologica Espanola*, *Mar 1:S2173-5735*(24), 12181–12187. https://doi.org/10.1016/j.otoeng.2023.10.010

FreeCAD. (2021). *FreeCAD Project*. Https://Www.Freecadweb.Org/. https://www.freecadweb.org/

Generalova, A. N., Vikhrov, A. A., Prostyakova, A. I., Apresyan, S. V., Stepanov, A. G., Myasoedov, M. S., & Oleinikov, V. A. (2024). Polymers in 3D printing of external maxillofacial prostheses and in their retention systems. *International Journal of Pharmaceutics*, *657*(124181), 1–26. https://doi.org/10.1016/j.ijpharm.2024.124181

Geomagic Control X. (n.d.). *Geomagic Control X*. Https://Oqton.Com/Geomagic-Controlx/.

Gibson, I., Rosen, D., & Stucker, B. (2015). *Additive Manufacturing Technologies* (Second Edition). Springer New York. https://doi.org/10.1007/978-1-4939-2113-3

Gibson, I., Rosen, D., Stucker, B., & Khorasani, M. (2021). Introduction and Basic Principles. In I. Gibson, D. Rosen, B. Stucker, & M. Khorasani (Eds.), *Additive Manufacturing Technologies* (Third Edition, pp. 1–21). Springer International Publishing. https://doi.org/10.1007/978-3-030-56127-7_1

Goiato, M. C., Pesqueira, A. A., Ramos da Silva, C., Filho, H. G., & Micheline dos Santos, D. (2009). Patient satisfaction with maxillofacial prosthesis. Literature review. *Journal of Plastic, Reconstructive and Aesthetic Surgery*, *62*(2), 175–180. https://doi.org/10.1016/j.bjps.2008.06.084

Gokharman, F. D., Kadirhan, O., Celik Aydin, O., Yalcin, A. G., Kosar, P., & Aydin, S. (2023). A Comprehensive Look at Maxillofacial Traumas: On the Basis of Orbital Involvement. *Diagnostics*, *13*(22). https://doi.org/10.3390/diagnostics13223429

Gómez Roselló, E., Quiles Granado, A. M., Artajona Garcia, M., Juanpere Martí, S., Laguillo Sala, G., Beltrán Mármol, B., & Pedraza Gutiérrez, S. (2020). Facial fractures: classification and highlights for a useful report. In *Insights into Imaging* (Vol. 11, Issue 1). Springer. https://doi.org/10.1186/s13244-020-00847-w

Gonzalez, J. B. (1978). Polyurethane elastomers for facial prostheses. *The Journal of Prosthetic Dentistry*, *39*(2), 179–187. https://doi.org/10.1016/S0022-3913(78)80018-3

Gordon, L. G., Elliott, T. M., Wright, C. Y., Deghaye, N., & Visser, W. (2016). Modelling the healthcare costs of skin cancer in South Africa. *BMC Health Services Research*, *16*(1). https://doi.org/10.1186/s12913-016-1364-z

Górski, F., Gapsa, J., Kupaj, A., Kuczko, W., Żukowska, M., & Zawadzki, P. (2024). Virtual Design Process of Customized 3D Printed Modular Upper Limb Prostheses. In F. Górski, R. Păcurar, J. F. Roca González, & M. Rychlik (Eds.), *Advances in Manufacturing IV* (pp. 206–218). Springer, Cham. https://doi.org/10.1007/978-3-031-56456-7_16

Gowd, M. S., Shankar, T., Ranjan, R., & Singh, A. (2017). Prosthetic consideration in implant-supported prosthesis: A review of literature. *Journal of International Society of Preventive and Community Dentistry*, *7*(7), S1–S7. https://doi.org/10.4103/jispcd.JISPCD_149_17

Goyal, M. K., Goyal, S., & Dhanasekar, B. (2014). Modern trends in modeling of extra-oral defects. *Indian Journal of Dental Research*, *25*(1), 128–132. https://doi.org/10.4103/0970-9290.131170

Guo, K., Li, M., Qi, J., Han, S., Wu, X., & Guo, F. (2024). Precise maxillofacial soft tissue reconstruction: A combination of cone beam computed tomography and 3dMD photogrammetry system. *Heliyon*, *10*(12: e32513), 1–10. https://doi.org/10.1016/j.heliyon.2024.e32513

G[illegible]rski’s, F., Zawadzki, P., Wichniarek, R., Kuczko, W., Slupinska, S., & Zukowska, M. (2022). Automated Design and Rapid Manufacturing of Low-Cost Customized Upper Limb Prostheses. *Journal of Physics: Conference Series Volume 2198:012040, 15th Global Congress on*

Manufacturing and Management (GCMM 2021) 25th-27th November 2020, *2198*(1), 1–11. https://doi.org/10.1088/1742-6596/2198/1/012040

Hevner, A. R., March, S. T., Park, J., & Ram, S. (2004). Design Science in Information Systems Research. *Design Science in IS Research MIS Quarterly*, *28*(1), 75–105. https://wise.vub.ac.be/sites/default/files/thesis_info/design_science.pdf

Hogg, N. J., & Horswell, B. B. (2006). Soft Tissue Pediatric Facial Trauma: A Review. *Journal of the Canadian Dental Association*, *72*(6), 549–552a. www.cda-adc.ca/jcda

Horváth, I. (2007). International Conference on Engineering Design, Iced'07 Comparison of Three Methodological Approaches of Design Research. In J.-C. Bocquet (Ed.), *Proceedings of the International Conference on Engineering Design, ICED 2007, the 16th International Conference on Engineering design* (pp. 1–11).

Hussain, S., Mubeen, I., Ullah, N., Shah, S. S. U. D., Khan, B. A., Zahoor, M., Ullah, R., Khan, F. A., & Sultan, M. A. (2022). Modern Diagnostic Imaging Technique Applications and Risk Factors in the Medical Field: A Review. *BioMed Research International*, *2022*, 1–19. https://doi.org/10.1155/2022/5164970

InVesalius Website. (n.d.). *InVesalius User Manual*. Https://Invesalius.Github.Io/Docs/User_guide/User_guide.Html.

Iqbal, T., Saaiq, M., & Ali, Z. (2013). Epidemiology and outcome of burns: Early experience at the country's first national burns Centre. *Burns*, *39*(2), 358–362. https://doi.org/10.1016/j.burns.2012.07.011

Irshad, T. Bin, Pascoletti, G., Bianconi, F., & Zanetti, E. M. (2024). Mandibular bone segmentation from CT scans: Quantitative and qualitative comparison among software. *Dental Materials*, *40*(8), e11–e22. https://doi.org/10.1016/j.dental.2024.05.022

Jablonski, R. Y., Coward, T. J., Bartlett, P., Keeling, A. J., Bojke, C., Pavitt, S. H., & Nattress, B. R. (2023). IMproving facial PRosthesis construction with contactlESs Scanning and Digital workflow (IMPRESSeD): study protocol for a feasibility crossover randomised controlled trial of digital versus conventional manufacture of facial prostheses in patients with orbital or nasal facial defects. *Pilot and Feasibility Studies*, *9*(110), 1–14. https://doi.org/10.1186/s40814-023-01351-w

Jablonski, R. Y., Veale, B. J., Coward, T. J., Keeling, A. J., Bojke, C., Pavitt, S. H., & Nattress, B. R. (2021). Outcome measures in facial prosthesis research: A systematic review. *The Journal of Prosthetic Dentistry*, *126*(6), 805–815. https://doi.org/https://doi.org/10.1016/j.prosdent.2020.09.010

James, S. L., Lucchesi, L. R., Bisignano, C., Castle, C. D., Dingels, Z. V., Fox, J. T., Hamilton, E. B., Henry, N. J., McCracken, D., Roberts, N. L. S., Sylte, D. O., Ahmadi, A., Ahmed, M. B., Alahdab, F., Alipour, V., Andualem, Z., Antonio, C. A. T., Arabloo, J., Badiye, A. D., … Mokdad, A. H. (2020). Epidemiology of injuries from fire, heat and hot substances: Global, regional and national morbidity and mortality estimates from the Global Burden of Disease 2017 study. *Injury Prevention*, *26*, i36–i45. https://doi.org/10.1136/injuryprev-2019-043299

Jardini, A. L., Larosa, M. A., de Carvalho Zavaglia, C. A., Bernardes, L. F., Lambert, C. S., Kharmandayan, P., Calderoni, D., & Maciel Filho, R. (2014). Customised titanium implant fabricated in additive manufacturing for craniomaxillofacial surgery: This paper discusses the design and fabrication of a metallic implant for the reconstruction of a large cranial defect. *Virtual and Physical Prototyping*, *9*(2), 115–125. https://doi.org/10.1080/17452759.2014.900857

Jeschke, M. G., van Baar, M. E., Choudhry, M. A., Chung, K. K., Gibran, N. S., & Logsetty, S. (2020). Burn injury. *Nature Reviews Disease Primers*, *6*(1). https://doi.org/10.1038/s41572-020-0145-5

Jindal, S. K., Sherriff, M., Waters, M. G., Smay, J. E., & Coward, T. J. (2018). Development of a 3D printable maxillofacial silicone: Part II. Optimization of moderator and thixotropic agent. *The Journal of Prosthetic Dentistry*, *119*(2), 299–304. https://doi.org/10.1016/j.prosdent.2017.04.028

Kamio, T., Suzuki, M., Asaumi, R., & Kawai, T. (2020). DICOM segmentation and STL creation for 3D printing: a process and software package comparison for osseous anatomy. *3D Printing in Medicine*, *6*(17), 1–12. https://doi.org/10.1186/s41205-020-00069-2

Kelly, L. M., & Cordeiro, M. (2020). Three principles of pragmatism for research on organizational processes. *Methodological Innovations*, *13*(2), 1–10. https://doi.org/10.1177/2059799120937242

Kharade, P. P. (2020). Maxillofacial prosthesis for Facial Defects- Evidence Based Approach. *The Journal of Indian Prosthodontic Society*, *20*(5), 19. https://doi.org/10.4103/0972-4052.306367

Kikinis, R., Pieper, S. D., & Vosburgh, K. G. (2014). 3D Slicer: A Platform for Subject-Specific Image Analysis, Visualization, and Clinical Support. In F. A. Jolesz (Ed.), *Intraoperative Imaging and Image-Guided Therapy* (pp. 277–289). Springer New York. https://doi.org/10.1007/978-1-4614-7657-3_19

Kim, C. H., Jeong, J. H., Bolch, W. E., Cho, K. W., & Hwang, S. B. (2011). A polygon-surface reference Korean male phantom (PSRK-Man) and its direct implementation in Geant4 Monte Carlo simulation. *Physics in Medicine and Biology*, *56*(10), 3137–3161. https://doi.org/10.1088/0031-9155/56/10/016

Korpela, M., Riikonen, N., Piili, H., Salminen, A., & Nyrhilä, O. (2021). Additive Manufacturing—Past, Present, and the Future. In M. K.-E. Collan (Ed.), *Technical, Economic and Societal Effects of Manufacturing 4.0 Automation, Adaption and Manufacturing in Finland and Beyond* (pp. 17–41). Palgrave Macmillan, Cham. https://doi.org/10.1007/978-3-030-46103-4_2

Kotzé, P., Van Der Merwe, A., & Gerber, A. (2015). Design Science Research as Research Approach in Doctoral Studies. *Twenty-First Americas Conference on Information Systems, Puerto Rico*, 1–14.

Kouhi, M., de Souza Araújo, I. J., Asa'ad, F., Zeenat, L., Bojedla, S. S. R., Pati, F., Zolfagharian, A., Watts, D. C., Bottino, M. C., & Bodaghi, M. (2024). Recent advances in additive manufacturing of patient-specific devices for dental and maxillofacial rehabilitation. *Dental Materials*, *40*(4), 700–715. https://doi.org/10.1016/j.dental.2024.02.006

Lanchimba, C., Díaz-Sánchez, J. P., & Velasco, F. (2023). Exploring factors influencing domestic violence: a comprehensive study on intrafamily dynamics. *Frontiers in Psychiatry*, *14*, 1–12. https://doi.org/10.3389/fpsyt.2023.1243558

Lee, C., Foo, Q., Wong, L., & Leung, Y. (2017). An Overview of Maxillofacial Trauma in Oral and Maxillofacial Tertiary Trauma Centre, Queen Elizabeth Hospital, Kota Kinabalu, Sabah. *Craniomaxillofacial Trauma & Reconstruction*, *10*(1), 16–21. https://doi.org/10.1055/s-0036-1584893

Leonardi, A., Buonaccorsi, S., Pellacchia, V., Moricca, L. M., Indrizzi, E., & Fini, G. (2008). Maxillofacial Prosthetic Rehabilitation Using Extraoral Implants. *The Journal of Craniofacial Surgery*, *19*(2), 398–405. https://doi.org/10.1097/SCS.0b013e318163e443

Lewis, D. H., & Castleberry, D. J. (1980). An assessment of recent advances in external maxillofacial materials. *The Journal of Prosthetic Dentistry*, *43*(4), 426–432. https://doi.org/10.1016/0022-3913(80)90215-2

Li, X., Xu, J., Fan, J., Xue, Y., Gu, X., Zhou, H., & Han, D. (2023). Current situation and development of facial prosthesis. *Chinese Journal of Plastic and Reconstructive Surgery*, *5*(1), 39–42. https://doi.org/10.1016/j.cjprs.2023.03.005

Liacouras, P., Garnes, J., Roman, N., Petrich, A., & Grant, G. T. (2011). Designing and manufacturing an auricular prosthesis using computed tomography, 3-dimensional photographic imaging, and additive manufacturing: A clinical report. *Journal of Prosthetic Dentistry*, *105*(2), 78–82. https://doi.org/10.1016/S0022-3913(11)60002-4

Lontz, J. F. (1990). State-of-the-Art Materials Used for Maxillofacial Prosthetic Reconstruction. *Dental Clinics of North America*, *34*(2), 307–325. https://doi.org/10.1016/S0011-8532(22)01149-1

Ma, J., He, Y., Li, F., Han, L., You, C., & Wang, B. (2024). Segment anything in medical images. *Nature Communications*, *15*(654), 1–9. https://doi.org/10.1038/s41467-024-44824-z

Mahajan, H. (2018). Research Paper on CREO. *International Journal Of Innovative Research In Technology*, *5*(3), 21–23.

Malik, S., Singh, G., Kaur, G., Yadav, S., & Mittal, H. C. (2017). Orofacial trauma in rural India: A clinical study. *Chinese Journal of Traumatology - English Edition*, *20*(4), 216–221. https://doi.org/10.1016/j.cjtee.2016.10.006

Mandolini, M., Brunzini, A., Facco, G., Mazzoli, A., Forcellese, A., & Gigante, A. (2022). Comparison of Three 3D Segmentation Software Tools for Hip Surgical Planning. *Sensors*, *22*(14:5242), 1–16. https://doi.org/10.3390/s22145242

Manero, A., Smith, P., Sparkman, J., Dombrowski, M., Courbin, D., Kester, A., Womack, I., & Chi, A. (2019). Implementation of 3D printing technology in the field of prosthetics: Past, present, and future. *International Journal of Environmental Research and Public Health*, *16:1641*(9), 1–15. https://doi.org/10.3390/ijerph16091641

Maritz, D., Wallis, L., Van Der Merwe, E., & Nel, D. (2012). The aetiology of adult burns in the Western Cape, South Africa. *Burns*, *38*(1), 120–127. https://doi.org/10.1016/j.burns.2010.12.007

Marro, A., Bandukwala, T., & Mak, W. (2016). Three-Dimensional Printing and Medical Imaging: A Review of the Methods and Applications. *Current Problems in Diagnostic Radiology*, *45*(1), 2–9. https://doi.org/10.1067/j.cpradiol.2015.07.009

Mazzoli, A. (2013). Selective laser sintering in biomedical engineering. *Medical & Biological Engineering & Computing*, *51*(3), 245–256. https://doi.org/10.1007/s11517-012-1001-x

Mduzana, L., Tiwari, R., Lieketseng, N., & Chikte, U. (2020). Exploring national human resource profile and trends of Prosthetists/Orthotists in South Africa from 2002 to 2018. *Global Health Action*, *13*(1), 1–13. https://doi.org/10.1080/16549716.2020.1792192

Memon, A. R., Wang, E., Hu, J., Egger, J., & Chen, X. (2020). A review on computer-aided design and manufacturing of patient-specific maxillofacial implants. *Expert Review of Medical Devices*, *17*(4), 345–356. https://doi.org/10.1080/17434440.2020.1736040

Meulepas, J. M., Ronckers, C. M., Smets, A. M. J. B., Nievelstein, R. A. J., Gradowska, P., Lee, C., Jahnen, A., Van Straten, M., De Wit, M. C. Y., Zonnenberg, B., Klein, W. M., Merks, J. H., Visser, O., Van Leeuwen, F. E., & Hauptmann, M. (2019). Radiation exposure from pediatric CT scans and subsequent cancer risk in the Netherlands. *Journal of the National Cancer Institute*, *111*(3), 256–263. https://doi.org/10.1093/jnci/djy104

Mian, S. H., Moiduddin, K., Abdo, B. M. A., Sayeed, A., & Alkhalefah, H. (2022). Modelling and evaluation of meshed implant for cranial reconstruction. *The International Journal of Advanced Manufacturing Technology*, *118*(5–6), 1967–1985. https://doi.org/10.1007/s00170-021-08161-5

Mitra, A., Choudhary, S., Garg, H., & Jagadeesh, H. G. (2014). Maxillofacial prosthetic materials-an inclination towards silicones. *Journal of Clinical and Diagnostic Research*, *8*(12), ZE08-ZE13. https://doi.org/10.7860/JCDR/2014/9229.5244

Mondal, S., Sikder, A., Das, S., Ray, A., & Das, S. (2023). Structural Design and Analysis of Below-knee Prosthetic Leg in Mechanical System. *Research Square*, 1–29. https://doi.org/10.21203/rs.3.rs-3249738/v1

Muneer, A., & Pearce, I. (2016). An Introduction to Prosthetic Devices. In A. Muneer, I. Pearce, & D. Ralph (Eds.), *Prosthetic Surgery in Urology* (p. 255). Springer International Publishing. https://doi.org/10.1007/978-3-319-13859-6

Ndlovu, B. C., Sengayi-Muchengeti, M., Wright, C. Y., Chen, W. C., Kuonza, L., & Singh, E. (2022). Skin cancer risk factors among Black South Africans—The Johannesburg Cancer Study, 1995–2016. *Immunity, Inflammation and Disease*, *10*(7), 1–8. https://doi.org/10.1002/iid3.623

Niiniluoto, I. (2014). Values in design sciences. *Studies in History and Philosophy of Science Part A*, *46*, 11–15. https://doi.org/10.1016/j.shpsa.2013.11.002

Nikitichev, D. I., Patel, P., Avery, J., Robertson, L. J., Bucking, T. M., Aristovich, K. Y., Maneas, E., Desjardins, A. E., & Vercauteren, T. (2018). Patient-Specific 3D Printed Models for Education, Research and Surgical Simulation. In *3D Printing* (pp. 115–135). InTech. https://doi.org/10.5772/intechopen.79667

Norval, M., Kellett, P., & Wright, C. Y. (2014). The Incidence and Body Site of Skin Cancers in the Population Groups of South Africa. *Photodermatology Photoimmunology and Photomedicine*, *30*(5), 262–265. https://doi.org/DOI: 10.1111/phpp.12106

Olatunji, G., Osaghae, O. W., & Aderinto, N. (2023). Exploring the transformative role of 3D printing in advancing medical education in Africa: a review. *Annals of Medicine & Surgery*, *85*(10), 4913–4919. https://doi.org/10.1097/ms9.0000000000001195

Ornaghi, H. L., Monticeli, F. M., & Agnol, L. D. (2023). A Review on Polymers for Biomedical Applications on Hard and Soft Tissues and Prosthetic Limbs. *Polymers*, *15*(19), 1–24. https://doi.org/10.3390/polym15194034

Ozdemir-Karatas, M., Cifter, E. D., Ozdemir-Ozenen, D., Balik, A., & Tuncer, E. B. T. (2011). Manufacturing Implant Supported Auricular Prostheses by Rapid Prototyping Techniques. *European Journal of Dentistry*, *5*(4), 472–477.

Pan, Y., Zhu, H., & Hou, L. (2022). Epidemiological analysis and emergency nursing care of oral and craniomaxillofacial trauma: a narrative review. *Annals of Palliative Medicine*, *11*(4), 1518–1525. https://doi.org/10.21037/apm-21-2995

Parry-Hill, J. L. (2019). *e-NABLE: DIY-AT Production in a Multi-Stakeholder System* [Rochester Institute of Technology]. https://repository.rit.edu/theses

Parthasarathy, J. (2014). 3D modeling, custom implants and its future perspectives in craniofacial surgery. *Annals of Maxillofacial Surgery*, *4*(1), 9. https://doi.org/10.4103/2231-0746.133065

Pawar, P. G., Bhoyar, A., & Sathe, S. (2023). Development, Evaluation, and Comparison of an Indigenous 'APDS' AI-based Digital Application for Effective Shade Selection of Silicone Maxillofacial Prosthesis: Protocol for A Cross-sectional Study. *Journal of Clinical and Diagnostic Research*, *17*(5), ZK05–ZK08. https://doi.org/10.7860/jcdr/2023/61326.17991

Paxton, N. C., Nightingale, R. C., & Woodruff, M. A. (2022). Capturing patient anatomy for designing and manufacturing personalized prostheses. *Current Opinion in Biotechnology*, *73*, 282–289. https://doi.org/10.1016/j.copbio.2021.09.004

Peck, M. D. (2011). Epidemiology of burns throughout the world. Part I: Distribution and risk factors. *Burns*, *37*, 1087–1100. https://doi.org/10.1016/j.burns.2011.06.005

Petrovic, V., Haro, J. V., Blasco, J. R., & Portolés, L. (2012). 7 Additive Manufacturing Solutions for Improved Medical Implants. In C. Lin (Ed.), *Biomedicine* (Vol. 7, pp. 147–180). Intechopen. https://doi.org/DOI: 10.5772/38349

Pieper, S., Halle, M., & Kikinis, R. (2004). 3D Slicer. *2004 2nd IEEE International Symposium on Biomedical Imaging: Macro to Nano (IEEE Cat No. 04EX821)*, 2, 632–635. https://doi.org/10.1109/ISBI.2004.1398617

Pilgway. (2021). *3D Coat*. Https://3dcoat.Com/. https://3dcoat.com/

Pilgway Studio. (n.d.). *3D Coat Website*. Https://3dcoat.Com/Articles/Article/Sculpting-in-3dcoat/.

Pillay, L., Mabongo, M., & Buch, B. (2018). Prevalence and aetiological factors of maxillofacial trauma in a rural district hospital in the Eastern Cape. *South African Dental Journal*, *73*(5). https://doi.org/10.17159/2519-0105/2018/v73no5a4

Pirozzi, M. A., Jacob, D., Pálsson, T., Gargiulo, P., Helgason, T., & Jónsson Jr, H. (2023). State of the art in 3D printing. In P. Gargiulo (Ed.), *Handbook of Surgical Planning and 3D Printing* (pp. 3–36). Elsevier. https://doi.org/10.1016/B978-0-323-90850-4.00014-4

Pixologic. (2021). *ZBrush*. Https://Pixologic.Com/. https://pixologic.com/

Prakash, P., Bahri, R., & Bhandari, S. K. (2021). Maxillofacial Defects: Impact on Psychology and Esthetics. In M. P. Levine & J. S. Santos (Eds.), *Beauty - Cosmetic Science, Cultural Issues and Creative Developments* (Beauty, p. 170). IntechOpen. https://doi.org/10.5772/intechopen.95830

Printz, C. (2019). American College of Radiology takes steps to lower CT scan radiation exposure. *Cancer*, *125*(2), 163–319. https://doi.org/10.1002/cncr.31948

Prusa3D. (n.d.). *Meshmixer Tutorial for 3D Printing Beginners*.

Purkait, R. (2016). External ear: An analysis of its uniqueness. *Egyptian Journal of Forensic Sciences*, *6*(2), 99–107. https://doi.org/10.1016/j.ejfs.2016.03.002

Rajaguru, K., Karthikeyan, T., & Vijayan, V. (2020). Additive manufacturing-State of art. *Materials Today: Proceedings*, *21*, 628–633. https://doi.org/10.1016/j.matpr.2019.06.728

Raju Jithin, K. S. S. (2024). *A Comprehensive Comparative Analysis of Catia V6 and PTC Creo Parametric* [Halmstad University]. http://hh.diva-portal.org/smash/get/diva2:1873002/FULLTEXT02.pdf

Reichard, C. A. (2020). *Test and Evaluation of an Artec Leo 3D Scanner* [Florida Institute of Technology]. https://repository.fit.edu/etd

Reis, B. B., Lins, L., Spínola, L. G., & Carvalho, F. M. (2018). Quality of life, work ability, and facial deformities. *Revista Brasileira de Medicina Do Trabalho*, *16*(3), 318–326. https://doi.org/10.5327/Z1679443520180278

Rengier, F., Mehndiratta, A., Von Tengg-Kobligk, H., Zechmann, C. M., Unterhinninghofen, R., Kauczor, H. U., & Giesel, F. L. (2010). 3D printing based on imaging data: Review of medical applications. In *International Journal of Computer Assisted Radiology and Surgery* (Vol. 5, Issue 4, pp. 335–341). Springer Verlag. https://doi.org/10.1007/s11548-010-0476-x

Road Traffic Management Corporation. (2022). *State of Road Safety in South Africa “January 2021 to December 2021.”* https://www.rtmc.co.za/images/rtmc/docs/reports/State-of-Road-Safety-Report_Final.pdf

Rorty, R., Putnam, H., Conant, J., & Helfrich, G. (2004). What is pragmatism? *Think*, *3*(8), 71–88. https://doi.org/10.1017/s1477175600001056

Saberpour, A., Otaran, A., Schmitz, M., Muehlhaus, M., Dabral, R., Luvizon, D., Maekawa, A., Inami, M., Theobalt, C., & Steimle, J. (2023). Computational Design of Personalized Wearable Robotic Limbs. *UIST 2023 - Proceedings of the 36th Annual ACM Symposium on User Interface Software and Technology*, 1–13. https://doi.org/10.1145/3586183.3606748

Safali, S., Berk, T., Makelov, B., Acar, M. A., Gueorguiev, B., & Pape, H. C. (2023). The Possibilities of Personalized 3D Printed Implants—A Case Series Study. *Medicina*, *59*(249), 1–12. https://doi.org/10.3390/medicina59020249

Sakib-Uz-Zaman, C., & Khondoker, M. A. H. (2023). Polymer-Based Additive Manufacturing for Orthotic and Prosthetic Devices: Industry Outlook in Canada. *Polymers*, *15*(6), 1–14. https://doi.org/10.3390/polym15061506

Sarstedt, I. (2012). *Comparisons of Sculpting Efficiency Between Mudbox and ZBrush* [Bachelor Thesis]. University of Gävle, Sweden.

Sarwer, D. B., Siminoff, L. A., Gardiner, H. M., & Spitzer, J. C. (2022). The psychosocial burden of visible disfigurement following traumatic injury. *Frontiers in Psychology*, *13*(979574), 1–11. https://doi.org/10.3389/fpsyg.2022.979574

Saunders, M. N. K., Bristow, A., Thornhill, A., & Lewis, P. (2019). Understanding research philosophy and approaches to theory development. In M. N. K.; Saunders, P. Lewis, & A. Thornhill (Eds.), *Research Methods for Business Students* (8th Edition, pp. 128–171). Pearson Education. https://www.pearson.com/en-gb/higher-education/educators.html?item=100000000652476

Saunders, M. N. K., Lewis, P., & Thornhill, A. (2009). Understanding research philosophies and approaches. In M. N. K. Saunders, P. Lewis, & A. Thornhill (Eds.), *Research Methods for*

Business Students (5th Edition, p. 852). Pearson Education. https://www.pearson.com/en-au/media/gnqjwj0v/9781292402727_sample.pdf?srsltid=AfmBOoo6QVJeWjIRcYxlLkqcwTqaMaZZ6uAqtrORGaMAVrig0nrbdYHC

Schipper, J. A. M., Merema, B. J., Hollander, M. H. J., Spijkervet, F. K. L., Dijkstra, P. U., Jansma, J., Schepers, R. H., & Kraeima, J. (2024). Reliability and validity of handheld structured light scanners and a static stereophotogrammetry system in facial three-dimensional surface imaging. *Scientific Reports*, *14:8172*(1), 1–10. https://doi.org/10.1038/s41598-024-57370-x

Sharma, S., Dhiman, M., Kalra, P., Banga, H. K., & Singh, M. (2023). Reverse engineering and CAD/CAM application in the design of maxillofacial prosthesis. *International Journal on Interactive Design and Manufacturing (IJIDeM)*. https://doi.org/10.1007/s12008-023-01503-5

Shbeer, A. (2024). Radiation in the intensive care units: A review of staff knowledge, practices, and radiation exposure. *Journal of Radiation Research and Applied Sciences*, *17*(100849), 1–7. https://doi.org/10.1016/j.jrras.2024.100849

Siegel, R. L., Giaquinto, A. N., & Jemal, A. (2024). Cancer statistics, 2024. *CA: A Cancer Journal for Clinicians*, *74*(1), 12–49. https://doi.org/10.3322/caac.21820

Spiriev, T., Nakov, V., Laleva, L., & Tzekov, C. (2017). OsiriX software as a preoperative planning tool in cranial neurosurgery: A step-by-step guide for neurosurgical residents. *Surgical Neurology International*, *8:241*(1), 1–9. https://doi.org/10.4103/sni.sni_419_16

Srivastava, G., Kumar Padhiary, S., Mohanty, N., Patil, P. G., Panda, S., Cobo-Vazquez, C., Çakmak, G., & Molinero-Mourelle, P. (2024). Digital workflow feasibility for the fabrication of intraoral maxillofacial prosthetics after surgical resection: a systematic literature review. *ACTA Odontologica Scandinavica*, *83*, 392–403. https://doi.org/https://doi.org/10.2340/aos.v83.40870

Statistics South Africa. (2023). *Cancer in South Africa (2008 - 2019): Vol. Report 03-08-00*. www.statssa.gov.za

Steuck, P.-F., Gottschewski-Meyer, P. O., Bierschwale, D., & Knackstedt, R. (2024). Questionnaires in Design Science Research-a Systematic Overview. *19th International Conference on Wirtschaftsinformatik*, 1–6. https://www.researchgate.net/publication/382088080

Supramaniam, P., Junus, S., Hashim, L., Chiew, S. C., & Devesahayam, P. R. (2024). Lost years, mortality burden: the impact of COVID-19 pandemic on premature death due to road traffic accidents in a northern state in Malaysia. *BMC Public Health*, *24*(1), 1520. https://doi.org/10.1186/s12889-024-19027-2

Suresh, N., Janakiram, C., Nayar, S., Krishnapriya, V. N., & Mathew, A. (2022). Effectiveness of digital data acquisition technologies in the fabrication of maxillofacial prostheses-A systematic review. *Journal of Oral Biology and Craniofacial Research*, *12*, 208–215. https://doi.org/10.1016/j.jobcr.2021.12.004

Sykes, B. E., Curtis, T. A., & Cantor, R. (1972). Psychosocial aspects of maxillofacial rehabilitation. Part II. A long-range evaluation. *The Journal of Prosthetic Dentistry*, *28*(5), 540–545. https://doi.org/https://doi.org/10.1016/0022-3913(72)90065-0

Tack, P., Victor, J., Gemmel, P., & Annemans, L. (2016). 3D-printing techniques in a medical setting: A systematic literature review. In *BioMedical Engineering Online* (Vol. 15, Issue 1). BioMed Central Ltd. https://doi.org/10.1186/s12938-016-0236-4

Tantisatirapong, S., Khunakornpattanakarn, S., Suesatsakul, T., Boonpratatong, A., Benjamin, I., Tongmeesee, S., Kangkorn, T., & Chanwimalueang, T. (2023). The simplified tailor-made workflows for a 3D slicer-based craniofacial implant design. *Scientific Reports*, *13*(2850), 1–14. https://doi.org/10.1038/s41598-023-30117-w

Tanveer, W., Ridwan-Pramana, A., Molinero-Mourelle, P., & Forouzanfar, T. (2023). Applications of CAD/CAM Technology for Craniofacial Implants Placement and Manufacturing of Auricular Prostheses—Systematic Review. *Journal of Clinical Medicine*, *12*(5950), 1–34. https://doi.org/10.3390/jcm12185950

Teo, A. I. C., Van As, A. B., & Cooper, J. (2012). A comparison of the epidemiology of paediatric burns in Scotland and South Africa. *Burns*, *38*(6), 802–806. https://doi.org/10.1016/j.burns.2012.04.010

The Skin Cancer Foundation. (2024). *Skin Cancer Facts & Statistics - The Skin Cancer Foundation*. https://www.skincancer.org/skin-cancer-information/skin-cancer-facts/

Tobin-Tyler, E. (2023). Intimate Partner Violence, Firearm Injuries and Homicides: A Health Justice Approach to Two Intersecting Public Health Crises. *Journal of Law, Medicine and Ethics*, *51*(1), 64–76. https://doi.org/10.1017/jme.2023.41

Tofail, S. A. M., Koumoulos, E. P., Bandyopadhyay, A., Bose, S., O'Donoghue, L., & Charitidis, C. (2018a). Additive manufacturing: scientific and technological challenges, market uptake and opportunities. In *Materials Today* (Vol. 21, Issue 1, pp. 22–37). Elsevier B.V. https://doi.org/10.1016/j.mattod.2017.07.001

Torres-Sanmiguel, C. R. (2022). Modeling and Simulation Process via Incremental Methods of a Production-Aimed Upper Limb Prosthesis. *Applied Sciences*, *12*(6:2788), 1–17. https://doi.org/10.3390/app12062788

Tóth, T., Varga, P., Štefanovič, B., Bednarčíková, L., Schnitzer, M., Hudák, R., & Živčák, J. (2021). Accuracy verification of an anatomical model manufactured using low-cost additive production. *Applied Sciences (Switzerland)*, *11*(2), 1–19. https://doi.org/10.3390/app11020594

Tria, G. (2023). Project Daniel, a Collaborative open-source 3D Prosthesis project led by Not Impossible Labs in Sudan. *Patient Innovation: Sharing Solutions, Improving Life*. https://patient-innovation.com/post/7608

Trieu, M. N., & Thinh, T. N. (2023). The Anthropometric Measurement of Nasal Landmark Locations by Digital 2D Photogrammetry Using the Convolutional Neural Network. *Diagnostics*, *13*(891), 1–16. https://doi.org/10.3390/diagnostics13050891

Tsalafoutas, I. A., Hassan Kharita, M., Al-Naemi, H., & Kalra, M. K. (2020). Radiation dose monitoring in computed tomography: Status, options and limitations. In *Physica Medica* (Vol. 79, pp. 1–15). Associazione Italiana di Fisica Medica. https://doi.org/10.1016/j.ejmp.2020.08.020

Unkovskiy, A., Spintzyk, S., Beuer, F., Huettig, F., Röhler, A., & Kraemer-Fernandez, P. (2022). Accuracy of capturing nasal, orbital, and auricular defects with extra- and intraoral optical scanners and smartphone: An in vitro study. *Journal of Dentistry*, *117*(103916). https://doi.org/10.1016/j.jdent.2021.103916

Unkovskiy, A., Spintzyk, S., Brom, J., Huettig, F., & Keutel, C. (2018). Direct 3D printing of silicone facial prostheses: A preliminary experience in digital workflow. *Journal of Prosthetic Dentistry*, *120*(2), 303–308. https://doi.org/10.1016/j.prosdent.2017.11.007

Vanaclocha-Saiz, A., Vanaclocha, V., Atienza, C. M., Clavel, P., Jorda-Gomez, P., Barrios, C., & Vanaclocha, L. (2022). Finite Element Analysis of a Bionate Ring-Shaped Customized Lumbar Disc Nucleus Prosthesis. *ACS Applied Bio Materials*, *5*(1), 172–182. https://doi.org/10.1021/acsabm.1c01027

Vennam, S., KN, V., & Pati, F. (2024). 3D printed personalized assistive devices: A material, technique, and medical condition perspective. *Applied Materials Today*, *40*. https://doi.org/10.1016/j.apmt.2024.102403

Ventola, C. L. (2014). Medical Applications for 3D Printing: Current and Projected Uses. *Pharmacy & Therapeutics*, *39*(10), 704–711. www.thingiverse.com

Vom Brocke, J., Hevner, A., & Maedche, A. (2020). Introduction to Design Science Research. In J. vom Brocke, A. Hevner, & A. Maedche (Eds.), *Design Science Research* (pp. 1–13). Springer Nature. https://doi.org/10.1007/978-3-030-46781-4_1

Weigand, H., Johannesson, P., & Andersson, B. (2021). An artifact ontology for design science research. *Data and Knowledge Engineering*, *133*(101878), 1–19. https://doi.org/10.1016/j.datak.2021.101878

Wendo, K., Barbier, O., Bollen, X., Schubert, T., Lejeune, T., Raucent, B., & Olszewski, R. (2022). Open-Source 3D Printing in the Prosthetic Field—The Case of Upper Limb Prostheses: A Review. *Machines*, *10*(6). https://doi.org/10.3390/machines10060413

World Cancer Research Fund International. (2020). *Skin cancer statistics*. https://www.wcrf.org/cancer-trends/skin-cancer-statistics/

World Health Organization. (2023). *Global status report on road safety 2023*. https://www.who.int/teams/social-determinants-of-health/safety-and-mobility/global-status-report-on-road-safety-2023

Yadav, S. K., & Shrestha, S. (2017). A study on posttraumatic experience of road traffic accident afflicted maxillofacial trauma patient at tertiary hospital. *Journal of Natural Science, Biology and Medicine*, *8*(1), 40–45. https://doi.org/10.4103/0976-9668.198358

Yap Abdullah, J., Manaf Abdullah, A., Zaim, S., Hadi, H., Husein, A., Ahmad Rajion, Z., & Malin Abdullah, J. (2024). Three-dimensional analysis of reconstructed skulls using three different open-source software versus commercial software. *Proceedings of the Institution of Mechanical Engineers, Part H: Journal of Engineering in Medicine*, *238*(1), 55–62. https://doi.org/10.1177/09544119231212034

Yushkevich, P. A., Gao, Y., & Gerig, G. (2016). ITK-SNAP: An interactive tool for semi-automatic segmentation of multi-modality biomedical images. *Proceedings of the Annual International Conference of the IEEE Engineering in Medicine and Biology Society, EMBS*, *2016-October*, 3342–3345. https://doi.org/10.1109/EMBC.2016.7591443

Zabala-Travers, S. (2021). Biomodeling and 3D printing: A novel radiology subspecialty. *Annals of 3D Printed Medicine*, *4*(100038), 1–15. https://doi.org/10.1016/j.stlm.2021.100038

Zardawi, F. M. (2012). *Characterisation of Implant Supported Soft Tissue Prostheses Produced with 3D Colour Printing Technology* (Issue November). http://etheses.whiterose.ac.uk/3299/1/Final_-Thesisi_7.pdf

Zardawi, F. M., Xiao, K., Van Noort, R., & Yates, J. M. (2015a). Investigation of Elastomer Infiltration into 3D Printed Facial Soft Tissue Prostheses. *Anaplastology*, *4*(1), 1–5. https://doi.org/10.4172/2161-1173.1000139

Zardawi, F. M., Xiao, K., Van Noort, R., & Yates, J. M. (2015b). Mechanical Properties of 3D Printed Facial Prostheses Compared to Handmade Silicon Polymer Prostheses. *European Scientific Journal*, *11*(12), 1–11.

Zhou, J., Pan, B., Yang, Q., Zhao, Y., He, L., Lin, L., Sun, H., Song, Y., Yu, X., Sun, Z., & Jiang, H. (2016). Three-dimensional autologous cartilage framework fabrication assisted by new additive manufactured ear-shaped templates for microtia reconstruction. *Journal of Plastic, Reconstructive and Aesthetic Surgery*, *69*(10), 1436–1444. https://doi.org/10.1016/j.bjps.2016.06.011

Appendixes

Appendix A

Central University of Technology, Free State

CENTRAL UNIVERSITY OF TECHNOLOGY, FREE STATE
SENTRALE UNIVERSITEIT VIR TEGNOLOGIE, VRYSTAAT
YUNIVESITHI E BOHARENG YA THEKENOLOJI, FOREISTATA

FACULTY RESEARCH AND INNOVATION COMMITTEE – HEALTH AND ENVIRONMENTAL SCIENCES

RESEARCH ETHICS APPROVAL LETTER

Date: 20 April 2018

This is to confirm that:

Applicant's Name	Izél van Heerden
Supervisor Name for Student Project	Prof Annabel Fossey and Dr Kobus van der Walt
Level of Qualification for Student	Doctor of Health Sciences in Biomedical Technology
Tittle of research project	Techno-economic assessment of process chains for the manufacturing of external maxillofacial prostheses for the South African ethnic demography using digital and Additive Manufacturing technologies

Ethical clearance has been provided by the Faculty Research and Innovation Committee on the 10th of October 2017 in view of the CUT Research Ethics and Integrity Framework, 2016, with reference number **FHES2017001.**

[x] None

[ ] Specific conditions

Further the approval of this committee, the candidate should now seek ethical approval from the Health Sciences Research Ethics Committee of the University of the Free State.

Wish you success with your research project.

____

(FRIC Chairperson)

Appendix B

UNIVERSITY OF THE FREE STATE
UNIVERSITEIT VAN DIE VRYSTAAT
YUNIVESITHI YA FREISTATA
UFS·UV
HEALTH SCIENCES
GESONDHEIDSWETENSKAPPE

Health Sciences Research Ethics Committee

23-Apr-2018

Dear **Izél Van Heerden**

Ethics Clearance: **Techno-economic assessment of process chains for the manufacturing of external maxillofacial prostheses for the South African ethnic demography using digital and Additive Manufacturing technologies.**

Principal Investigator: **Izél Van Heerden**

Department: **Biomedical Technology - CUT**

APPLICATION APPROVED

Please ensure that you read the whole document

With reference to your application for ethical clearance with the Faculty of Health Sciences, I am pleased to inform you on behalf of the Health Sciences Research Ethics Committee that you have been granted ethical clearance for your project.

Your ethical clearance number, to be used in all correspondence is:**UFS-HSD2018/0051/2404**

The ethical clearance number is valid for research conducted for one year from issuance. Should you require more time to complete this research, please apply for an extension.

We request that any changes that may take place during the course of your research project be submitted to the HSREC for approval to ensure we are kept up to date with your progress and any ethical implications that may arise. This includes any serious adverse events and/or termination of the study.

A progress report should be submitted within one year of approval, and annually for long term studies. A final report should be submitted at the completion of the study.

The HSREC functions in compliance with, but not limited to, the following documents and guidelines: The SA National Health Act. No. 61 of 2003; Ethics in Health Research: Principles, Structures and Processes (2015); SA GCP(2006); Declaration of Helsinki; The Belmont Report; The US Office of Human Research Protections 45 CFR 461 (for non-exempt research with human participants conducted or supported by the US Department of Health and Human Services- (HHS), 21 CFR 50, 21 CFR 56; CIOMS; ICH-GCP-E6 Sections 1-4; The International Conference on Harmonization and Technical Requirements for Registration of Pharmaceuticals for Human Use (ICH Tripartite), Guidelines of the SA Medicines Control Council as well as Laws and Regulations with regard to the Control of Medicines, Constitution of the HSREC of the Faculty of Health Sciences.

For any questions or concerns, please feel free to contact HSREC Administration: 051-4017794/5 or email EthicsFHS@ufs.ac.za.

Thank you for submitting this proposal for ethical clearance and we wish you every success with your research.

Yours Sincerely

Dr. SM Le Grange
Chair : Health Sciences Research Ethics Committee

Health Sciences Research Ethics Committee
Office of the Dean: Health Sciences
T: +27 (0)51 401 7795/7794 | E: ethicsfhs@ufs.ac.za
IRB 00006240; REC 230408-011; IORG0005187; FWA00012784
Block D, Dean's Division, Room D104 | P.O. Box/Posbus 339 (Internal Post Box G40) | Bloemfontein 9300 | South Africa

Appendix C

PROJECT INFORMATION

Title of study:
Techno-economic assessment of process chains for the manufacturing of external maxillofacial prostheses for the South African ethnic demography using digital and Additive Manufacturing technologies

Principal Investigator:
This study will be conducted by Izél van Heerden, under the guidance of Professor Annabel Fossey and Doctor Kobus van der Walt in the Centre for Rapid Prototyping and Manufacturing (CRPM), Department of Mechanical and Mechatronics Engineering at the Central University of Technology (CUT), Free State. This study is undertaken towards a degree of Doctor of Health Sciences in Biomedical Technology.

E-mail: ivanheerden@mweb.co.za
Cell number: 083 662 3427

Background:
In the medical world, numerous patients suffer one or other disfigurement. These disfigurements may be as a result of birth defects, cancer, burns or accidents. Facial defects are of particular concern, because these patients often suffer psychological distress and tend to withdraw from their social environments. Therefore, patients suffering such facial disfigurements usually visit medical doctors requesting some or other treatment. Many of these treatments require the rebuilding of body parts, such as ears and noses. In an attempt to improve their appearances, these patients, thus may need artificial ears, noses or eyes.

Many of these patients are government funded and cannot afford expensive first world technologies to improve their facial disfigurements. These technologies include advanced computer design programs and advanced manufacturing technologies. Therefore, the need for mechanisms and systems through which such patients can access medical help has been recognised. Because such medical help is expensive, research is needed to determine what methods are available that are affordable, and still result in good quality artificial ears and noses. This information will help all South Africans, particularly those with low income to obtain such medical help.

The purpose of this study is:
The purpose of this study is to determine which design and manufacturing procedures are available to produce relatively low costing artificial ears and noses of acceptable quality. A component of this project will be to produce a catalogue of design information of ears and noses for South Africans of different ethnic groups. The purpose of this catalogue will be to help with the design and manufacturing of low-cost artificial facial parts. The data that will be used to achieve the purpose of this project will be obtained by applying digital scanning technologies.

To conduct this study, two types of digital data will be collected. From most participants, digital data of the head will be collected through the use of a hand-held digital scanner. Computed tomography data will also be obtained from two control participants, who are the principal investigator and one of the study supervisors.

Appendix D

Central University of Technology, Free State

LETTER OF CONCENT

Invitation to participate:
You are invited to take part in a research project. Before you decide to participate in this project, it is important that you understand why the research is being conducted and what it will involve.

Please take the time to read the accompanying information brochure carefully. Please ask the researcher if there is anything that is not clear or if you need more information.

Study procedure:
You will be subjected to a computed tomography (CT) scanner to generate digital data of your head. People are exposed to radiation from natural sources all the time. All x-rays involve a small extra dose of radiation. The dose of radiation used for CT examinations is carefully controlled to ensure the smallest possible amount is used that will still give a useful result. However, all radiation exposure is linked with a slightly higher risk of developing cancer. The size of any increased risk depends on the age of the participant and the total amount of radiation received. The risk of any one scan is very small but increases if many scans are needed.

Risks:
I understand the procedure has the following specific risks and limitations:

- There is a very small risk associated with radiation exposure. This cannot be avoided.
- If you are pregnant or think that you may be pregnant, or suffer epilepsy or have a tendency to seizures, or suffer claustrophobia, you are requested to withdraw from participating.

Benefits:
There will be no direct benefit to you for your participation in this project. However, we hope that your digital data will help many South Africa patients who are in need of cost-effective external facial prostheses, who under normal circumstances would not be able to afford such prostheses.

Confidentiality:
Only your digital data will be used and processed anonymously in this research project and subsequent research papers that may follow. Your name will not be mentioned in any scientific documentation.

Costs to subject:
There are no costs to you for your participation in this project.

Compensation:
There is no monetary compensation to you for your participation in this project.

Consent:
By signing this consent form, I confirm that I have read and understood the information and have had the opportunity to ask questions. I understand that my participation is voluntary and that I am free to withdraw at any time, without giving a reason and without cost. I understand that I will be given a copy of this consent form. I voluntarily agree to take part in this study.

……………………………………………… ………………………………………………
Signature of participant **Date**

Appendix E

LETTER OF CONCENT

Invitation to participate:
You are invited to take part in a research project. Before you decide to participate in this project, it is important that you understand why the research is being conducted and what it will involve.

Please take the time to read the accompanying information brochure carefully. Please ask the researcher if there is anything that is not clear or if you need more information.

Study procedure:
You will be subjected to a hand-held digital scanner to generate digital data of your head. This procedure is painless and will take approximately 40 minutes. This scanner generates digital data through blue light technology. Display screens of computers, electronic notebooks, smartphones and other digital devices also emit significant amounts of blue light.

Risks:
The risks to blue light exposure are minimal. However, in order to protect the interior of your eyes, you are requested to keep your eyes closed during the scanning process.

Benefits:
There will be no direct benefit to you for your participation in this project. However, we hope that your digital data will help many South Africa patients who are in need of cost-effective external facial prostheses, who under normal circumstances would not be able to afford such prostheses.

Confidentiality:
Only your digital data will be used and processed anonymously in this research project and subsequent research papers that may follow. Your name will not be mentioned in any scientific documentation.

Costs to subject:
There are no costs to you for your participation in this project.

Compensation:
There is no monetary compensation to you for your participation in this project.

If you are pregnant or think that you may be pregnant, or suffer epilepsy or tendency to seizures, you are requested to withdraw from participating.

Consent:
By signing this consent form, I confirm that I have read and understood the information and have had the opportunity to ask questions. I understand that my participation is voluntary and that I am free to withdraw at any time, without giving a reason and without cost. I understand that I will be given a copy of this consent form. I voluntarily agree to take part in this study.

……………………………………………… ………………………………………………
Signature of participant **Date**

Appendix F

Van Heerden, Fossey, Van der Walt, 2018. Maxillofacial prostheses production through computer-aided design and manufacturing technologies – review of state of the art. *RAPDASA 2018 Conference Proceedings*, pp.77 – 83. ISBN 978-0-620-80987-0.

Appendix G

Van Heerden and Fossey, 2019. Changing world of external maxillofacial prosthesis manufacturing. *RAPDASA 2019 Conference Proceedings*, pp.362 – 370. ISBN 978-0-6398390-0-4.